

AD-A121 242 MERCURY CADMIUM TELLURIDE SPUTTERING RESEARCH(U) NEW
JERSEY INST OF TECH NEWARK DEPT OF ELECTRICAL
ENGINEERING R H CORNELI 28 AUG 82 AFOSR-TR-82-0936
UNCLASSIFIED AFOSR-77-3249

F/G 13/8

1/1

NL

END

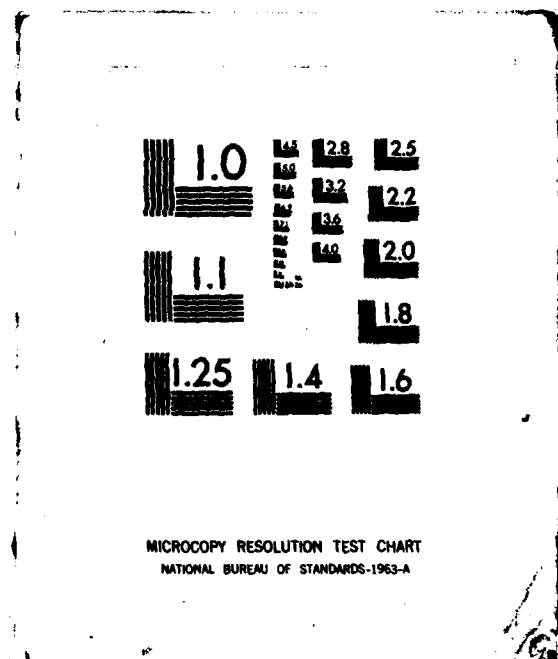
DATE

FILED

200

DTIC

CLASSIF



ED AF
FOSR-TR- 82-0936

(12)

AD A121242

FINAL SCIENTIFIC REPORT
HgCdTe Sputtering Research

Prepared for:

Air Force Office of Scientific Research
Bld. 410
Bolling Air Force Base
Washington, D. C. 20332

New Jersey Institute of Technology
323 High Street, Newark, N.J. 07102

August 28, 1982

DTIC
ELECTE
NOV 8 1982

A

Roy H. Cornely, Ph.D.
Principal Investigator
Department of Electrical Engineering

Approved for public release;
distribution unlimited.

DTIC FILE COPY

82 11 08 001

UNCLASSIFIED

SECURITY CLASSIFICATION OF THIS PAGE (When Data Entered)

REPORT DOCUMENTATION PAGE		READ INSTRUCTIONS BEFORE COMPLETING FORM
1. REPORT NUMBER AFOSR-TR- 82-0936	2. GOVT ACCESSION NO. AD-A121242	3. RECIPIENT'S CATALOG NUMBER
4. TITLE (and Subtitle) Mercury Cadmium Telluride Sputtering Research		5. TYPE OF REPORT & PERIOD COVERED Final Technical Report
7. AUTHOR(s) Roy H. Cornely, Electrical Engr. Dept.		6. PERFORMING ORG. REPORT NUMBER
9. PERFORMING ORGANIZATION NAME AND ADDRESS New Jersey Institute of Technology 323 High Street Newark, New Jersey 07102		8. CONTRACT OR GRANT NUMBER(s) AFOSR 77-3249
11. CONTROLLING OFFICE NAME AND ADDRESS Electronic and Solid State Sciences, Div. AFOSR Bldg. 410, Bolling Air Force Base Washington, D.C. 20332		10. PROGRAM ELEMENT, PROJECT, TASK AREA & WORK UNIT NUMBERS 61102F 2386/K2
14. MONITORING AGENCY NAME & ADDRESS (if different from Controlling Office)		12. REPORT DATE August 28, 1982
		13. NUMBER OF PAGES 92
		15. SECURITY CLASS. (of this report) Unclassified
		15a. DECLASSIFICATION/DOWNGRADING SCHEDULE
16. DISTRIBUTION STATEMENT (of this Report) Approved for public release; distribution unlimited.		
17. DISTRIBUTION STATEMENT (of the abstract entered in Block 20, if different from Report) N/A		
18. SUPPLEMENTARY NOTES Co-investigator for some of the work reported here was Dr. Lawrence Suchow, Professor of Chemistry in Dept. of Chem.Engr. and Chemistry		
19. KEY WORDS (Continue on reverse side if necessary and identify by block number) Mercury Cadmium Telluride, Semiconductor Thin Films Prepared by rf Triode Sputtering; Optical, Structural and Electrical Properties of Mercury Cadmium Telluride Thin Films, WDX Compositional Analysis of (Hg,Cd)Te Films, Annealing of (Hg,Cd)Te Thin Films.		
20. ABSTRACT (Continue on reverse side if necessary and identify by block number) A large number of 10 micron thick Mercury Cadmium Telluride films with 20 mole percent CdTe were triode-sputtered on silicon substrates. The sensitivity of carrier concentration and electron mobility to small changes in sputtering par- ameters (particularly Hg sputtering gas pressure and substrate d.c. bias and temperature) and to post-deposition annealing parameters was studied. Carrier concentrations of ten to the fifteenth per cubic cm at one hundred degrees Kelvin were obtained in n-type films after annealing at 553 degrees Kelvin.		

UNCLASSIFIED



Application For

NAME: [REDACTED]

DATE: [REDACTED]

TIME: [REDACTED]

PLACE: [REDACTED]

REASON: [REDACTED]

REMARKS: [REDACTED]

Signature: [REDACTED]

UNCLASSIFIED

TABLE OF CONTENTS

<u>SECTION</u>	<u>TITLE</u>	<u>PAGE</u>
1.0	FOREWARD	1
2.0	RESEARCH REPORT	3
2.1	Film Sputter-Deposition Equipment, Procedures and General Experimental Results	3
2.1.1	Sputtering System	3
2.1.2	Target Materials and Fabrication Procedure	4
2.1.3	Summary of Research on Chemical and Physical Changes of Sputtered Targets	5
2.1.4	Substrates and Their Preparation	6
2.1.5	Control of Hg Sputtering Gas Pressure	7
2.1.6	Film Flaking Problems	8
2.1.7	Some Experimental Results	8
2.2	Structural Properties of Sputtered Films	12
2.3	Determination of Film Composition by Electron Microprobe and Optical Absorption Measurements	17
2.3.1	Theory and Procedure for Optical Absorption Curve Calculations	17
2.3.2	Experimental Procedure for Optical Measurements	19
2.3.3	Optical Measurements Results	19
2.3.4	Procedure for Determining Film Composition by Microprobe Analysis	20
2.3.5	WDX Microprobe Results	21
2.3.6	Discussion of Compositional Results Obtained by Optical WDX Measurements	21
2.4	Dependence of Electrical Properties of Sputtered Films on Sputtering Parameters	33
2.4.1	Introduction	33
2.4.2	Hall-effect Measurement Equipment and Procedure	33
2.4.3	Hall Mobility of Sputtered Films Versus Film Thickness	34

AIR FORCE OFFICE OF SCIENTIFIC RESEARCH (AFOSR)

NOTICE OF TRANSMITTAL TO DTIC

This technical report has been reviewed and is approved for public release IAW AFR 190-12.

Distribution is unlimited.

MATTHEW J. KERPER

Chief, Technical Information Division

	2.4.4	Hall Mobility of Sputtered Films Versus Substrate Temperature	35
	2.4.5	Hall Mobility Versus Applied R.F. Power and Substrate Temperature	35
	2.4.6	Comparison of Hall Mobilities for CdTe and Silicon Substrates	36
	2.4.7	Hall Mobility and Carrier Concentration Versus Substrate Bias	36
	2.4.8	Hall Mobility and Carrier Concentration Versus Hg Pressure	36
	2.4.9	Hall Mobility Versus Exposure Time to Ambient Atmosphere	37
	2.4.10	Sputtering With D.C. Voltage Applied to the Target	37
	2.4.11	Dependence of Conduction Results on Film Composition	37
2.5		Electrical Properties of Annealed Films	46
	2.5.1	Introduction	46
	2.5.2	Background on Annealing (Hg,Cd)Te Material	46
	2.5.3	Annealing Procedure	47
	2.5.4	Conduction Properties of Annealed Films; Discussion of Results	48
	2.5.5	Study of the Magnetic Field Dependence Conduction Properties of Annealed Films	52
	2.5.6	Conclusions on Optimum Annealing and Sputtering Parameters for Nearly-Intrinsic Films	53
2.6		Appendix A; Appendix B	62
3.0		SUMMARY AND SUGGESTIONS FOR FUTURE WORK	66
4.0		REFERENCES	72
5.0		INTERACTIONS AND PUBLICATIONS	75
6.0		LIST OF CONTRIBUTING PERSONNEL IN 1977-1982 GRANT	79
7.0		ACKNOWLEDGEMENT	88

The objective of this research was to develop sputtering and post-deposition annealing techniques for preparation of single crystal, thin films of Mercury Cadmium Telluride (Hg,Cd)Te on large area, low cost substrates. The research concentrated on finding ways to control the film properties so that the thin film layers would be suitable for fabrication of either photovoltaic or photoconductive cells for wide-angled infrared sensing in wavelength regions of interest such as 3 - 5, 8 - 14 and 18 - 25 microns. The research involved R. F. (Radio-frequency) sputtering in a mercury vapor atmosphere using a triode-sputtering system, an approach that allows the Hg pressure to be low enough (about one micron) for nearly stoichiometric films of $(\text{Hg}_{1-x}, \text{Cd}_x)\text{Te}$ to be sputtered with any desired x value in the 0.18 to 0.27 compositional range. The sputtering approach at NJIT used targets made of cold-pressed powder mixtures composed of low-cost HgTe and CdTe powders. The effective x value of the target can be shifted by simply changing the relative volume of the two powders.

The triode-sputtering approach allows material to be deposited at higher energy than by MBE or LPE deposition methods and therefore higher substrate temperatures can be used and crystalline growth on low-cost silicon substrates, with (111) surface orientation, can be obtained. The NJIT research concentrated on optimizing film deposition parameters to obtain high quality films on silicon substrates because of its low cost and the potential use of its electronic properties. The behavior of carrier concentration and mobility with changes in temperature in the 87-300°K range was studied by Hall-effect measurements because of the strong dependence of this behavior on film stoichiometry and crystallinity. The very sensitive dependence of the conduction behavior on key sputtering parameters (Hg sputtering gas pressure, film deposition rate, substrate dc bias and temperature, and silicon surface treatment) was clearly established and studied. Extensive work was done on improving the properties by post-deposition annealing in a Hg atmosphere using a two-zone furnace. The conduction properties were studied as a function of the annealing temperature and time and the pressure of the Hg.

For films with an x compositional value of 0.2, carrier concentrations as low as 10^{15}cm^{-3} at 100°K were obtained. Electron mobilities at 87°K up to 16% of bulk crystal values were measured for 5 - 10 micron thick films. The most promising results were obtained using a small dc substrate bias, which was found to be very effective for removal of sputtered impurities from the target. The starting target materials were only 5 nines pure. The experimental conduction results indicate that further fine-tuning of the sputtering and annealing parameters can probably enable nearly intrinsic films with high electron mobilities to be obtained on silicon substrates.

A further objective of the research was to demonstrate that the sputtered film's compositional parameter x matched that of the target. By using Wavelength Dispersive Electronprobe Microanalysis and optical absorption measurements, the composition were shown to match (within the four percent accuracy of the measurement) for the films measured in the 0.2-0.27 x value range. The optical measurements, along with the dependence of the Hall-effect coefficient on magnetic field, enabled the conductivity type of compensated films to be found.

The research was very relevant to the science and technology of heteroepitaxial growth of the compound semiconductor (Hg,Cd)Te. There presently is much interest in (Hg,Cd)Te material, particularly in thin films. Scientific information obtained that would be useful to other researchers included: the effect of different annealing conditions on the control of the stoichiometry and the conduction properties of (Hg,Cd)Te thin films; the Wavelength Dispersive Electronprobe Microanalysis(WDX) and x-ray diffraction method for analysis of the structural and compositional properties of (Hg,Cd)Te thin films; the relation of film compositional properties to changes in target composition, as measured under a separate grant devoted to a scientific investigation of target sputtering phenomena.

The research had long-range applications to many present and future infrared detector programs. Among the application areas are: (a) low cost megabit arrays for long wavelength response (9-25) microns); (b) (Hg,Cd)Te detectors deposited on substrates containing CCD circuitry; (c) low-cost high-speed photovoltaic detectors; (d) long-wavelength, high gain avalanche and graded junction photo-diodes; (e) low noise, high gain photoconductors with reduced surface trapping effects due to either sputtered passivation layers or surface depletion regions formed in-field effects structures.

2.0 RESEARCH REPORT

2.1 Film Sputter-Deposition Equipment, Procedures and General Experimental Results

The deposition of $(\text{Hg}_{1-x}\text{Cd}_x)\text{Te}$ films by sputtering is a complex process involving consideration of the deposition system, the sputtering gas, the substrate material including its surface chemical and physical preparation, and other sputtering parameters involved in the nucleation and growth of the film. Research on NJIT on the behavior of sputtered $(\text{Hg,Cd})\text{Te}$ targets revealed that to maintain a sputtering target surface with sufficient Hg concentration, Hg must be used as the sputtering gas. It was also found that the pressure of the bombarding Hg vapor must be about 1.2 microns or less, dependent on sputtering rate and desired X value of the film, to maintain a target surface concentration of Cd high enough to sputter away sufficient Cd for stoichiometric films with desired X value. This low pressure requires the use of triode, rather than diode, sputtering systems; fortunately low-pressure triode sputtering was the NJIT approach from the beginning of this research. The following section will discuss in detail the NJIT triode sputtering system, including its operation and maintenance. Other sections will give details for the preparation and sputtering of the targets and the sputtering deposition parameters as they relate to some of the general experimental properties of the sputtered $(\text{Hg,Cd})\text{Te}$ films.

2.1.1 Sputtering System

The modified Material Research Corporation 8800 sputtering system used to deposit the $(\text{Hg}_{1-x}\text{Cd}_x)\text{Te}$ thin films by the triode-mode is shown in Fig. 1-1.(1) A rotating turret head accommodates 4 targets fitted with grounded shields to assure sputtering of only the target. RF power (P_{rf}) as well as dc power (P_{dc}) can be applied to the targets to produce rf or dc sputtering. A moveable anode contains a resistive heater to heat the substrates to a specified temperature (T_s) as well as cooling lines that can carry air (when the anode is very hot) and water (once the anode is below 120°C) to quench the samples. The samples are placed on a copper platen and can be moved without breaking vacuum from the intervac to the anode by means of a pneumatic plunger. The anode is normally grounded through a high impedance but can also carry either dc (V_b) or rf for bias sputtering or sputter etching. The system was modified for this research to have a triode confinement box, with a split three-part construction so that the central portion is at floating potential with respect to the plasma and therefore does not sputter. [One end of the triode box is at ground potential while the other end is at the biased filament potential V_{dc} . Without the box being split by insulators the central region would have a D.C. potential with respect to the plasma.] The system was also modified so that almost all metal parts exposed to the Hg vapor are made of stainless steel, which can withstand the corrosive Hg atmosphere. The electron flow produces increased ionization of the sputtering gas (Hg) allowing sputtering to occur at a lower pressure. The electrons are produced by thermionic emission from a filament supplied with approximately 65 amps at 60 hertz (I_{fil}). The electron flow (I_{dc}) is collected by a dc biased filament (V_{dc}) at the opposite end of the confinement box. This arrangement may be switched if the emitting filament burns out.

The sections of the box surrounding the filaments and the filament feedthroughs as well as the targets are cooled with water whose temperature can be controlled. Temperatures are monitored by thermocouples at the outlets. It was found that the filament current feedthrough cooling lines, which previously carried only cold water, needed to carry warm water since Hg tended to condense on the feedthroughs and cause intermittent arcing. This was a problem that plagued initial depositions and led to eventual loss of vacuum through feedthrough insulator (teflon) softening. While investigating this problem it was also found that a gradual buildup of conducting film occurs on the filament feedthrough insulator. The insulator was redesigned to minimize this buildup. A regular maintenance program also included cleaning the triode box, viewing ports, the intervac door and all exposed areas. This was determined to be the best way to assure trouble-free runs and to minimize contaminants. (1)

The mercury pressure (P_{Hg}) is monitored with a pirani gage. The mercury source is a pool of mercury in a stainless steel bottle connected to the vacuum chamber via a valve. The mercury pressure in the chamber is controlled by heating the bottle with a resistive heating tape. To prevent condensation, the walls and roof are also heated with resistive tapes, shown as resistors in Fig 1-1. To maintain a constant flow of mercury (and as a coarse control of the pressure) the gate valve angle is adjusted. Sometimes argon is needed to increase the pressure high enough to ignite the plasma. After ignition the argon supply is shut off and system is allowed to purge itself.

To obtain a "good" vacuum both before and after sputtering, the system is heated to accelerate outgassing. The criteria for good vacuum, that is, adequate for sputtering, was both a low base pressure (less than 1.0×10^{-6} Torr) and a long rise time (greater than 2 minutes). The rise time ($t_{r \text{ cold}}$) was defined as the time for the pressure to rise to 10×10^{-6} Torr (on the ionization gage) with the gate valve closed and the system cold. It was found, however, that it was better to leave the heat on continually since more outgassing can be accomplished and the chamber will be ready to sputter sooner. Also, this method saves time on the day of sputtering since no time is required waiting for the system to heat up. Of course the rise time is much shorter with the chamber hot; therefore, a new hot rise time ($t_{r \text{ hot}}$) was used. It is defined as the time for the pressure to rise to 5×10^{-5} Torr with the gate valve closed. It was determined that in this case a rise time of at least one minute was satisfactory for sputtering.

2.1.2 Targets Materials and Fabrication Procedure

The fabrication of many pressed-powder targets was required to deposit the large number of films required for deposition and annealing methods for optimizing the properties of sputtered (Hg,Cd)Te films. Altogether about 80 target discs of (Hg,Cd)Te were fabricated between 1977 and 1982 for film deposition purposes. These targets were almost all made by the relatively inexpensive method of pressing powder mixtures, obtained by grinding HgTe and CdTe polycrystalline ingots, into relatively firm discs, 5.7 cm. diameter, epoxied onto five inch diameter backing plates. Figures 2 and 3 show the details of mounting the target disc in the sputtering system. The average sizes of the HgTe and CdTe particles were about 9 and 7.3 microns respectively. A plot of the size distribution is given in reference 2. The 5.7 diameter discs were usually 0.3 cm thick

and made with an 80 ton press in the NJIT M.E. Lab. Data on the densities of target discs (before sputtering) versus applied pressure, disc thickness and composition were obtained in the ARO research and reported.^{2,3,4} [Typical results for discs with X=0.25 composition were: for 7.72 cm diameter, 0.42cm thick discs, a density of 5.6 g/cm^3 is obtained with an applied pressure of $0.4 \times 10^8 \text{ newtons/m}^2$; for 5.72cm diameter, 0.165cm thick discs, a density of 6.8 g/cm^3 is obtained with $1.6 \times 10^8 \text{ newtons/m}^2$ applied pressure; for 2.86cm diameter, 0.15cm thick discs, a density of $7\text{--}7.15 \text{ g/cm}^3$ is obtained with an applied pressure of $2.16 \cdot 10^8 \text{ newtons/m}^2$. To obtain the same densities for X=0.2 discs requires only about 90% of the applied pressure for X=0.25 discs.] More important than applied pressure in fabricating good targets, without cracks and soft areas, are the techniques for leveling the powder in the die before pressing and the techniques for removing the disc from the die after pressing the powder. As detailed in Bourne's thesis,⁽³⁾ a key factor is waiting several hours to let pressurized air escape from the die-disc interface before opening the die for removal of the disc. If this is not done, tiny and even large cracks appear on the target surface resulting in material from the target falling on growing films during sputtering.

The economics of the pressed-powder target approach to sputtering thin films can be seen by the following example. A 40 gram X=0.2 disc, about 0.3cm thick, requires 33.82 grams of HgTe and 6.18 grams of CdTe. The cost of 300 grams of HgTe purchased from Atomergic Chem. Corp., Plainview, N.Y., was \$900 or \$3 per gram, up from a cost of \$2.35/gram in 1978. The cost of CdTe powder from Two-Six Corp., Saxonburg, Pa. was \$1.55/gram between 1980 and 1982. Thus the cost of the materials for a 5.7cm. 0.3cm thick target is only \$111.04. This target can sputter 10-15 μ m thick films on Si substrates over a 150 cm^2 area in the NJIT triode system before a groove erodes through to the stainless steel backing plate. [The groove is caused by a stainless steel mask, positioned in front of the target, which focuses the ion beam near the edge of the disc.] The target would last three times as long if the sputtering system had been originally designed for 5.7cm rather than 12.7cm diameter targets. A similar target made from polycrystalline (Hg_{0.8} Cd_{0.2})Te material, which is difficult to purchase, might cost more than \$3000.

A problem with the sputtering approach is the purity of the available starting materials. The HgTe and CdTe materials purchased for this research (prices given above) were guaranteed to be only five nines pure. With this purity, uncompensated films with impurities and carrier concentrations at best in the 10^{17} cm^{-3} range can be obtained by normal (no substrate bias) sputtering methods.

An important factor to save time and vacuum problems when doing sputtering research, is to be able to change targets without breaking the main target vacuum seal, which in the MRC 8800 requires 3 to 4 hours of labor. A new target design was tested and implemented that enabled (Hg,Cd)Te discs mounted onto special, thin stainless steel backing plates, with recessed grooves for the discs, to be mounted into the front of the main, modified MRC backing plates. The total target system required 3 stainless steel pieces per disc, but provided a low thermal impedance for the dissipated target power. The details of the design are given in reference 2.

2.1.3 Summary of Research on Chemical and Physical Charges of Sputtered Targets

Extensive research on the physical and chemical charges of sputtered targets was done under sponsorship of the Army Research Office, N.C. and reported in detail

in references 2 and 3 and summarized and updated with recent results in reference 4. For brevity, the major results of importance for thin film deposition of (Hg,Cd)Te will be just summarized here. One result from this research was that most of the pressed powder particles of HgTe and CdTe tend to fuse together forming (Hg,Cd)Te, although large cones formed on a relatively smaller number of particles greater than 30-40 microns kept their original composition of HgTe and CdTe. The dynamic changes in the distribution of Hg, Cd, and Te atom in the 1000-3000 Å thick target region (altered layer) influenced by Hg bombardment of the target surface were studied as a function of Hg sputtering gas pressure. [The targets used in this study were flat polycrystalline pieces of $(\text{Hg}_{0.8}\text{Cd}_{0.2})\text{Te}$ ingots expoxied onto pressed-powder surfaces. The distributions of Hg, Cd, and Te atoms as a function of sputtering time were obtained by the combination of slow backetching of the ingots with dilute Bromine Methanol solution at 77°K and XPS (X-ray-induced photoelectron spectroscopy) surface analysis of 10 Å depths]. One conclusion from this work was that Cd tends to be completely depleted from the target surface when the sputtering gas pressure rises above about 1.2 micron. This result explained the poor film results for Hg pressures above 1.2 microns with applied rf target power densities of 3-10 watts/cm². It was also found that the time for the target surface (first 10 Å) to reach equilibrium is less than 5 minutes--a longer time, yet unknown, is required for the pressed powder particles to fuse together to form (Hg,Cd)Te. A first order math model to describe the altered layer formation and its growth with time was developed. The model accounts for removal of the three different atoms by sputtering, the influx of Hg from the target surface, and the diffusion of atoms into the altered layer from the bulk region with constant composition. Six diffusion constants and coefficients for the model were found by curve fitting the experimental results.

2.1.4 Substrates and Their Preparation

The substrates used in this research were low-cost, high resistivity silicon (2 to 3 dollars per wafer), expensive CdTe (\$150 for each 0.9cm square, 0.2 cm thick substrate) and precleaned glass slides. Each deposition run had 10-15 substrates pieces of Si, of sufficient size for either Hall-effect or optical measurements, glass slides, and often one CdTe substrate. The glass slides were used mainly to prevent deposition onto the platen, from which films could peel off during the deposition run. Because sputtered (Hg,Cd)Te films even on glass substrates tend to grow with (111) surface orientation, as determined by X-ray diffractometry, Si substrates with (111) surface orientation were used. Most of the wafers were from two n-type batches with resistivities in the 70-90 and 1000-3000 ohm-cm range. The CdTe substrates, having little or no native oxide, required no preparation for sputtering other than to be "dusted off" with compressed Helium. The silicon substrates, however, are received from the manufacturer with a micron or two of thermally grown oxide. The oxide stripping procedure used was standard for all runs and is as follows: a) etch 20-30 minutes in hydrofluoric acid under a venting hood; b) rinse in methanol; c) rinse in trichlorethylene; d) rinse twice in isopropyl alcohol; and e) transport to intervac immersed in fresh isopropyl. For some deposition runs, the samples were left submerged overnight in the isopropyl alcohol (to allow the substrates to be prepared the day before the run) to inhibit room temperature oxide growth. It was found that this change in procedure did not affect film results.

Loading the platen (substrates holder) was a straightforward procedure, but one that required expeditiousness. The glass slides and CdTe were leisurely

placed on the perimeter and in the center, respectively, since there was concern for oxidation. The Hall effect mask was placed on the CdTe wafer glass chips were placed on the glass slides for thickness measurements. Then each silicon substrate was quickly but carefully taken out of the isopropyl bath by its edges with a pair of fine tweezers and blown dry with Helium before placed on the platen. Hall effect masks were placed on the desired silicon samples and glass chips for thickness measurements were placed in different locations. The placement of Si substrates took less than one minute. No difference in electrical properties for films placed at different times during the one minute Silicon Substrate Set-up time was observed. After roughing the intervac chamber about 15 minutes the platen was transferred to lie on the anode which was preheated to the substrate temperature used during the deposition. As little as 20 or as much as 40 minutes later the shield between the samples and the target (and plasma) was removed and the samples were exposed to the sputtered species. (The target was always sputtered for at least 15 minutes before the samples were exposed). The CdTe substrates were single crystal 111 oriented square wafers approximately 0.9 cm on a side and 0.2 cm thick. The lattice constant (5) of CdTe is 6.481 angstroms and that of HgTe is 6.462 angstroms. Assuming that the lattice constant is a linear function of X, (5) $(\text{Hg}_{0.8}\text{Cd}_{0.2})\text{Te}$ has a lattice constant of 6.464 angstroms. Silicon, by comparison, has a lattice constant of 5.43 angstroms. The closeness of CdTe's lattice constant to that of $(\text{Hg}_{0.8}\text{Cd}_{0.2})\text{Te}$ is the reason why CdTe is used as a substrate. It was assumed that the small lattice mismatch would produce better films on CdTe than those grown on silicon substrates. However, the results with both types of substrates were similar; the optimization of the sputtering and annealing parameters was based on the much more numerous Hall-effect results obtained from films on Si substrates.

2.1.5 Control of Hg Sputtering Gas Pressure

Sputtering at controlled values of Hg pressure is a difficult task which was increasingly important as thin film analysis results indicated the significant effects of Hg pressure on film properties. The Hg pressure was controlled by heating a stainless steel bottle outside the vacuum chamber (see figure II-1) and controlling the temperature of the walls and fixtures inside the vacuum system. The mercury pressure was read with CVC PiraniGauge, GP 310, calibrated for Hg and checked occasionally by a Granville Phillips Series 224 Ionization Gauge.

The highest Hg pressure used for a film deposition run was 2.0 μm . At this pressure using a 5.72 cm diameter target, and an R.F. input power of 200 watts, the deposition rate was still 20 $\text{\AA}/\text{sec}$. The Hg bottle had to be heated to 46°C, heated cathode cooling water had to be used (to prevent Hg condensation on the three targets not bombarded with Hg), and the coldest point measured inside the chamber was 7 to 9°C. The surface area of the Hg and the position of the Hg source with respect to the pumpout port appear to be factors influencing the maximum achievable Hg pressure. The highest pressure obtained in this research was only 2.5 μm ; to obtain higher pressures, the temperature of the chamber and the Hg source must be raised and the temperature and thermal gradients throughout the vacuum system monitored using many thermocouples attached to a multi-thermocouple readometer. Heating of the chamber, when not carefully controlled, has produced vacuum leaks. It was found that the Hg pressure continued to be "pinned" at 2.5 μm by cold spots inside the vacuum chamber, even though external wall temperatures were above 50°C and heated cathode cooling water was used. Both the film analysis and target research eventually made it clear that it was not desirable to have Hg pressure above 1.3-1.5 μm for film deposition runs because of the depletion of Cd from the surface of (Hg,Cd)Te targets due to the influx of Hg. Therefore research to raise the Hg sputtering pressure above 2.5 μm by heating the coldest fixtures in the vacuum system was discontinued.

2.1.6 Film Flaking Problems

The surface of good films were smooth, shiny and uniform in all respects. In some runs the films appeared pockmarked and it was discovered that this was due to flakes that fell on the films during the run. (The flakes did not adhere to the film and only shielded the film under it from growing and further - thus the pockmarks.) It was discovered (by watching the samples through the viewing port during the run) that flakes were peeling off the cooper platen and stainless steel Hall effect masks. It was decided to predeposit films on the platen and Hall-effect shields (preferably on the day before the run, to save time) at an even higher applied target power, 200W, to produce better adhesion. The predeposition on the platen and Hall effect masks was also an absolute necessity for bias sputtering since back sputtering of cooper or steel would contaminate the films. Another source of flaking that was eventually discovered was from the target shield. Flaking from all sources increased as the deposition time increased. This was attributed to the film relaxing to its lowest energy configuration by growing with a structure with the theoretically proper lattice constant. As the upper layers of the film (being less influenced by the substrates lattice constant) coalesce into the more proper configuration, the lower layers are influenced (energy-wise) into assuming that same configuration. The result of this is a strain that eventually causes peeling of the film from the metal fixture substrate. The best solution that could be found for the target shields was simply to clean off all previous films with steel wool or sand paper before each run, to minimize the film thickness reached during the run.

Strain can also be induced by temperature changes due to differences in the linear coefficient of expansion of the two materials. The rate of change of the temperature is also an important factor. A clear illustration of this took place during one particular deposition run, T91. The substrate temperature (T_S) inadvertently rose from 250°C to 265°C within three minutes. About ten minutes later, flaking from the platen was noticed. Other instances where T_S went off track but was allowed to return slowly to the proper setting produced no such effect.

The cause of considerable flaking in run T82 was attributed to the change in substrate temperature after 30 minutes to 150°C from that used in the predeposition and initial part of the deposition run (250°C).

2.1.7 Some Experimental Results

The data and results of tables 2.1 and 2.2 are a comprehensive listing for nineteen deposition runs made in 1980-81 by M. Mulligan and not previously reported to AFOSR. Table 2-1 shows values for the deposition and predeposition parameters most recently used in the research. Table 2-2 shows Hall-effect measurements results which were used to optimize deposition parameters. The Hall-effect results will be grouped and discussed detail in section 2.4, which is concerned with the electrical properties of you as-deprinted films.

TABLE 1-1 SUMMARY OF DEPOSITION PARAMETERS¹

RUN	Disc ²	STEADY STATE					START ⁴		Time of Δ to ss (min)	PREDEPOSITION ⁴			
		P _{rf} (W)	V _B (Vdc)	T _s (°C)	P _{Hg} (μm)	Time (Hr) ss+st	P _{rf} (W)	T _s (°C)		Time (min)	P _{rf} (W)	T _s (°C)	P _{Hg} (μm)
T-73	75	150	None	250	0.90	8	-	-	-	None	None	None	None
T-74	75	100	None	250	0.90	8	-	-	-	None	None	None	None
T-75	78	100	None	200	0.90	8	-	-	-	None	None	None	None
T-76	78	150	None	200	0.90	8	-	-	-	None	None	None	None
T-77	81	100	None	200	0.90	11	200	250	30	None	None	None	None
T-78	81	75	None	250	0.90	12	150	250	30	2006	200	1.0	10
T-79	87	75	None	200	0.90	10	150	250	30	2006	200	1.1	15
T-80	87	75	None	280	0.80	12	150	250	30	200	250	0.9	15
T-81	88	75	None	250	1.20	12	150	250	30	200	250	0.9	15
T-82	89	75	None	150	0.90	8	150	250	30	200	250	N.A.	15
T-83	89	75	None	250	0.60	12	150	250	30	200	250	0.7	15
T-84	90	75	14	250	0.90	12	150	250	30	200	250	0.8	15
T-85	91	75	28	250	0.90	12	150	250	30	200	250	0.9	15
T-86	91	75	14	250	1.20	7.5	150	250	30	200	250	1.0	15
T-87	88	75	14	250	1.20	11.5	150	250	30	200	250	1-1.2	15
T-88	92	75	18	250	1.20	11.5	150	250	30	300	250	1-1.3	15
T-89	92	75	18	250	1.20	12	150	250	30	200	250	1.2	15
T-90	93	<u>5</u>	14	250	1.20	12	1600 ⁵	250	30	9.6 ⁵	250	1.2	15
T-91	93	75	7	250	0.90	9	150	250	30	200	250	0.9	15
T-92	94	75	14	250	1.20	12	150	250	30	200	250	1.2	15
T-93	94	75	14	250	1.40	12	150	250	30	200	250	1.4	15
T-94	95	75	10	200	0.95	9	150	250	30	200	250	0.9	15

1. All targets made from a pressed powder physical mixture of HgTe and CdTe with $x = 0.20$
2. Targets were usually used twice for a total sputtering time of 24 hours.
4. DC bias used for predeposition was the same as for the run.
5. DC sputtering with a voltage of 100V (1600V for predeposition) and a current of 6 mA.
6. Only platen, not Hall effect masks, predeposited.

TABLE 1-2 Summary of Electrical Results

RUN	ROOM TEMP.		AVERAGE HALL VALUES		High Value In Run (87°K)	Number of Samples in Average	COMMENTS
	Mobility (cm ² /vs)	Carr. Conc. Range 4 (10 ¹⁶ cm ⁻³)	Mobility (cm ² /vs)	Carr. Conc. Range 4 (10 ¹⁶ cm ⁻³)			
T73	1610	8.2/15	1760	6.7/12	2180	6	Slightly pockmarked
T74	925	52/97	1340	52/97	1610	7	No pockmarks
T75	1420	35/65	2140	36/67	540	6	Very pockmarked
T76	1080	46/86	1490	47/87	1760	5	Moderately pockmarked
T77	1560	46/85	2310	49/91	2960	8	Flaking ended run
T78	1780	30/56	2930	32/60	4310	8	No flaking
T79	910	61/110	1280	64/120	1430	6	Flaking ended run--target shield & HZ mask
T80	1240	58/110	1770	61/110	2090	6	No flaking
T81	1670	37/68	2330	40/74	2750	6	No flaking
T82	916	52/97	1390	57/100	1870	5	Flaking ended run (from platen)
T83	1860	61/110	2810	63/120	3420	5	No flaking
T84	4610	3.0/5.5	4330	2.1/3.8	7400 ¹	6	No flaking
T85	569	6.1/11-P	135	21/39-P	--	4	No flaking
T86	1760	5.6/10	3670	4.4/8.2	2960	6	Flaking ended run
T87	2930	5.9/11	5150	3.4/6.3	6080	7	Flaking ended run
T88	1470	2.8/5.3	2300	1.8/3.4	2860	3	Flaking ended run
T89	905	2.3/4.3-P	439	0.66/1.2-P	--	3	No flaking
T90	1270	4.1/7.6	1430	1.8/3.4	1850	3	No flaking
T91	910	17/32	1340	17/32	--	3	Flaking ended run ²
T92	250	3	188	2	445	1	No flaking
T93	900	3/7	1226	2/2	1253	3	No flaking
T94	1075	6/20	1633	4/14	2321	3	No flaking

1. All samples in this run had highest mobility at an intermediate temperature = 175°K. Average mobility at that temperature was 6020.

2. After T₉ drifted to 2650C, air cooling to anode was applied and T₉ dropped quickly (3 min) to 250°C. Flaking noticed 10 minutes later.

3. P type films.

4. Based on thickness uncertainty of ±30%.

2.2 STRUCTURAL PROPERTIES OF SPUTTERED FILMS

The structural properties of triode-sputtered (Hg,Cd)Te films on silicon substrates were studied by X-ray diffraction. The broad X-ray scans were generated for diffraction angles from 0 to 160° on GE X-ray equipment (GE11GN1). Typical X-ray diffractometry scans showing the high amount of 100 per cent (111) orientation of some films on Si substrates with (111) surface orientation, with correspondingly good conductivity and optical absorption properties, were shown on page 24 of ref. 5 and published.^(6,7) Also shown were scans for poorly oriented films, with 200, 311, 331, and 422 orientations. Many diffraction measurements were done at two different magnifications in order to see the entire height of the major peaks and also to detect the presence of short peaks representing orientations other than the preferred orientation. A typical trace⁽¹¹⁾ is shown in figure 2.1. Results, such as shown in figure 2.2, showed that the (444) peak had a half width of only 0.8° in highly oriented films.^(7,11) This width is the same as that reported for (Hg,Cd)Te films made by LPE that were thought to be single crystal.⁽⁸⁾

Further study of the structural properties of triode-sputtered (Hg,Cd)Te films on (111) oriented Si substrates was done at Martin Marietta.⁽⁹⁾ Two film samples, T81-S12 and T52-S9, that yielded above-average electron mobility results were measured by X-ray beam, rocking curve analysis and Laue diffraction pattern analysis. Broad diffractometer scans of the films were first taken and the results were identical to those obtained at NJIT.^(5,6,7,11) Rocking curve measurements were then made on the Si(111) and (Hg,Cd)Te(111) peaks, which occur at nearby diffraction angles, 24° and 28° . The rocking curve measurement is done by leaving the X-ray source and detector fixed at the angle for the specified peak but rotating the sample about the axis which is normal to the plane of the source, sample and detector. The curves can be used to indicate the degree of orientation of the (111) crystallites. The rocking curves for both (Hg,Cd)Te samples had widths of 4° compared with the 0.4° (instrument limited) width of the Si single crystal substrate. This result indicated that Martin Marietta's X-ray topography scan technique, to determine the crystallite size, could not be successful on the T81 and T52 films. This is because the primary beam in the X-ray topography camera at Martin Marietta is collimated to within six seconds of arc, so that only a extremely small portion of the 4° peak would be sensed by the camera. [X-ray topography was tried on the films and the crystallinities were not observed.] To use X-ray topography, films with a higher degree of orientation of the (111) crystallinities would have to be selected (or prepared). As suggested by Dr. Beck⁽⁹⁾, the rocking curve measurement technique should be implemented at NJIT and the results used to select films for X-ray topography. Rocking curve measurements could also be used to optimize the film preparation parameters.

The degree of preferred (111) orientation of some triode-sputtered films as a function of sputtering parameters was studied⁽¹¹⁾. The results are given in table 2.1. One notes that in some runs the degree of preferred orientation was different for films on different pieces of substrates. From these results and others, it can be concluded that the degree of orientation was usually nearly 100% for substrate temperatures of 250°C , independent of Hg pressure, deposition rate, and film x-value; for substrate temperatures of 300°C and $150\text{--}200^\circ\text{C}$, poorer oriented films were obtained. The value of the preferred orientation, a figure of merit,⁽²²⁾ was calculated from the powder intensity of the (111) line ($I_{111}=100$), the sum of all intensities other than (111) and parallel lines (I_{other}), the sum of all intensities for the starting material excluding the (111) and

parallel line intensities (I_7), and the intensity of the (111) line of the sample. (I_{111}). (For X values of 0.20 and 0.25, the I_7 values were calculated as 342 and 336 respectively). The equation for the % preferred orientation along the (111), PPO is:

$$PPO = 1 - \frac{I_3 I_6}{I_7 I_{111}} \times 100 \quad (1)$$

Diffraction data for both CdTe and HgTe powders, constituting the starting material for the targets, were taken at NJIT and reported (23), as the values in the ASTM card files were found to be old values in error.

Change in preferred orientation with annealing in Hg atmosphere was briefly studied(11). Sample T52-S17 had no noticeable change in the 100% preferred orientation after annealing. Sample T74-S15 showed a slight increase from 91.5 to 93.2% after annealing. (The annealing conditions for these samples are given in section 2.5.2).

Determination of the size of the crystallites in the films was also attempted by chemical etching techniques. The samples were chemically polished and etched to bring out the grain boundaries before SEM photographs were taken. The polish and etch mixture consisted of a solution (by volume) of 15 parts concentrated nitric acid, 15 parts distilled water, 1 part concentrated hydrochloric acid, and one part of 5% bromine in 95% methanol. The etching was done for about 10 seconds for each sample prior to silver pasting them onto aluminum mounts for insertion into the SEM. The results for the samples studied indicated that the grain size was at least 1 micron. Etched vertical lines as shown in these samples (24,25) were not observed when the same chemical etching treatment was applied to annealed film samples, indicating that the grain sizes of the annealed films were much greater. Direct observation of the crystallites by some technique, such as X-ray topography, is required before a firm conclusion on the effect of annealing on grain size can be drawn.

Table 2.1

No	MM	Target 'y'	Dg Press (mm)	Cathode Volt. (volt.)	Substrate Temp. (°C)	Forward Power (Watts)	Deposition Rate (µm/hr)	Film 'y'	Prof. Orientation Max Min
1	749	0.25	1.3	2200	300	200	1.0	0.25 ± 0.01	(88) (95)
2	750	0.25	1.4	2200	300	200	-	-	(85) (87)
3	751	0.10	1.2	1500	250	200	1.0	-	100 100
4	752	0.10	1.4	1500	250	200	1.0	-	100 100
5	753	0.23	1.25	2100	250	200	-	-	(813) (820)
6	754	0.23	1.3	2100	300	200	-	-	94 94
7	755	0.10	1.3	2250	300	200	-	-	96 96
8	764	0.25	1.2	1500	250	200	1.0	0.23 ± 0.01	(816) (87)
9	769	0.27	0.7	1000	250	150	0.70	0.26 ± 0.01	(88) (92)
10	773	0.20	0.9	1750	250	150	-	-	(88) (93)
11	774	0.20	0.9	1450	250	100	0.50	0.23 ± 0.01	(814) (82)
								0.21 ± 0.01	93 73

Note: Sample numbers are shown in parenthesis.

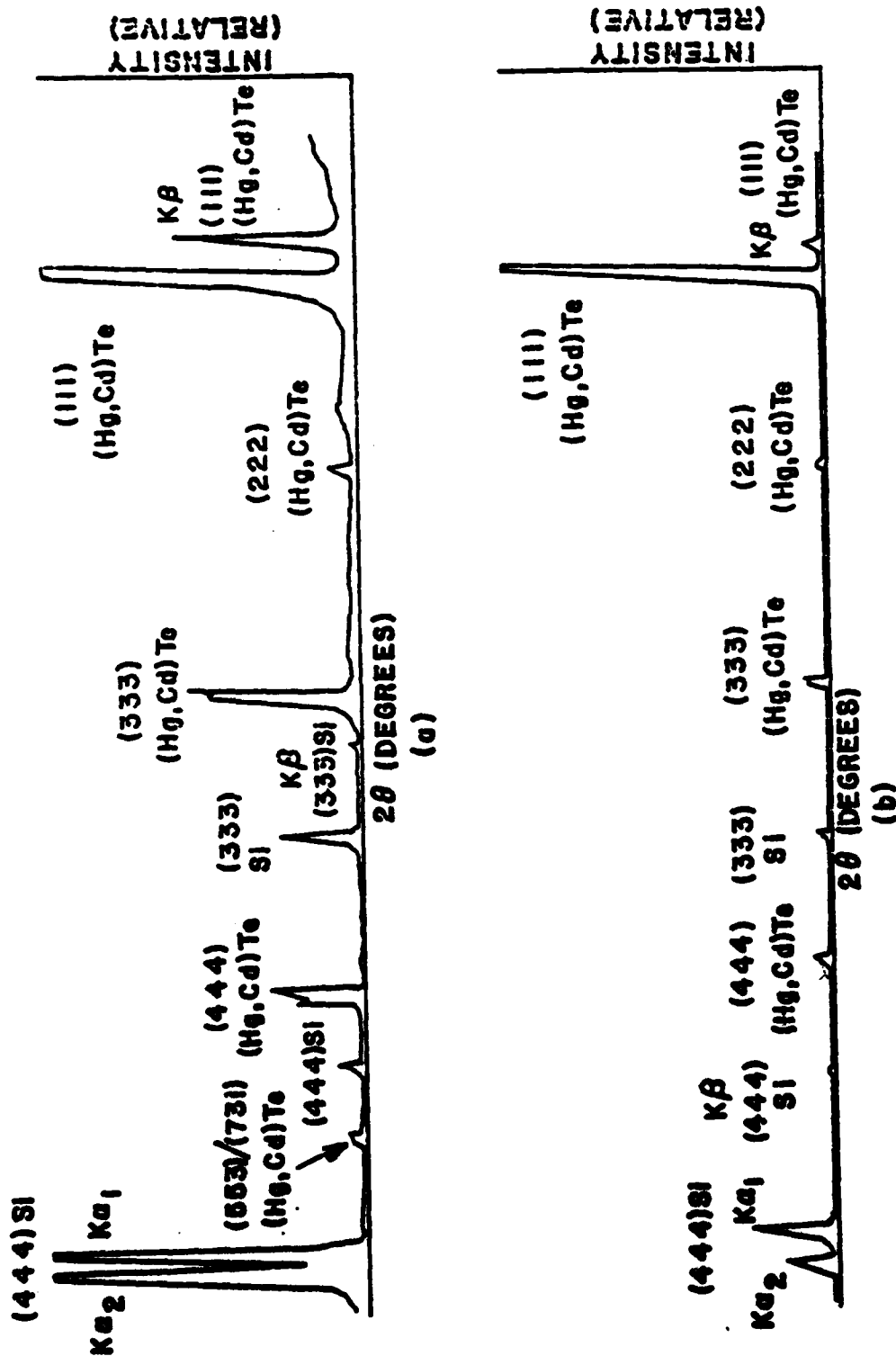


Figure 2.1: X-ray diffraction patterns of a typical film at two different values of gain

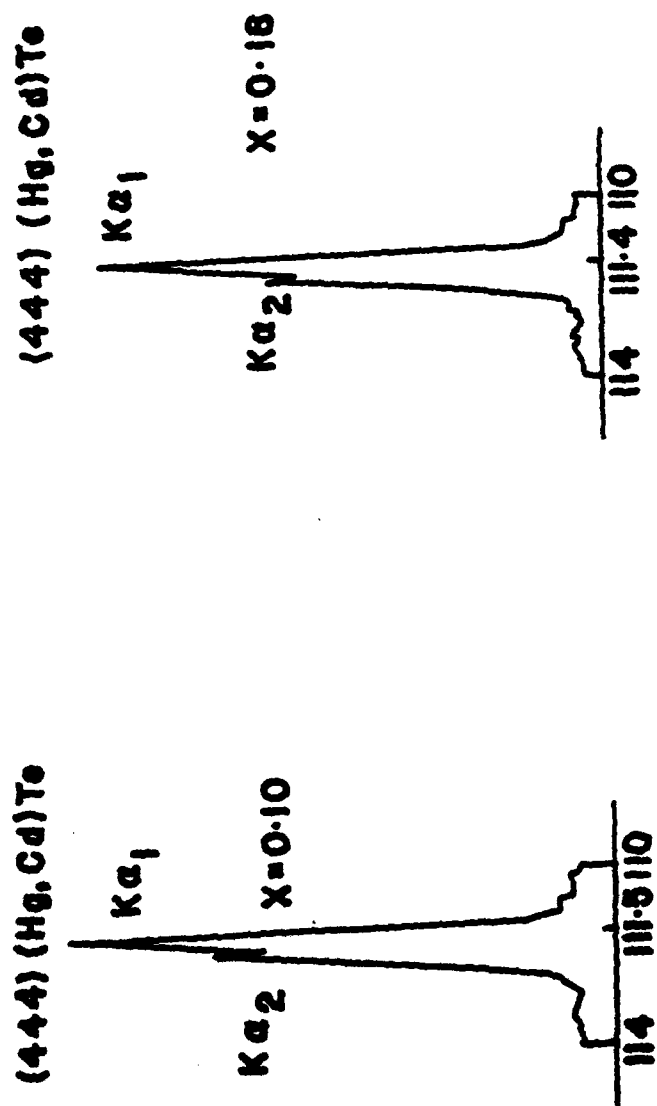


Figure 3.2: Typical (444) peaks used for calculating lattice constants of thin films.

2.3 DETERMINATION OF FILM COMPOSITION BY ELECTRON MICROPROBE AND OPTICAL ABSORPTION MEASUREMENTS

The compositions of six sputtered films with different X compositional values, were determined by two methods: relatively expensive, wavelength dispersive electron microprobe analysis and optical absorption curves obtained from IR transmission measurements. The dual measurement approach was necessary to confirm the measurement accuracy of each method; it was useful in that it ultimately showed that as-deposited films were p-type even though the Hall coefficients were negative. Optical absorption curves were also calculated theoretically, accounting for the possible Burstein Moss shift due to filling of the conduction band states by free-carrier electrons, and compared with the absorption curves found by experiment. The results of the two compositional measurements showed that the X value of triode-sputtered $(\text{Hg}_{1-x}\text{Cd}_x)\text{Te}$ films usually matched that of the target in the 0.18-0.25, within the accuracy of the measurements which was less than four percent.

2.3.1 Theory and Procedure for Optical Absorption Curve Calculations

Optical absorption in narrow semiconductors can be calculated by the k.p theory which uses time-independent perturbation theory for solving the energy eigenvalue equation. The k.p theory was successfully applied by Kane⁽¹⁰⁾ to calculate the energy bands in InSb. The method was extended to calculate the optical absorption in other narrow gap semiconductors, particularly $(\text{Hg},\text{Cd})\text{Te}$. The theory of optical absorption in $(\text{Hg},\text{Cd})\text{Te}$ is reviewed in detail in reference 11 and will be briefly discussed here.

The total absorption coefficient, α , in $(\text{Hg},\text{Cd})\text{Te}$ can be written as

$$\alpha = \text{BM}_{hh} \alpha_{hh} + \text{BM}_{lh} \alpha_{lh} \quad (1)$$

where BM_{hh} and BM_{lh} are the Burstein-Moss factors for the heavy hole (hh) and light hole (lh) valence bands. The BM factor given in equation 2, can be calculated for different incident angular frequencies, ω , if the energy gap, E_g , and Fermi level, F , are known.

$$\text{BM} = \frac{1 - \exp\left(\frac{-\hbar\omega}{kt}\right)}{\left[1 + \exp\left(\frac{-\hbar\omega - E_g + 2F}{2kt}\right)\right] \left[1 + \exp\left(\frac{\hbar\omega + E_g - 2F}{2kt}\right)\right]} \quad (2)$$

The Fermi energy, measured with respect to the valence band edge, will be a function of temperature and carrier concentrations and can exceed the bandgap

energy ($F > E_g$) for degenerate n-type material. In the degenerate situation, the BM factor is less than 1, Q_v decreases, and there is a shift of the absorption edge to higher incident energies as shown in figure 3.1. The Burstein-Moss shift is only significant in n-type films because of the sharp curvature of the conduction band compared with the valence band. For p-type films, the Fermi level goes only slightly below the valence band even for very large hole concentrations, i.e. greater than 10^{18}cm^{-3} . The Fermi level was calculated for a given free electron concentration by first calculating the Fermi-Dirac integral⁽¹²⁾ given in equation 3 below.

$$F(\epsilon, \eta) = \frac{2}{\sqrt{\pi}} \int_0^\infty \frac{x^4 \left(1 + \frac{x}{\epsilon}\right)^4 \left(1 + \frac{2x}{\epsilon}\right)}{1 + \exp(x - \eta)} dx$$

$$\text{where } F(\epsilon, \eta) = \frac{n}{N_C}$$

$$N_C = 2 \left(\frac{3E_g kT}{8\pi P^2} \right)^{3/2} \quad (3)$$

$$\eta = \frac{E_g}{kT}$$

$$\epsilon = \frac{F - E_g}{kT}$$

$$\text{and } x = \frac{E}{kT} \text{ where } E \text{ is energy above conduction band minimum.}$$

The quantities n, η, ϵ , and x are the free electron concentration, reduced band-gap energy, reduced Fermi energy and reduced energy above the conduction band minimum respectively. From η and $F(\epsilon, \eta)$, a corresponding value of ϵ can be looked up in Bebb and Ratliffe⁽¹³⁾ and the Fermi energy found. Fortran programs were written, Appendix A, to calculate the absorption coefficient at different incident energies for mercury cadmium telluride films of known band gap energy for a) non-degenerate p-type films and b) n-type films with given free electron concentrations. The programs used the following constants^(14,15,16): the matrix element between valence and conduction bands, $8.5 \times 10^{-8} \text{eV-cm}$; m_{hh} , the effective heavy hole mass, $0.4m_0$; and ϵ_∞ , the dielectric constant, 12. Curves, such as figure 3.1 were calculated⁽¹¹⁾ for compositions $x=0.18, 0.20, 0.23$, and 0.25 for free electron concentrations of $10^{16}, 10^{17}$, and 10^{18}cm^{-3} . The curves in fig. 3.2 were computed for intrinsic material. The values of the bandgap energy for different values of the compositional parameter, x , were obtained from the empirical relation of J. Schmit and E. Stelzer:⁽¹⁷⁾

$$E_g(x, T) = 1.59x - 0.25 + 5.233(10^{-7})T(1 - 2.08x) + 3.27x^3 \quad (4)$$

2.3.2 Experimental Procedure for Optical Measurements

Transmittance of samples was measured on a Perkin-Elmer Model 457 dual-beam infrared spectrophotometer. The samples were placed in the sample beam aperture and a plain substrate was inserted in the reference beam aperture. The plain substrate used as optical reference was of the same specifications as the sample substrate. Not only did the optical reference substrate attenuate the reference beam to permit the transmittance measurements of highly absorbing (Hg,Cd)Te films but it also cancelled the effect of sample substrate absorption. The resultant data, therefore, represented the transmittance through the (Hg,Cd)Te film only. In case of thick substrates, the measurements were made in slow scan mode and frequent checks (as recommended by the manufacturer of the instrument) were made at a number of different wavelength to ensure accuracy of data.

Sample thickness t and transmittance ratio $\frac{I}{I_0}$ at several different wavelengths on the optical scan were used to calculate the optical absorption coefficients α by the formula:

$$\alpha = t^{-1} \ln (I/I_0) \quad (5)$$

The reflectance of the samples was ignored in calculating the absorption constants because a) the refractive indices of the plain silicon substrates were approximately the same as those of the film samples and b) the sample surfaces were as mirrorlike in appearance as the plain substrates in the reference beam. The reflectance of Si is calculated as 0.299 for a refractive index of 3.42 (obtained from the accepted dielectric constant of 11.7). The reflectance of (Hg,Cd)Te is 0.304, using refractive index of 2.46 corresponding to a dielectric constant value of 12. Thus the difference in air-reflectance of the two semiconductors is only 0.005, which has no effect on the measurement.

2.3.3 Optical Measurement Results

Figures 3.3, 3.4, and 3.5 show absorption curves calculated from transmission data for five samples from runs T49, T67, T69, and T74. The available electron microprobe data for these samples were used to calculate the compositional parameter X and bandgap (from equation 4 of section 2.3.1). From the value of the bandgap, the theoretical absorption curves were plotted. The closest fit to the experimental data was obtained only by assuming the film samples were non-degenerate p-type. This agreed with the fact that the samples were all as-deposited, unannealed, films which were found from Hall-effect measurements to have either p-type or mixed conduction. Therefore the optical behavior of the films was in agreement with the electrical measurements.

Although the absorption edges for the samples are not quite as sharp as predicted by the optical absorption theory which assumes perfect homogeneity, the experimental absorption edges are sharp enough to indicate good compositional uniformity in the area of the film exposed to the infrared beam. As previously reported (7,25) the sharpness of the absorption edge compares favorably with data reported by others. (24)

The compositional uniformity of triode-sputtered films was further investigated through microprobe analysis by determining compositions at a number of points on the film surfaces of samples of various shapes about 4mm^2 or more in area and the compositions were found to be the same.

23

The 'x' values of five samples were estimated through the experimental optical data by two different methods described as follows: (i) The experimental absorption curves were compared with the closely spaced (interval $\Delta x = 0.002$) theoretical absorption curves for intrinsic material with 'x' values in the neighborhood of the expected composition; (ii) the incident energies at $\alpha = 1000\text{cm}^{-1}$ from the absorption curves were used as the bandgap energies E_g and the corresponding 'x' values were found from Schmidt and Stelzer equation.⁽¹²⁾ The use of these two procedures for estimating the 'x' values is shown in fig. 3.6. It should be pointed out that optical measurements require a sample with about 1 square cm area, while Hall effect samples are smaller in size and have different shape. The optical samples, when subjected to annealing, tended to peel and produce pinholes. It was therefore not possible to make optical measurements on annealed samples, which were known to be n type. The peeling problem is one that can be solved with time and optical absorption measurements of n-type films should reveal a Burstein-Moss shift of the absorption edge.

2.3.4 Procedure for Determining Film Composition by Microprobe Analysis

The composition of films were measured very accurately by Wavelength Dispersive Electroprobe Microanalysis (WDX)⁽¹⁸⁾ at Structure Probe Inc. using standards of known composition. WDX spectroscopy is considered a more accurate method than the more commonly used energy dispersive x-ray (EDX) spectroscopy.^(19,11) Both methods use an incident electron beam on the standard and the specimen to be measured. Energy dispersive x-ray analysis (EDX) uses an x-ray detector whose output pulse amplitudes are proportional to the energy of photons emitted from a standard and the samples being measured. The output pulses are then processed in a multi-channel analyzer for determining the quantities of the various elements in the sample. On the other hand, wavelength dispersive x-ray analysis (WDX) uses crystal spectrometers (preset at known Bragg angles for the elements being measured) to measure the wavelength and the intensities of x-rays from the samples and the standards after the x-rays are scattered from a crystal built into the spectrometer.

The accuracy of the WDX techniques is due to three reasons:

- 1) WDX eliminates the possible error due to any extraneous high-energy particles in the system because it relies on detection of x-ray wavelengths rather than the measurements of energy scattered from the sample being analyzed:
- 2) WDX detects and measures only one element at a time thereby ensuring better accuracy;
- 3) Since WDX electron microprobe is especially designed for quantitative work rather than producing high-resolution pictures, the current source of electron microprobe is much more stable than the current source of an SEM used in EDX analysis.

The accuracy of the WDX is dependent on the accuracy of the standards. The best available standards were obtained by NJIT from Joe Schmidt of the Honeywell Research Center in Bloomington, MN. These standards were prepared by solidification of molten mixtures of weighed quantities of Hg, Cd and Te. The precision of the density measurement of these standards was within $\pm 0.01\%$. The composition was then determined by using Wooley and Ray's composition vs. density curves^(20,21). Because of the inclusion of Hg droplets in the standard ingots, the accuracy of the composition of these standards was estimated to be within ± 0.7 of a mole percent. In any case, according to Schmitt, it is not worse than ± 1.0 mole percent. The composition of the standards ranged from $x = 0.10$ to $x = 0.50$. Their values were verified at Structure Probe by using HgTe, CdTe, and Te standards.

25

The experimental WDX procedure used at Structure Probe Inc. was as follows: The samples were epoxied on a metallic mount with a highly polished surface. The standards were also arranged in a similar manner. The samples were inserted into MS-46 electron probe microanalyzer of CAMECA Instruments, Inc. and the column was pumped down to less than 1×10^{-4} torr for analysis. The vacuum within the spectrometer itself was less than 1×10^{-2} torr. To decrease the diffusion of Hg away from the electron beam the samples were cooled using an anti-contamination cold finger to -100°C during the analysis. The analysis was done at a beam voltage of 20 Kv and a specimen current of 100 nA. The analysis of the samples was done in two steps. First, intensity readings for all three elements were taken on the standards, then the sample, and again on the standards. In order to ensure the independence of the composition measurements from surface morphology, three regions were taken per sample, and three readings were taken per region. This approach also ensured good statistics as well as compensation for current loss during analysis. Atomic percentages of the elements were calculated from the intensity readings by a computer program which took in account the necessary corrections of data for atomic number, absorption and fluorescent effects during analysis.

2.3.5 WDX Microprobe Results

The atomic percents for Cd, Te, and Hg found by WDX electron microanalysis of six sputtered thin film samples are given in table 3.1. Five different methods were used to calculate the compositional parameter x from the atomic percentages⁽¹¹⁾. These methods are shown in appendix B. The results of these calculation methods are shown in table 3.2. Method IV was selected as the procedure for calculating the x -values of the films for three reasons: First, it yielded results for the the (Hg,Cd)Te standards, whose compositions were determined by precision density measurements at Honeywell,⁽²⁰⁾ that were in closest agreement with the Honeywell values; second, it is the widely accepted as the standard procedure by industrial researchers; and finally because the results agreed most closely with the " x value" of the sputtered target based on the relative percent of CdTe powder particles and the results obtained from the optical measurements. In order to estimate the accuracy of the WDX measurement at the S.P. Inc., the five Honeywell standards with x values of 0.217, 0.212, 0.320, 0.245, and 0.165 were measured using pure HgTe, pure CdTe and pure Te standards and calculated by procedure (iv) as 0.209, 0.216, 0.323, 0.247 and 0.159 respectively. The discrepancy between the two sets of value ranges from a minimum of $\pm 0.82\%$ to a maximum of $\pm 3.69\%$.

2.3.6 Discussion of Compositional Results Obtained by Optical and WDX Measurements

The bandgap energies were calculated from the compositional parameter x found from WDX measurements, using equation (4) of section 2.3.1. These values are given in table 3.3 and compared with the bandgap energies calculated from the optical absorption data, using the bandgap value for $\alpha = 1000 \text{ cm}^{-1}$ (method ii in section 2.3.3). The two methods of finding the bandgap from absorption data give nearly identical values as can be seen by comparing the composition values calculated from the Schmidt and Stelzer equation using the bandgaps found from the two optical methods. These values are given in the first two columns for composition in table 3.4. From table 3.3, it can be seen that with the exception of sample T69-S7, sputtered using an $x=0.27$ target, the bandgap energies are very close and certainly within the $\pm 5\%$ accuracy of the WDX measurement. The source of discrepancy for T69-S7 may either be a slight error in the measurement of thickness and/or the electron microprobe measurement having an error of more than $\pm 5\%$ because of the sample ' x ' value being more distant from those of the standards

25

($x=0$ and $x=1$) than for the rest of the samples. Table 3.4 compares the x values calculated from the absorption data and WDX microprobe measurements with the x value of the target. [The reader is reminded that the target x value is the mole percent of CdTe particles in the powder mixture of HgTe and CdTe and that research indicated that most of the particles fuse together to form (Hg,Cd)Te. The uncertainty in the target x value is due to the weighing and mixing procedures in fabricating the target.] With the exception of samples T74-S1 and T64-S16, the x values for all samples were within the possible total error due to the inaccuracies of the microprobe measurement and target preparation procedures. The compositional values for these samples were only 0.006 and 0.005 outside the possible range of error. It can also be said from this limited data that there may be a tendency for targets with lower x values (e.g. $x=0.2$) to produce films, under the sputtering conditions for these samples, with x slightly greater than 0.2 while films made with higher x values (e.g. $x=0.25$) may be depleted of Cd. More sputtering experiments and more accurate compositional measurements are required to see if this tendency is real.

From the results in tables 3.3 and 3.4, it can be concluded that the composition of sputtered films in the compositional parameter range of 0.2 to 0.27 (and most probably over a wider range of 0.18 to 0.3,) can be controlled to match the target x value. [The results shown were the only results obtained due to the cost of the WDX measurements, about \$150 per sample.] Thus it has been shown that by simply changing the relative volume of the CdTe and HgTe particles the film composition can be shifted to any desired x value. From the results in tables 3.3 and 3.4, it can also be concluded that optical transmission measurements, which are much less expensive and faster than the WDX measurements, can be used to accurately measure the film x value.

Table 3.1: Atomic Percents Found by Electron Microanalysis*

No.	Sample	Tellurium	Cadmium	Mercury
1.	T-74-S15 (Annealed)	52.48	8.71	38.81
2.	T-74-S1	55.47	7.07	37.45
3.	T-49-S7	54.35	9.29	36.36
4.	T-64-S16	52.23	9.83	37.94
5.	T-67-S4	53.93	7.02	39.05
6.	T-49-S7	53.59	10.35	36.06

*The measurement technique permits accuracy within $\pm 5\%$.
However, the precision (repeatability) of the equipment
used is within $\pm 0.1\%$

TABLE 3.2: COMPOSITION 'X' VALUES CALCULATED FROM ATOMIC PERCENTS IN TABLE 7.1

Sample Method	1 <u>T74-S15</u> <u>(0.20)</u>	2 <u>T74-S1</u> <u>(0.20)</u>	3 <u>T49-S7</u> <u>(0.25)</u>	4 <u>T64-S16</u> <u>(0.25)</u>	5 <u>T67-S4</u> <u>(0.20)</u>	6 <u>T69-S7</u> <u>(0.27)</u>
(i)	0.17	0.14	0.19	0.20	0.14	0.21
(ii)	0.20	0.20	0.23	0.22	0.18	0.24
(iii)	0.17	0.13	0.17	0.19	0.13	0.19
(iv)	0.21	0.23	0.25	0.23	0.20	0.26
(v)	0.18	0.16	0.20	0.21	0.15	0.22

Values in parantheses represent target compositions.

Table 3.3: Bandgap energies of thin film samples

No.	Sample	Bandgap Energy (ev)	
		calculated from microprobe measured λ_g	optical estimate at $\alpha=1000 \text{ cm}^{-1}$
1.	T74-S15	0.180	0.175
2.	T74-S1	0.197	0.191
3.	T49-S7	0.226	0.210
4.	T64-S16	0.203	-
5.	T67-S4	0.166	0.167
6.	T69-S7	0.241	0.218

Table 3.4: Compositions 'x' as measured by different methods

No.	Sample	Composition 'x'			
		optical(i)	optical(ii)	Electron Microprobe	Target
1.	T74-S15-A	0.208	0.209	0.21±0.01	0.200±0.004
2.	T74-S1	0.219	0.221	0.22±0.01	0.200±0.004
3.	T49-S7	0.238	0.238	0.24±0.01	0.250±0.005
4.	T64-S16	-	-	0.23±0.01	0.250±0.005
5.	T67-S4	0.200	0.204	0.20±0.01	0.200±0.004
6.	T69-S7	0.239	0.242	0.26±0.01	0.270±0.006

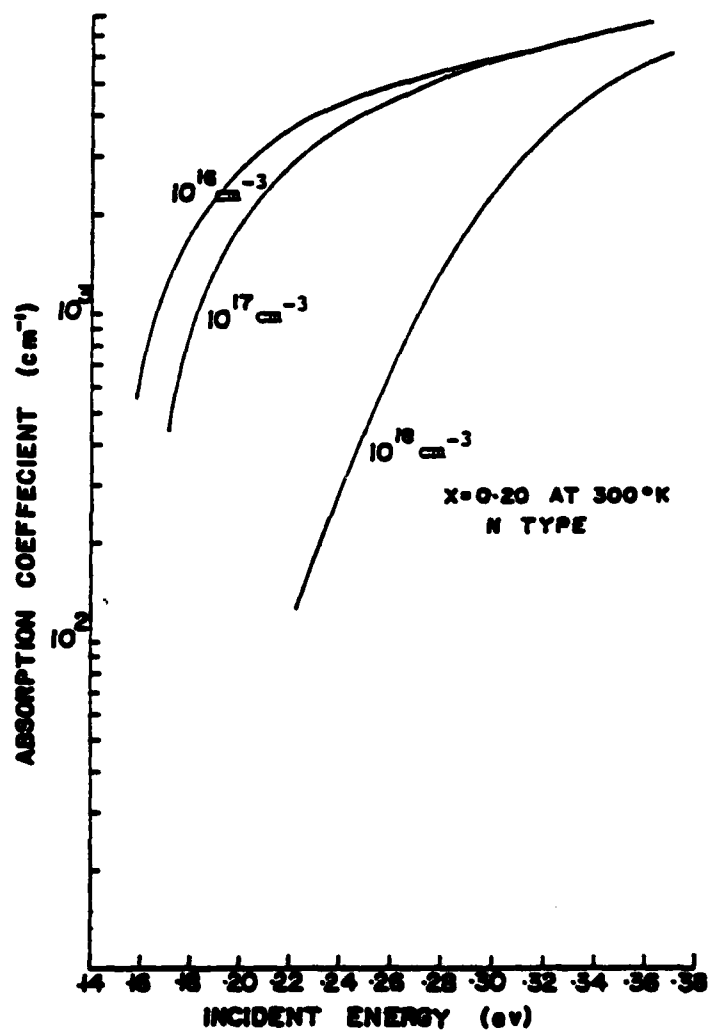


Fig. 3.1: Calculated Optical Absorption Curves showing Burstein-Moss shift for n-type $\text{Hg}_{0.80}\text{Cd}_{0.20}\text{Te}$ with Electron Concentrations of 10^{16} , 10^{17} and 10^{18} cm^{-3} .

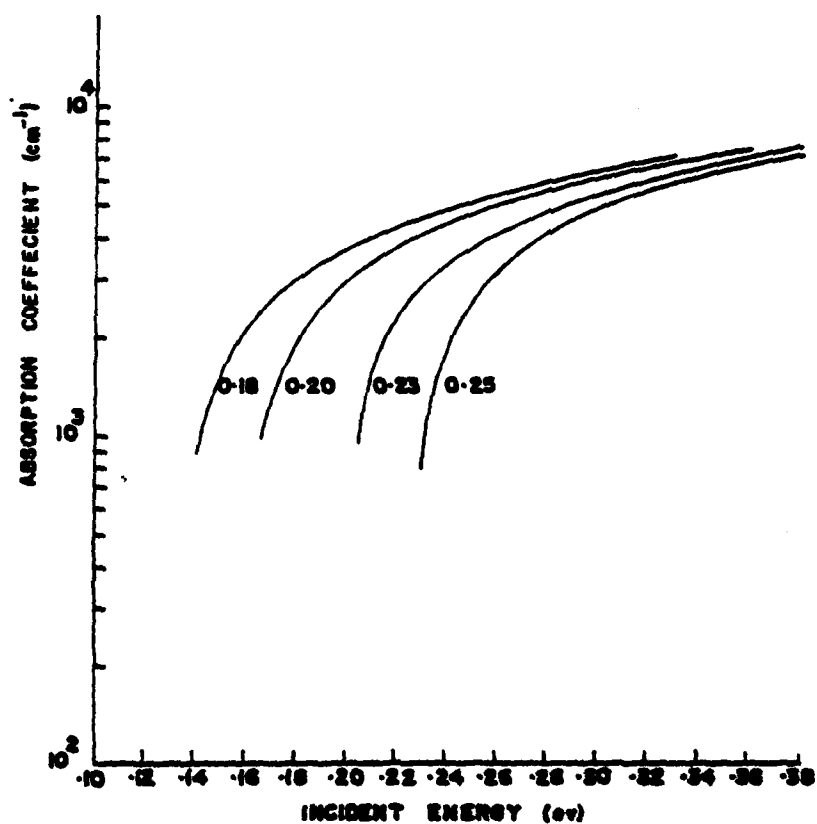


Fig. 3.2: Calculated Optical Absorption Curves for Intrinsic $\text{Hg}_{1-x}\text{Cd}_x\text{Te}$ with $x = 0.18, 0.20, 0.23$ and 0.25 .

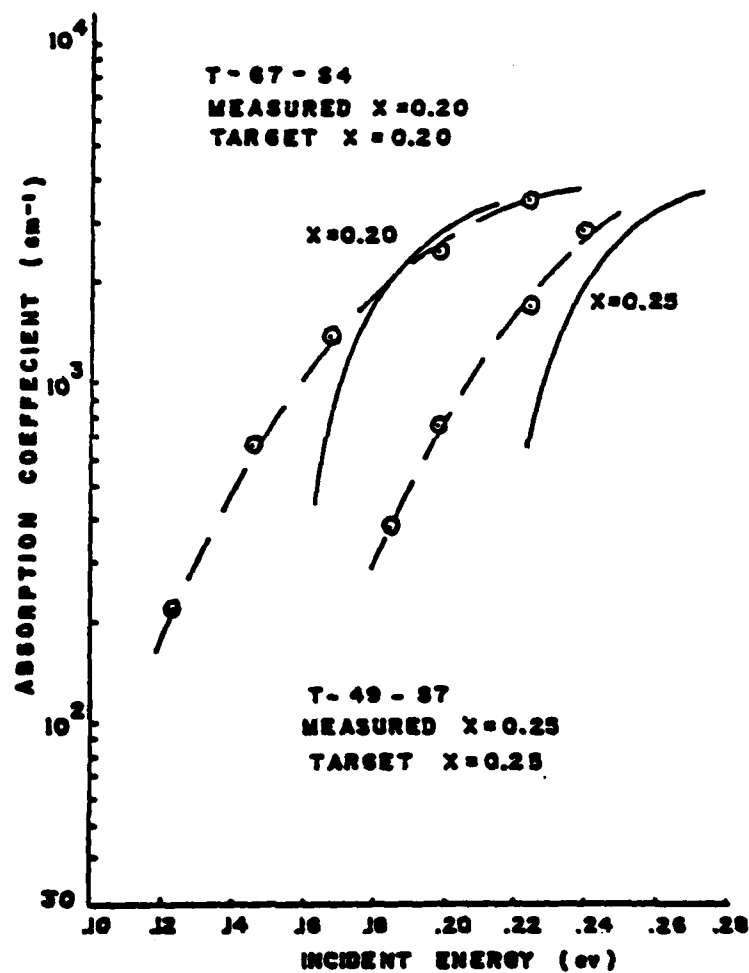


Fig. 1.3: Comparison of Theoretical Absorption Curves (Solid Curves) for $Hg_{1-x}Cd_xTe$ with $X = 0.20$ and 0.25 as Measured by Electron Microprobe and Experimental Absorption Data (circles) for Samples T67-84 and T49-87 respectively.

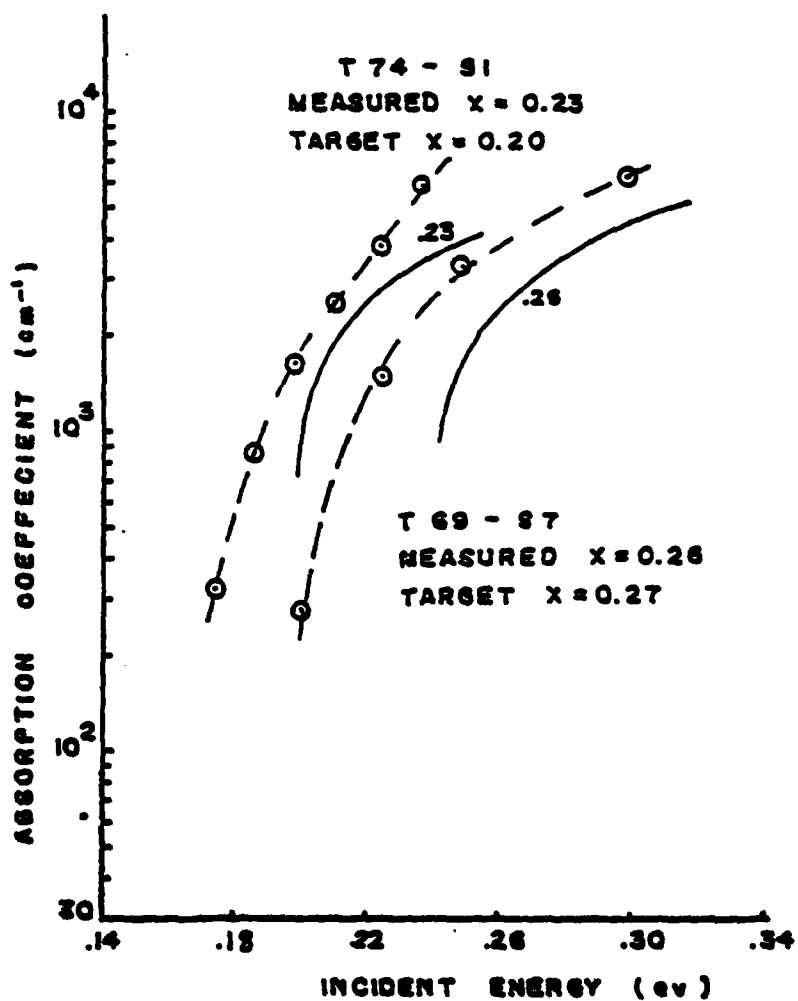


Fig. 3.4: Comparison of Theoretical Absorption Curves (solid curves) for $X = 0.23$ and 0.26 as measured by Electron Microprobe and Experimental Absorption Data (circles) for Samples T74-S1 and T69-S7.

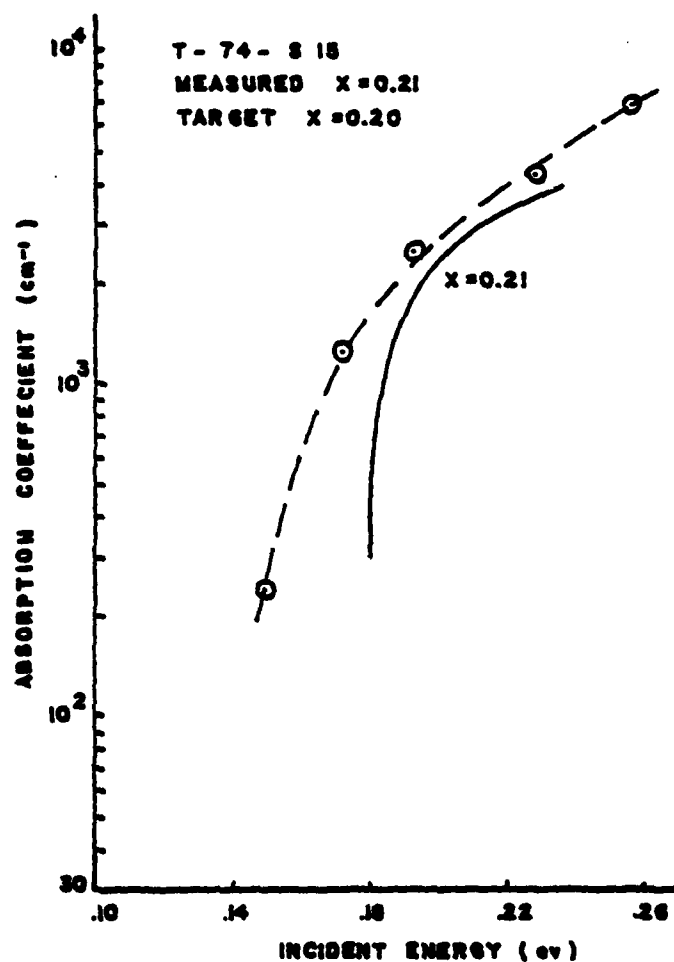


Fig. 3.5: Comparison of Theoretical Absorption Curves (solid curves) for $x = 0.21$ as measured by Electron Microprobe and Experimental Absorption Data (circles) for sample T74-815.

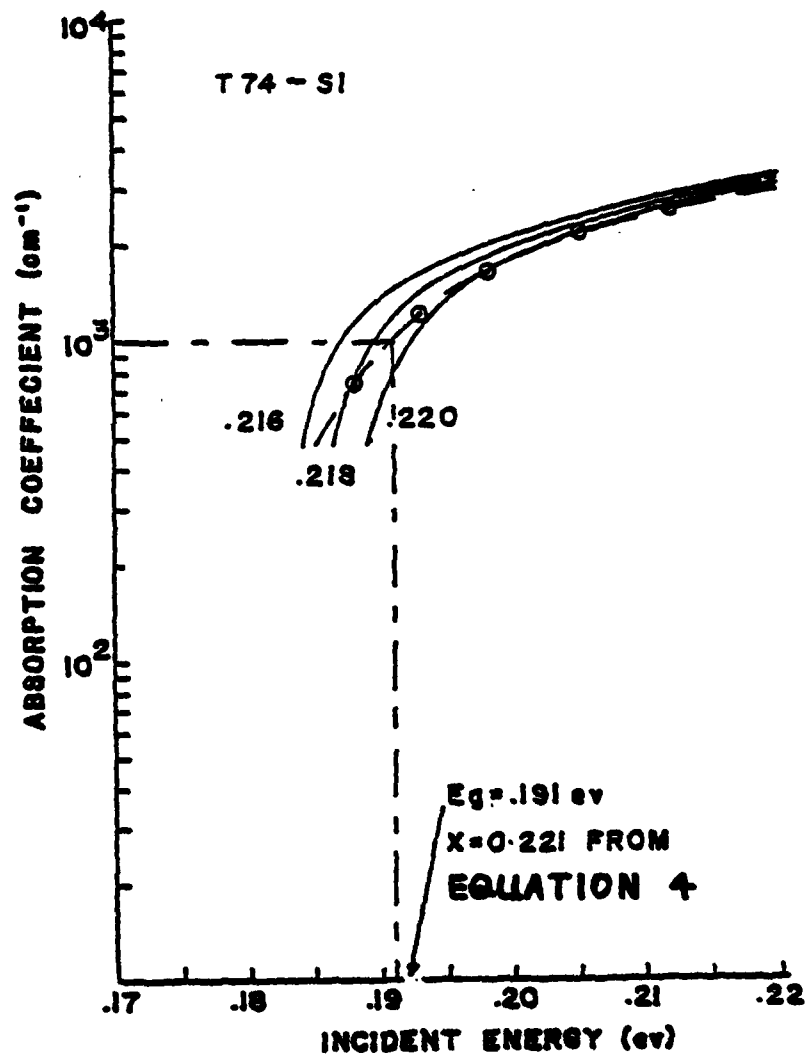


Fig. 3. 6: Use of Optical Curves for Determining Band-gap Energy and Composition of Sample T74-SI. Calculated Absorption for $X = 0.216, 0.218$ and 0.220 is shown by Solid Curves and Circles represent Experimental Absorption Data.

2.4 DEPENDENCE OF ELECTRICAL PROPERTIES OF SPUTTERED FILMS ON SPUTTERING PARAMETERS

2.4.1 Introduction

The data presented in tables 1.1 and 1.2 were obtained with the objective of studying specific relationships between electrical properties (particularly Hall-effect mobility and carrier concentration) and sputtering parameters (e.g. applied rf power to the target, Hg sputtering gas pressure and substrate bias and temperature). Understanding these relationships is the key to optimizing sputtering parameters to obtain a particular film property. The properties that were the main objective of the optimization of the sputtering parameters were high electron mobility, and low free carrier concentration (necessary for high mobility). Since electron mobility is a sensitive function of crystal quality, obtaining high electron mobility would prove that the films had properties similar to bulk single-crystal material and that the conduction properties of sputtered films could be controlled. On the other hand, low electron mobility may be due to many factors that can be potentially eliminated with further sputtering research: a) Hg or Cd vacancies in otherwise high quality crystals due to unoptimized Hg gas pressure and substrate temperature. The vacancies can cause the films to be either p-type or compensated; b) acceptor-like impurities due to impurities in the starting target materials not completely removed by substrate bias; c) poor growth conditions at Si-film interface causing a high density of crystal defects. This could be due to unoptimized substrate surface preparation methods. The cause of low mobility can be difficult to pinpoint because the type and level of impurities in (Hg,Cd)Te can not be directly measured.

2.4.2 Hall-effect Measurement Equipment and Procedure

The theory of the Hall-effect and the Van der Pauw method of Hall measurements are described in complete detail in NJIT theses and will only be briefly discussed here. The geometry and dimensions of the Hall-effect film samples are shown in figure 4.1. The four outer diameter areas (labeled A,B,C,D) serve as pads (evaporated indium) that are contacted by mechanical probes. Two opposite, narrow arms feed constant current, I_{MA} , into the central film region (whose resistivity, carrier concentration and mobility are measured) and two arms act as extremely low current carrying, point contact, voltage probes connected to a 10^{14} input impedance digital voltmeter (Keithley 616 electrometer). A digital potentiometer-thermometer (Omega model 400A), a water cooled dc Varian electromagnet (that provided magnetic fields between 100 and 5 kilogauss), and a vacuum-evacuated dewar with a cold-finger probe holder complete the apparatus. Figure 4-2 shows an improved probe assembly holder⁽¹⁾. [It was recently further modified so that two samples on opposite sides of the cold finger can be tested in a single vacuum pumpdown.] The old assembly is a standard method that has the disadvantage that the probes can not be individually positioned or pressure adjusted and all four probes must be simultaneously positioned over the sample, which can be viewed only from the side. With vertical probes, the sample can be easily damaged by puncturing the indium dots and underlying film during testing. With the berrillium-copper probe design,⁽¹⁾ the contacts to the pads are easily made and observed. Wiring to the pressure adjusted screw is conveniently made. Ohmic behavior of all contacts was verified before measurements were made.

With the VanderPauw method, values for the resistivity and Hall voltage can be calculated from eight measurements. With no magnetic field, four measurements

are made: First, current is injected from A to B and the voltage between contacts D and C is measured; second, current is injected from B and C and the voltage between contacts A and D is measured; the third and fourth measurements are made by injecting current from B to D and then D to B, each time measuring the voltage between contacts A and C. The final four measurements are done by repeating the last two measurements with magnetic field in both directions. The resistivity is calculated from the first two measurement values using equation 1.

$$\rho = \frac{\pi t}{\ln 2} \frac{[1] + [2]}{2I} f \quad (1)$$

Where t is the sample thickness in cm., $[1]$ and $[2]$ are the voltage values from the first two measurements, I is the dc current, and f is a correction factor obtained from the ratio of $[1]$ to $[2]$ using a standard curve.⁽¹⁾ The Hall voltage is obtained from equation 2 using the voltage values of the last six measurements. Equations 3 are used to calculate the Hall coefficient (R_H), free carrier mobility (square cm per volt second) and free carrier concentration (carriers per cubic cm) based on the assumption of single carrier, noncompensated material. If V_H is negative, the carriers are electrons. The magnetic field, B , is in webers per square cm for the above units, (one gauss = 10^{-8} webers per square cm.)

$$V_H = \frac{|[5] - [3]| + |[6] - [4]| + |[7] - [4]| + |[8] - [3]|}{4} \quad (2)$$

$$R_H = \frac{V_H t}{IB} \quad ; \quad \mu_H = \frac{R_H}{\rho} \quad ; \quad c.c. = \frac{1}{q R_H} \quad (3)$$

The measurements are repeated at several temperatures between 300 and 77°K. The temperature of the cold finger can be quickly lowered by pouring a small amount of liquid nitrogen, which evaporates into the dewar flask. Because of the large number of measurements necessary for this research, the equations were programmed on a calculator for quick computation of the material properties from equations 1, 2, and 3. Measurements and calculations for five temperatures in the 80-300°K range can be obtained in less than one hour.

2.4.3 Hall Mobility of Sputtered Films Versus Film Thickness

Two pairs of deposition runs listed in table 1.1, at the end of section 2.1, (T75-T77, T86-T87) had identical key sputtering parameters: applied rf target power (P_{rf}), substrate temperature (T_s), and Hg sputtering gas pressure (P_{HG}). The runs differed only in length of time. The rate of deposition (thickness) was not measured for each run but the rate can be assumed to be about 0.8 $\mu\text{m/hr}$ for $P_{rf} = 75$ watts. In both pairs of runs, the electron mobility is greater for the thicker films. The cause for the decrease in mobility with decreasing film thickness could be attributed to the increase in surface scattering; however, the

mean free carrier path (and mobility) is believed to decrease even more rapidly with film thickness due to the effect of decreasing grain size with decreasing film thickness. SEM photographs of the sides of etched films⁽⁵⁾ indicated that the grain boundaries, perpendicular to the substrate surface, were more dense near the film-substrate interface and that the grains become larger away from the interface (perhaps due to an annealing effect as the grains grew.) Also thinner films may have much more strain associated with them, because of the substrate-film lattice mismatch, which could change the conduction band curvature and lower the electron mobility. Mobility versus thickness data for films on CdTe would help in understanding the relative importance of the mobility lowering mechanism; the high cost of CdTe substrates prevented a series of deposition runs with CdTe substrates from being done.

2.4.4 Hall Mobility of Sputtered Films Versus Substrate Temperature

Figure 4.3 plots the measured electron mobility at 87°K of films on Si substrates from deposition runs made in 1981-82 with different substrate temperatures. [The mobility values at the lowest measured temperature for n-type films are considered to be most significant with regard to crystalline quality.] Note that the two other most important sputtering parameters, target power and Hg pressure, are constant for the four runs but that there were some variations in deposition times. Of the five substrate temperatures used, best results were almost always obtained at 250°C. It is quite possible that 250°C is not optimum temperature and that the dotted curve, or some similar curve, might be obtained if additional mobility versus substrate temperature data between 280 and 200 degrees were taken. The low mobility values, compared to possible values greater than 200,000 that could be obtained, could be due to a) film thickness, b) strain, c) grain boundaries d) impurities from the target (no substrate bias was used), and e) either Hg or Cd vacancies. A more ideal Hg pressure for 250°C is now believed to be in the 1-1.1 micron range, from the standpoint of Cd vacancies. Films with low Hg pressure are less likely to have Cd defects and are more ideal for annealing experiments.

2.4.5 Hall Mobility Versus Applied R.F. Power and Substrate Temperature

The data in figure 4.4 show mobility results for films on Si substrates deposited at different substrate temperatures and applied rf power to the targets but with constant Hg pressure and deposition time. Observing the room temperature data from table 1.2, we see that all four runs yielded films with n-type behavior in that mobility increased with decreasing temperature. It was expected that film crystallinity and mobility would increase as the deposition rate was decreased since deposited atoms would have more time to move to their optimum positions. This was the case comparing the films from run T76 with run T75. The data in figure 4.3 indicate that increasing temperature should result in an increased mobility. This was the case comparing the film results from run T73 and T76. However, the deposition run T74, which should have yielded films with the highest mobility, did not. From table 1.2, it is seen that the carrier concentrations for this film set were in the mid to high ten to the seventeenth range. It should also be noted from table 1.2 that only when dc bias was applied to the substrate (T84-T91) did the carrier concentrations reduce to the necessary low ten to the sixteenth range - a minimum value required for bulk mobility values. This result suggests foreign impurities are the major factor limiting mobility to low values.

2.4.6 Comparison of Hall Mobilities for CdTe and Silicon Substrates

There was usually little difference in the mobility values measured for films on CdTe and Si; the difference was almost always in favor of the silicon (See table 4.1). There are two possible explanations for this difference. When designing future experiments, choices for deposition parameters were based on observed results from previous runs. These results were mobilities that were an average of all the values measured on both CdTe and Si, and since there were more Si samples the average was weighted in its favor. Therefore conditions were optimized for growth on Si rather than CdTe. The other possible reason depends on the positioning of the samples on the platen. Since the CdTe was always directly and fully under the target, it experienced the highest deposition rate. Lower deposition rates have been previously shown to produce better films.

The major conclusion that can be drawn from lack of sensitivity of mobility on substrate material and the low mobility values, is that grain size is probably not limiting the electron mean free path and mobility values. [Grains were not observed in the films on CdTe substrates]. It is much more probable that impurities, either native or foreign, are the major controlling factor effecting conduction properties of the films.

2.4.7 Hall Mobility and Carrier Concentration Versus Substrate Bias

Negative d.c. substrate bias had a strong effect on conduction properties. A negative dc bias on the substrate anode accelerates positive Hg ions to it. As the kinetic energy of the ions is increased, they become energetic enough to "loosen" weakly or poorly bonded Hg, Cd or Te atoms and to inhibit the incorporation of weakly bonded impurity atoms or interstitial Hg atoms. As the bias is increased further, it also creates vacancies, most likely of the volatile atoms. This can be seen in the results presented in Table 4.2 with the order of increasing bias being: T78, 84, 85 for a Hg pressure of 0.9 microns and T81, 87, 89 for a Hg pressure of 1.2 microns. At both Hg pressures, with an intermediate bias, a dramatic decrease in carrier concentration occurs from that without bias. This suggests the level of foreign impurities have been reduced. The mobility increases due to decreased impurity scattering. For the largest bias conditions, the films become p-type as evidence by the decrease of mobility with decreasing temperature. The results suggest that bias values less than fourteen volts may be sufficient for removal of impurities without creating Hg vacancies leading to compensated film behavior.

2.4.8 Hall Mobility and Carrier Concentration Versus Hg Pressure

Table 4.3 compares film results for deposition runs where only the Hg pressure was changed. Comparing the results for the three runs without substrate bias (T83, T78, and T81) we see that there is a surprisingly small difference in conduction results. Since the results should be a strong function of Hg pressure, this lack of dependence is attributed to the dominance of foreign impurities in the starting target materials when no substrate bias is applied. Comparing the two minus fourteen volt bias runs, it could be said that the Hg pressure for T84 was too low for fourteen volt bias level, as evident by the decrease in mobility with measuring temperature suggesting compensated material due to Hg vacancies. From the ARO sponsored research⁽⁴⁾, it was found that for Hg pressures above 1.2 microns, Cd tends to be depleted from the target surface and therefore from the films. It is possible that for Hg pressures even less than 1.2 microns, Cd may

23

not arrive at a sufficient rate as the film grows to prevent Cd vacancies. Therefore T87 films may be lacking in Cd, which would cause increased scattering and a reduction in mobility. In further experiments, the values of Hg pressure between 0.9 and 1.2 microns must be slowly changed at various bias settings and with CdTe as well as Si substrates. It is firmly believed by the author that much higher values of mobility for triode-sputtered films can be obtained by further fine tuning of the sputtering parameters.

2.4.9 Hall Mobility Versus Exposure Time to Ambient Atmosphere

To see what effect the time of exposure to the ambient atmosphere of the silicon substrates (while loading the platen) had on the film's growth and properties, an experiment was designed. In it the first substrate loaded (with the longest exposure) was placed the same distance from the center as the last sample loaded, which had the shortest exposure. The time of exposure was between 5 and 30 seconds for the last-in sample and from 3 to 6 minutes of exposure for the first-in samples. The results are given in Table 4.4. As can be seen, there is no clear tendency indicating whether the amount of oxidation at this stage has any effect on growth. The experiment should be repeated when higher mobility films were obtained after further fine tuning of the sputtering parameters.

2.4.10 Sputtering with D.C. Voltage Applied to the Target

An experiment was conducted with a d.c. voltage of 100 volts applied to the target since it was reported that good results were obtained by this method.⁽²⁷⁾ The conduction properties of films from this run can be compared to those from the rf run, T87, which had similar values for Hg pressure, substrate bias and temperature, and sputtering time. However, an important parameter—deposition rate—has not yet been measured for T90. The conduction results for T90 films were somewhat comparable to the films for T87. Both films sets are probably dominated by nonoptimized values for Hg pressure and substrate bias and temperature and not strongly dependent on target voltage. Therefore the dc sputtering approach must be considered in future work, due to the simple required sputtering apparatus, even though rf sputtering is known to give a more constant deposition rate and cleaner films when used with metal targets.

2.4.11 Dependence of Conduction Results on Film Composition

In research prior to 1981, conduction properties of films deposited with targets with x values other than 0.2 were obtained. These results were reported in AFOSR annual reports for 1978-1981 grants. The conduction results did not differ to any significant degree from those for x=0.2 films emphasized in this section. The past research with different compositions served the purpose of demonstrating that the composition of the film can follow that of the target and that films with any desired composition in at least the 0.18 - 0.27 compositional range can be obtained. However, the results in this section show that many sputtering parameters must be finely tuned to obtain optimum conduction results and that the optimization is difficult research. The optimum sputtering parameters would obviously be a function of desired film composition. Therefore the decision in 1981 to concentrate all ARO and AFOSR research on a single material composition of 0.2 appears to have been correct.

Table 4.1 CdTe vs Si Substrates

Run	Mobility (cm^2/vs)				Number of Silicon Samples in Average	Si as % diff. of CdTe Value (87OK)
	CdTe		Si Average			
	Rm. Temp	Liq. N ₂ (87OK)	Rm. Temp.	Liq. N ₂ (87OK)		
T79	900	1220	912	1290	5	+5.7
T80	1100	1610	1260	1800	5	+12
T81	1900	2750	1670	2250	5	-18
T82	885	1230	922	1430	4	+16
T83	1570	2480	1930	2890	4	+16
T86	1370	2250	1840	2750	4	+22
T87	1960	2812	3090	5540	6	+97

Table 4.2 Hall Mobility and Carrier Concentration vs Bias

Deposition Parameters			Electrical Results				
Run	P Hg mHg	Time Hrs.	Bias V(dc)	Room Temp.		Liq. N2 Temp. (87°K)	
				Mobility cm ² /vs	Car. Conc. Range (10 ¹⁶ cm ⁻³)	Mobility cm ² /vs	Car. Conc. Range (10 ¹⁶ cm ⁻³)
T78	0.9	12	None	1782	30/56	3932	32/60
T84	0.9	12	-14	4610	3.0/5.5	4332	2.1/3.8
T85	0.9	12	-28	569	6.1/11	135	21/39
T81	1.2	12	None	1674	37/68	2330	40/74
T87	1.2	11.5	-14	2929	5.9/11	5150	3.4/6.3
T89	1.2	12	-18	905	2.3/4.3	439	0.66 /1.2

Note: All runs had some P_{rf} (75 watts) and T_s (250°C).

Table 4.3 Hall Mobility and Carrier Concentration vs Hg Pressure

Deposition Parameters			Electrical Results				
Run	Bias V(dc)	Time Hrs.	P _{Hg} mHg	Room Temp.		Liq. N ₂ Temp. (87°K)	
				Mobility cm ² /vs	Car. Conc. Range (10 ¹⁶ cm ⁻³)	Mobility cm ² /vs	Car. Conc. Range (10 ¹⁶ cm ⁻³)
T84	-14	12	0.9	4610	3.0/5.5	4330	2.1/3.8
T87	-14	11.5	1.2	2930	5.9/11	5150	3.4/6.3
T83	None	12	0.6	1860	61/110	2810	63/120
T78	None	12	0.9	1780	30/56	2930	32/60
T81	None	12	1.2	1670	37/68	2330	40/74

Note: All runs had some P_{rf} (75 watts) and T_s (250°C).

Table 4.4 Exposure to Ambient Atmosphere
Between Etching and Sputtering

FIRST LOADED (Most Exposure)			LAST LOADED (Least Exposure)		
Sample	$\mu_H(\frac{cm^2}{vs})$		Sample	$\mu_H(\frac{cm^2}{vs})$	
	Rm. Temp.	Liq. N ₂ (87°K)		Rm. Temp.	Liq. N ₂ (87°K)
T76-52	1200	N.A.	T76-55	1070	1420
T77-511	1500	2000	T77-57	1230	1770
T78-57	1720	4310	T78-58	1520	2340
T79-512	983	1390	T79-511	963	1400
T80-59	1160	1630	T80-510	1150	1740
T81-59	1700	2030	T81-510	1690	2500
T83-511	1740	2780	T83-59	2500	3420

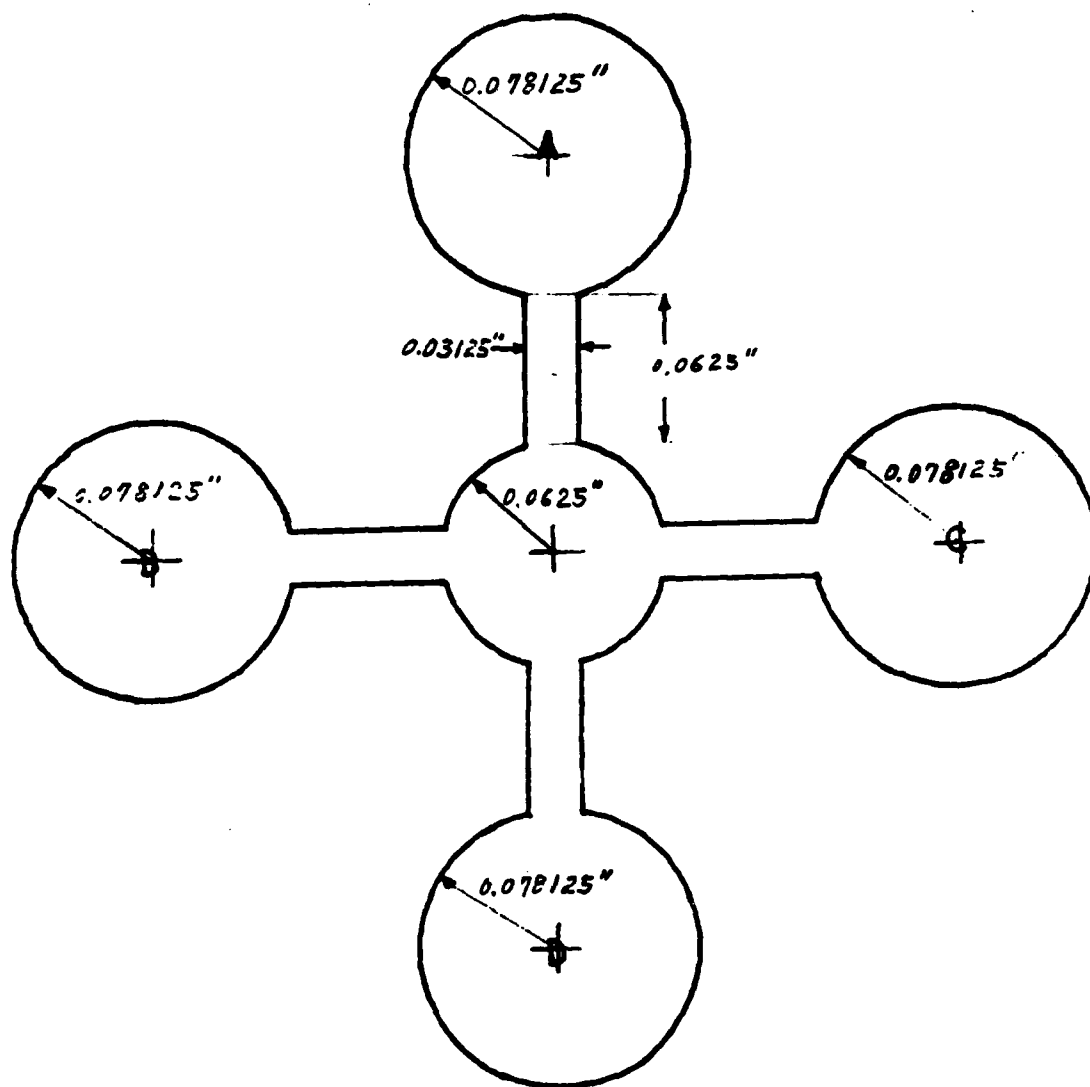


Figure 4-1 Mask/Thin Film Shape.

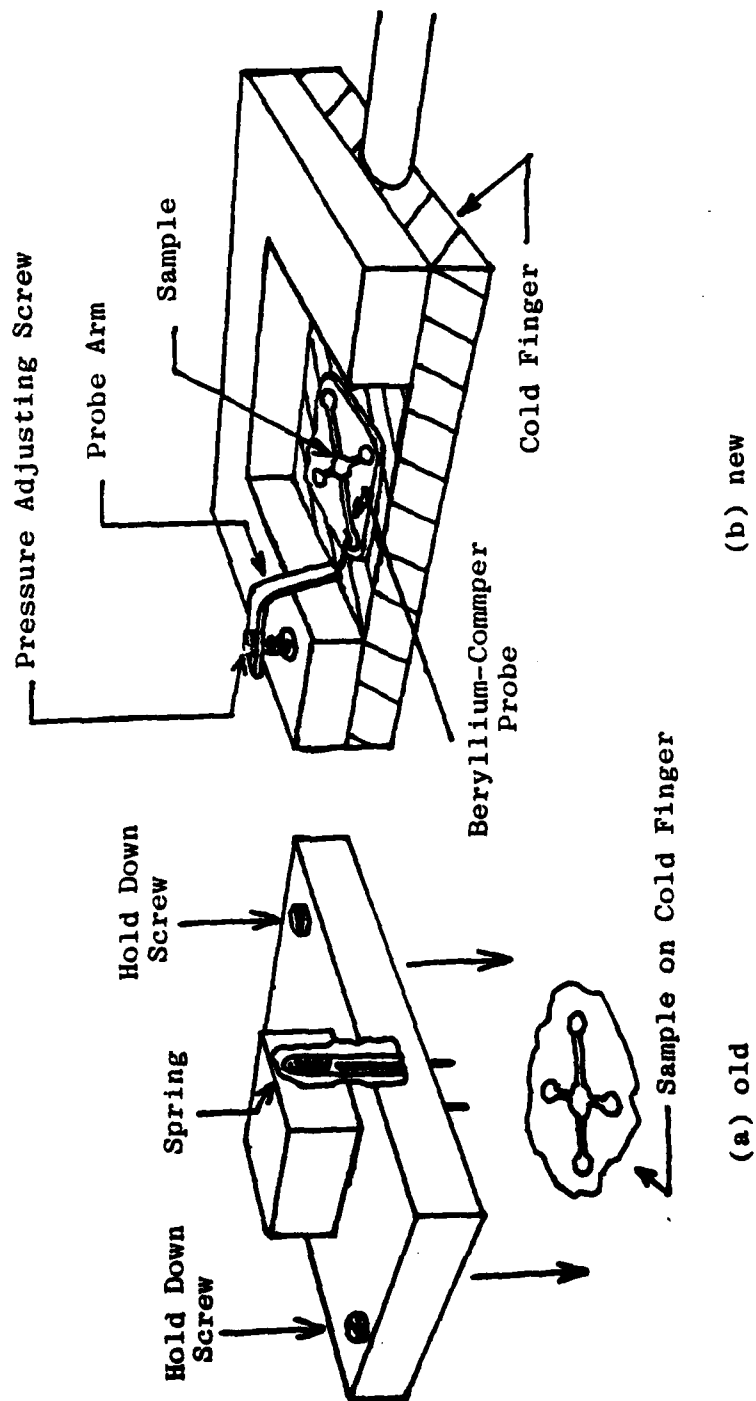
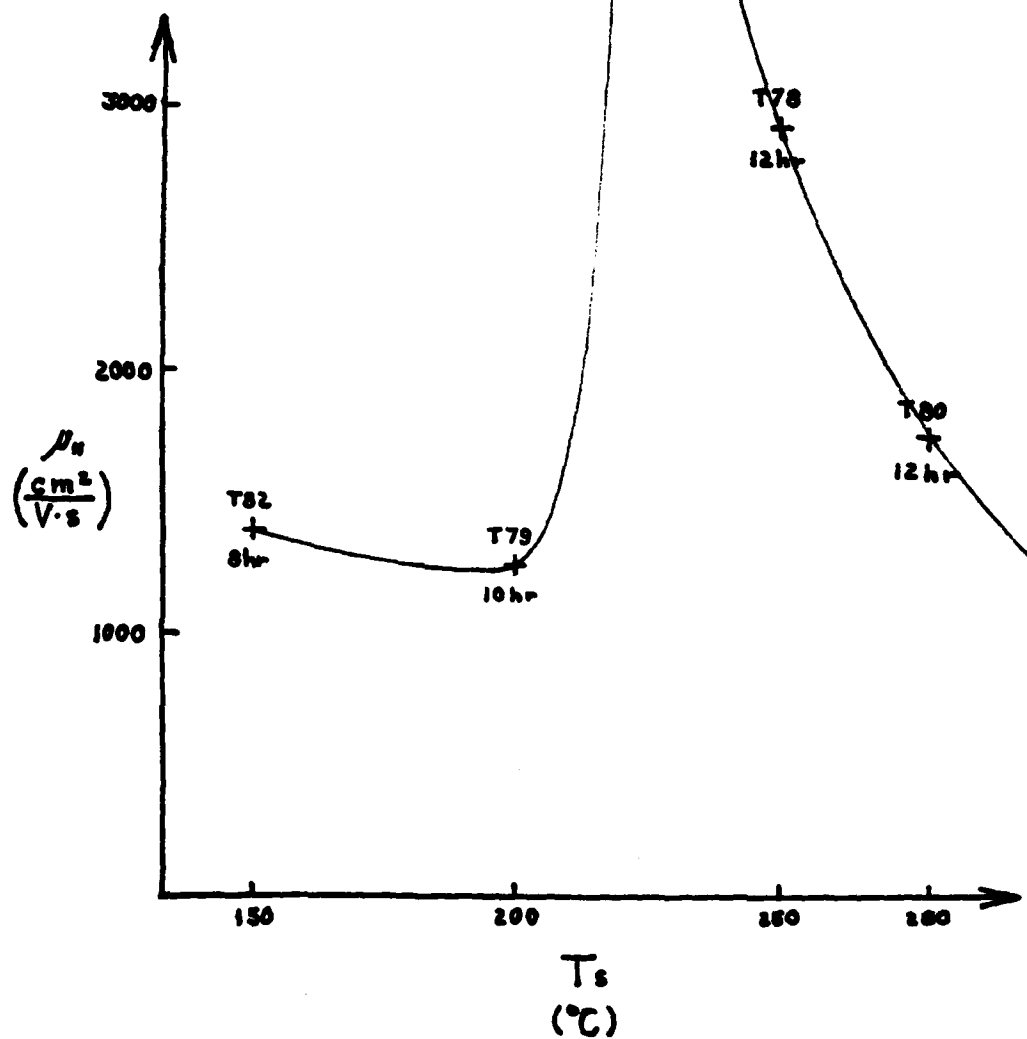
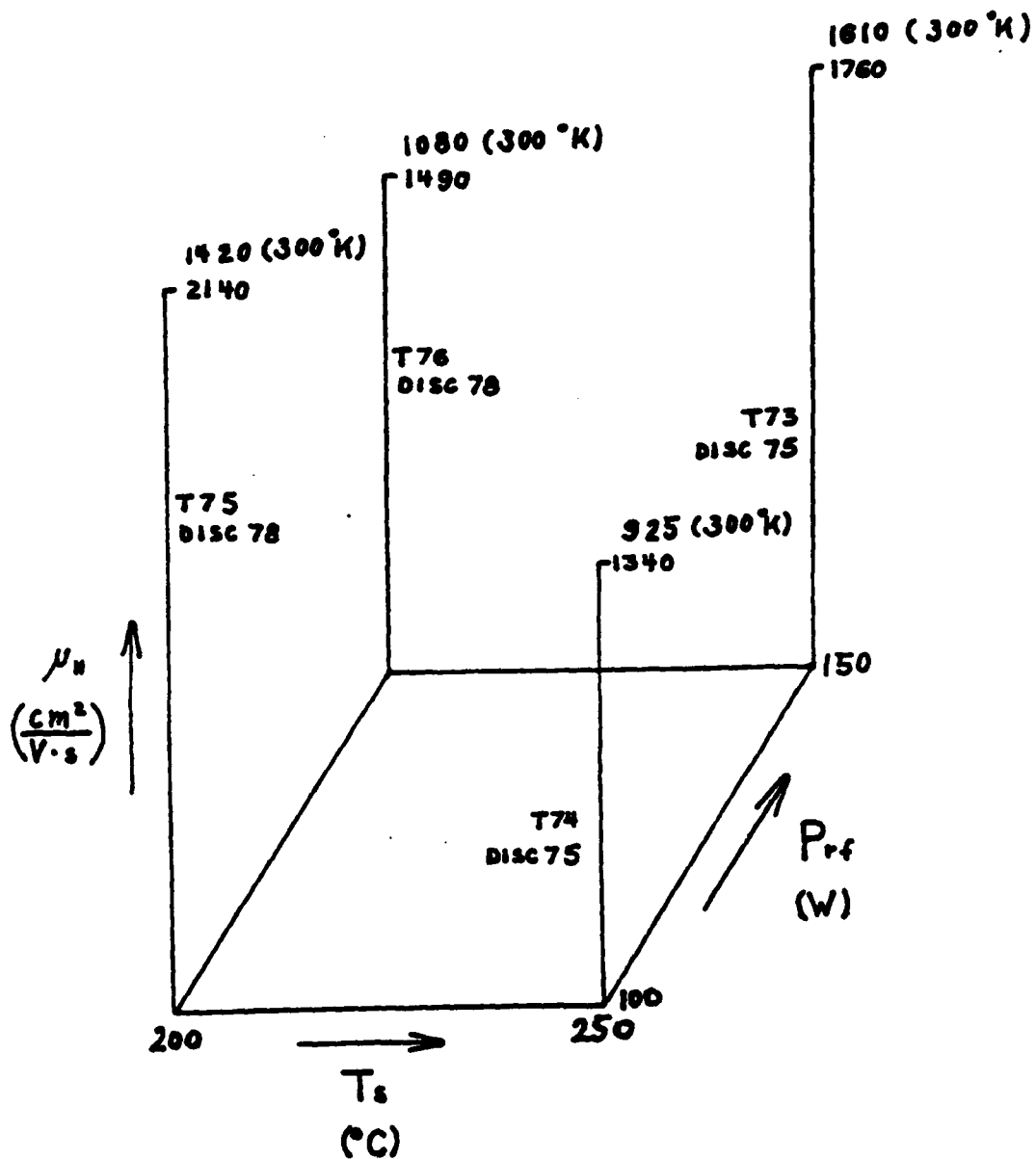


Figure 4-2 Probe Assemblies



All runs deposited with $P_{rf} = 75W$ and $P_{n_2} = 0.9\mu m$

Figure 4.3 Hall Mobility @ 87°K vs Substrate Deposition Temperature for Films Deposited Without Substrate Bias.



All runs 8 hrs., $P_{H_2} = 0.90 \mu\text{m}$, no bias, μ_H measured @ 87°K

Figure 4-4 Hall Mobility vs Deposition Power and Substrate Deposition Temperature.

2.5 ELECTRICAL PROPERTIES OF ANNEALED FILMS

2.5.1 Introduction

The main objective of this work was to obtain annealed films with high electron mobility and low native defects and carrier concentrations, to demonstrate the quality of the sputtered films. A second objective was to demonstrate control of the electrical properties by annealing methods. A final objective was to use the annealing experiments to get better description of the impurities and other defects in the film. The highest value for electron mobility obtained for the annealed sputtered films was only about one eighth of the maximum possible value. However, although ideal mobility values have not yet been obtained, the annealing results suggest that this objective is obtainable if the films to be annealed are prepared by optimized bias sputtering techniques so that the films do not contain a large number of foreign impurities.

2.5.2 Background on Annealing and Doping (Hg,Cd)Te Material

By annealing (HgCd)Te material in a Hg atmosphere, Hg vacancies (acting as acceptors) can be filled and the material changed from p to n-type. In the case of polycrystalline material, crystallites can be enlarged. Whether the annealed material becomes p or n-type is known⁽²⁸⁾ to be a sensitive function of the Hg partial pressure and the equilibrium annealing temperature with the general behavior expected to follow the data shown in figure 5.1. [For annealed (Hg,Cd)Te thin films, the conduction properties will depend also on the number and type of defects in the film and therefore on the sputter deposition parameters; for bulk materials and other types of thin films, such as LPE films, the original growth parameters may also influence the conduction behavior.] Annealing results have been reported for $(\text{Hg}_{0.6}\text{Cd}_{0.4})\text{Te}$ bulk materials^(29,30) and thin films⁽³¹⁾ and for $(\text{Hg}_{0.6}\text{Cd}_{0.2})\text{Te}$ bulk materials^(32,33,34) and thin films.⁽³⁵⁾ From data such as shown in figure 5.1, it can be seen that crystalline $(\text{Hg}_{0.6}\text{Cd}_{0.2})\text{Te}$ material annealed under Hg saturated conditions converts to n-type below 360°C and the electron concentration is practically independent of the annealing temperature below 360°C. Schmidt and Brebrick^(29,30) found that $(\text{Hg}_{0.6}\text{Cd}_{0.4})\text{Te}$ undoped samples also turned n-type at annealing temperatures below 350°C under Hg saturated conditions. The conversion temperatures were found to be different for samples with different carrier concentrations. This indicated that the type-conversion in these samples was due to residual foreign donors and not native donor defects. In the Hg vapor annealing process, atoms of Hg from the vapor will diffuse into the (Hg,Cd)Te and either occupy interstitial sites or fill Hg vacancies.⁽³¹⁾ In the former case, Te from the lattice will appear as a second phase. In stoichiometric crystals, the presence of Hg vacancies is associated with Hg atoms in interstitial positions which act as n-type Frenkel defects in the Hg-Cd sublattice. Cd vacancies can behave similarly. Other types of defects may also be present. For example, a high concentration of Hg vacancies created during the growth of a crystal can lead to clusters of excess Te atoms, which may prevent Hg atoms from filling Hg vacancies during annealing. Dislocation and grain boundaries can also cause an increase in free carrier concentrations. In thin films, lattice strains caused by mismatch in the coefficient of expansion of film and substrate during either growth or annealing processes can result in local changes of the forbidden gap, which can introduce additional free carriers.

23

Indium is commonly used as a contact material to n-type regions of (Hg,Cd)Te devices. It can also be introduced into (Hg,Cd)Te as a donor as shown in fig 5.2. (36,37) Its influence on the native defect structure has been investigated in the closely related II-VI compounds of CdS (38,39) and CdTe. (40,41,42,43) As a donor, it acts as a substitute for either Hg or Cd in the metal sublattice. Indium deposited by evaporation onto (Hg,Cd)Te material as a contact material will diffuse into the lattice since it has a high value for its diffusion coefficient, D, in the (Hg,Cd)Te host crystal. (e.g. $D = 1.1 \times 10^{-12}$ microns squared per second at 300°K and $D = 5.0 \times 10^{-9}$ at 400°K for a host crystal with $x = 0.2$) The diffused region of Indium for contacts will further diffuse into a sample if it is annealed. In further research, a defect model for Indium in $x=0.2$ material was developed where the Indium is incorporated as dissolved In_2Te_3 with only a small fraction of the Indium acting as a single donor in a Hg lattice site. (45) Figures 5.2 and 5.3 summarize the expected doping behavior of other elements in (Hg,Cd)Te.

2.5.3 Annealing Procedure

Samples to be annealed were mounted in pairs on a quartz fixture placed at the end of an 18mm ID, 21mm OD quartz tube, which was bathed thoroughly in trichlorethylene solvent. A small pool of Hg, typically a 0.5cm diameter droplet, was placed in the tube 11 cm from the sample. The tube was pumped down to a vacuum pressure of about 1×10^{-5} Torr (1.3×10^{-3} Pa) and then sealed off. The tube was held in a programmable two zone furnace (Ohio Thermal Inc, Model S11C-0431-22-2K, Barber Colman Co., 520 Solid State Controller) so that the samples and Hg droplet could be heated to different temperatures. The ambient Hg pressure in the tube was obtained corresponding to the vapor pressure of Hg at the lower temperature and was independent of the Hg in the tube. To avoid possible peeling effects and to allow for the interdiffusion of material at the film-substrate interface (to minimize lattice mismatch) the furnace temperatures were slowly raised at a convenient rate of 130C per hour. The samples were kept at an equilibrium temperature for 38.5 to 64 hours in earlier reported research (47,7) and in the recent work in table 5.2 for 48 to 54 hours. In earlier work reported in table 5.1 temperatures were slowly decreased to 300°K over a period of 7.5 hours. For the results reported in table 5.2, the samples were quenched in water for reproducible results and to preserve as much as possible the high temperature equilibrium defect concentration.

The annealing sample temperature range for these experiments was chosen to be between 230 and 350°C since the optimum annealing temperature for sputtered thin films could be possibly different from that for bulk crystals (which is generally accepted to be about 280°C) and since very good results were obtained initially at 350°C. It was therefore decided to study at first the change in film conduction properties over a wide range of annealing temperatures and Hg pressures. In recent work the temperature of the zone with the Hg pool was chosen to be about 5°C lower than the sample temperature to provide maximum Hg pressure to minimize Hg vacancies and yet not allow Hg to condense on the films as it will if the Hg droplet temperature exceeds the sample temperature. The different annealing conditions for various samples are given in tables 5.1 and 5.2.

The annealed samples in table 5.2 were of 2 types: those that had indium contacts evaporated onto their contact pads before annealing and those that did not, designated by AANI in table 5.2 (NI for no indium). The conduction properties of the AANI samples were not measured before being annealed, to avoid the possible problem of diffused regions under the contacts further diffusing through the arms into the center region. The AA samples were electrically measured after

25

being sputtered and then had their evaporated indium contacts removed by concentrated HCl solution followed by distilled water bath. After annealing, indium dots were evaporated on the contact pads and Hall-effect measurements made by changing the measurement temperature from 300°K to 77°K and the magnetic field from 4600 to 100 Gauss. In all cases, ohmic behavior of the contacts were verified with the IV curve tracer.

2.5.4 Conduction Properties of Annealed Films; Discussion of Results.

Hall effect data for films annealed in a Hg atmosphere are shown in Table 5.1B. The data in fig. 5.1A are the sputter-deposition parameters for the anneal films. The film number indicates whether the substrate was Cadmium Telluride (CT) or silicon (Si). In table 5.1B, the film mobility and carrier concentration values are compared with accepted values for bulk crystals, which are presented in brackets. These data were obtained and reported in 1980-81 (7,25) and were the first results for annealed films. Note the relatively high mobility values obtained for the last two film entries in table 5.1B. The mobility value of 23,800 about 16 percent of the maximum expected value, since the film is only 5.1 microns thick, was a good value from which to further optimize results.

As discussed in 2.5.3 the slow increase in temperature to the annealing value was necessary to prevent peeling of the films, particularly off the Si substrates. Protrusions shown in previously published photographs⁽²⁵⁾ are the first step in the peeling process. It is important to note that the protrusions always appear in the large circular areas of the sputtered film and not in the thin arms 1.7 by .5mm connecting the contact regions to the central region, 31 mm diameter. It is therefore believed that arrays of photoconductors, which would have dimensions similar to the arms, would not have peeling problems.

The film samples whose results are given in table 5.1B were not quickly cooled quenched, at the end of their annealing runs. This was because in a few initial annealing experiments quenched films peeled, for some unknown reason. Therefore unfortunately these annealed samples were cooled after annealing by slowly decreasing the temperatures of the two zone furnace over a period of five hours. On the basis of the data obtained from June 81 to June 82, it appears the film stoichiometry changed during the cooling procedure at the end of the run, actually improving the result. The annealing procedure used to obtain the results of samples with relatively high mobility in table 5.1B was not reproducible. However, when experiments were again done by quenching the quartz tube at the end of the annealing, no peeling effects were observed.

In Table 5.2, results for annealing experiments of June 81 - June 82 are presented. The annealing experiment number is the leftmost entry. Forty-one experiments were conducted, each yielding useful information pointing toward the sputtering and annealing conditions required to obtain nearly intrinsic films with high electron mobility.

The information in column 2 identifies the annealing run. As previously pointed out, the AA samples had indium deposited on the contact regions. The indium that did not diffuse into the sample during the evaporation process was etched away prior to the annealing run; the AANI samples were not tested before annealing and therefore, did not have any indium at the contact regions prior to annealing. Column 3 identifies the sputtering run. For example, T88-53 means the sample was from triode-sputtering run T88 and that the particular

silicon substrate was S3. The parameters of the sputtering runs are in table 1.1 and repeated in columns 4-7 and the conduction properties of samples in that run in table 1.2. The Hg pressure used during the sputter-deposition runs were in the 0.9-1.4 micron range and had a strong effect on properties of films after they were annealed. Subsequent to most of the deposition and annealing runs, it was clearly established from ARO research that Hg sputtering gas pressures above 1.2 micron would probably result in films with Cd vacancies as Cd was found depleted from the target surface.

Analysis of the conduction properties of sputtered films (1,11,52) pointed to the strong possibility that impurities introduced during the sputtering process were tending to make the films p-type. Therefore, emphasis was put on using negative DC substrate bias, to prevent impurities from being incorporated into the film, and on annealing bias-sputtered films. The values of the DC bias are given in column seven. In column 8 are the temperatures in the two zone furnace, with the higher value being that for the film sample location and the lower value that for the pool of Hg. From table 5.3, the pressure of Hg over the film sample corresponding to the temperature of the pool of Hg can be found. As previously discussed, for most annealing runs the two temperatures were chosen to be nearly identical to maximize the Hg concentration at the film surface that serves as a source of Hg to diffuse into the film to fill Hg vacancies. The runs made with large temperature differences were done to try to reproduce the conditions that led to the best results of table 5.1.

The final four columns give values for the measured mobility and carrier concentrations at film temperatures of 77 and 300°K. The notation p or n refers to the sign of the Hall-coefficient and not to whether the film actually has more holes than electrons. If the mobility is above 3000 cm. square per volt second the mobility increases with decreasing temperature and is not strongly effected by magnetic field changes, the film can be considered to be definitely n-type. If the mobility falls with decreasing temperature or if the mobility values are below 1000 and change by more than 10 percent with magnetic field changes, the film can be considered to be p-type.

The data of table 5.2 will now be discussed in terms of the purpose of the annealing experiment and the probable reasons for the conductivity results. The two general purposes of these annealing experiments were: a) to find the optimum annealing parameters required to modify as-deposited film properties to obtain intrinsic or slightly n-type films with high electron mobility and b) to obtain an understanding of the nature of the defects and impurities in as-deposited and annealed films.

Film samples 1 to 15 were sputtered without substrate bias. The annealing results support the belief that p-type impurities are present when bias is not applied. For samples 1,2 and 3 the annealing temperatures were those found to be close to ideal. Both samples 1 and 2 were p-type. The interpretation of the results for sample 2 is difficult because of pock marks due to flaking (see table 1.2 for T75). Of the films without bias in Table 5.2, sample 3 had the best result - its mobility was improved by about a factor of 3 and its carrier concentration decreased by a factor of 5.

Samples 4 and 5, which had carrier concentrations and mobilities similar to sample 3 before annealing, became clearly p-type after annealing with two zone temperatures of 325/200. This result suggested that the sample annealing temperature of 325°C was too high for the low Hg pressure provided by the 200°C of the pool of Hg. Samples 6, 7 and 8 also had p type behavior after annealing; results were quite different than what was expected from the samples of Table 5.1 with 350/200 annealing temperatures which were annealed without quenching as the final process. The annealing temperatures of 325/200 and 325/175 were lowered somewhat from the 350/200 temperature of the successful run of Table 5.1 because at the lower temperatures there were no protrusions or peeling of the film off the Si substrate during the run while peeling occurred occasionally for some samples at 350°C.

Sample 9, annealed under more ideal annealing temperatures, gave very poor results. Comparison with samples 17 and 18 strongly suggest that the cause was impurities from the target not removed by substrate bias.

Sample 11 can be compared with sample 6, which had a stronger p-type behavior. The difference can be attributed to the higher P_{Hg} of sample 11 (1.2 vs. 0.9 microns).

Samples 12, 13 and 14 with lower T_s and probably more Hg incorporated in the film had n-type behavior even after the 325/175 anneal. Sample 15 with much less Hg incorporated in the film during the sputtering run ($P_{Hg} = 0.6$ microns, $T_s = 250^\circ\text{C}$) had strong p-type behavior.

Sample 16 was the first sample prepared with substrate bias. A big improvement in mobility and a lowering of the carrier concentration by more than a factor of 10 due to substrate bias can be observed by comparing the results with sample 8. Sample 18 gave the best results of all annealing runs. Note the very low carrier concentration, down to nearly 10^{15} cm^{-3} at 85°K and 5.3×10^{15} at 300°K, and the increase in mobility when compared with films without bias, samples 1, 2 and 3. It should be noted that the carrier concentration of T87 was lower by a factor of about 10, before annealing, compared to the no bias runs T74, T75, and T76. Samples 17 and 18 can be compared since the annealing parameters were nearly the same. Ten volt bias is clearly advantageous but the -20 volt bias, with $P_{Hg} = 0.9$, probably causes Hg as well as impurities to be removed from the film by sputtering. There is also a probability that a high density of grain boundaries are introduced due to the high value of bias.

For the next two samples, 19 and 20, the annealing temperatures were increased slightly. The carrier concentration is seen to increase, probably due to interstitial Hg being introduced into the film. The relatively large increase in mobility for the measuring temperature decrease from 300 to 258°K suggests that the higher substrate annealing temperature is necessary for larger grains but at these temperatures the stoichiometry is not optimum. This result suggests that two-step annealing processes may be most effective (e.g. a 320/300 anneal followed by a 40 hour 280/278 anneal).

The seven samples 21-27 all had 13 volt substrate bias P_{Hg} equal to 12 microns and were from the same sputtering run T88. The annealing temperatures had three sets of values 280/275, 230/225 and 310/305 for the purpose of confirming that 280/275 is really close to optimum annealing temperatures. The film results for the 310/305 confirm that annealing at higher temperatures result in a Hg pressure that is too high and causes films to have interstitial Hg and high carrier concentrations. From figure 5.3, (at 310°C P_{Hg} is twice that

at 280°C). At this point in the research, experiments were also done to see the effect of diffused indium under the contacts. Note that sample 26 without indium had a positive Hall coefficient at 300°K and lower mobility while sample 23 was n type at 300°K. This result indicates that indium had some effect (perhaps compensation at 300°). The samples annealed at 230/225 had low mobilities and again the indium sample was n-type at 300°K. Since the diffusion coefficient of Hg in (Hg,Cd)Te is known ⁽⁴⁴⁾ to decrease more rapidly with temperature at temperatures below 250°C, due to a change in the diffusion mechanism, it is now felt that the 230/225 annealing would be successful if the annealing time was much longer than 40 hours. (The important basic information on the value of the diffusion coefficient of Hg and various impurities in (Hg,Cd)Te versus temperature has not been published in the U.S.)

Comparison of the 280/275 runs for samples 25 and 21 shows that indium from the contact regions diffused into the central film region during the anneal and plays a role in making the film more n-type. The poorer result for sample 21 versus sample 18 shows that 10 volt bias is closer to an optimum value than 13 volt bias and that future experiments should study the influence of the small difference in temperature of the Hg pool and the sample temperature.

Sample 27 differed from sample 21 in one respect. Indium was deliberately evaporated over the whole sample, including the central region, and then removed by etching. Again the sample was more n-type as opposed to sample 25 but the indium concentration was too high as indicated by the 10^{18} values of the carrier concentrations.

The d.c. sputtered films from run T90, with 10 volt bias, appeared to be n-type (see table 1.2). The sample 28 from this run annealed at 230/225, without the presence of indium, had p-type behavior. Experiments to anneal these films at 280/278 are planned.

The film samples 29 and 30 were part of a set of three. The 280/275 sample was accidentally destroyed. The results for both these samples were poor. The cause of the very high carrier concentration of sample 30, annealed at a much lower annealing temperature than that for sample 29, is not known.

Film samples 31-34 were all sputtered with higher Hg pressure, 1.4 microns. At the time it was not known that this would probably result in Cd vacancies in the film. Comparing the results for samples 31 and 32, it is seen that the film annealed with indium present had a somewhat lower inversion temperature, indicating lower acceptor concentration. Samples 34, annealed at 310/305, also had p-type behavior. The presence of Cd vacancies seems to require a different optimum annealing temperature since the film 33, annealed at 230/225, had the best result.

The samples 35-41 were studied to see the effects of changes in annealing parameters on films sputtered with lower Hg pressure, $P_{\text{Hg}} = 0.9$ microns, to insure that there would not be a problem with Cd vacancies. To compensate for the decrease in Hg pressure and possible increase in Hg vacancies, the substrate temperature was lowered to 200°C and somewhat lower d.c. substrate bias was used, - 8 volts. The lower substrate temperature was expected to decrease the size of the grains of as sputtered films; the formation of nearly single crystal films would then depend on the annealing process. Comparing samples 35 and 36, it is seen that the films annealed at even these low temperatures can be very sensitive to the presence of indium. A longer anneal of sample 35 to promote grain growth and the filling of possible Hg vacancies might yield very good results. Comparing samples 35 and 37, it is surprising that there is no decrease in carrier concentration and increase in mobility with the rise in annealing temperature as in the case of the films sputtered at 250°C . One explanation is that sample 35 might have been inadvertently doped with an n-type dopant that compensated the Hg vacancies. On the basis of the comparison of 35 and 37, 270-280 is not the optimum annealing temperature range for films sputtered with the parameters of T94.

Samples 38-41 were annealed in the presence of diffused indium. Comparing with Sample 37, the influence of indium is to make the room temperature carrier concentration significantly higher and to make the mobility versus measuring temperature behavior more n-type. Raising the annealing temperatures to 350/345, to possibly enable additional grain growth resulted in very high carrier concentrations. A second annealing step at a lower annealing temperature should be tried on sample 41. Also to complete the study additional AANI samples should be annealed at 270/265 and 280/275 and studied.

2.5.5 Study of the Magnetic Field Dependence of the Conduction Properties of Annealed Films.

The magnetic field dependence of the Hall coefficient, R , has been recently studied at 300°K and at a low temperature ($87-100^{\circ}\text{K}$) for applied magnetic fields in the 0.165-4.65 kilogauss range. Figure 5.4 (for 300°K) and fig. 5.5a (for 100°K) show measurement results for the dependence of R , carrier concentration, and mobility on magnetic field; data for an n-type sample, No. 35, and two samples with p-type behavior, No. 23 and 25. For the n-type sample No. 35, and others such as No. 18, there is little variation of R with magnetic field between 4.6 and 0.5 kilogauss. A sharp drop in mobility and R is seen for fields below 0.5 kg due to the magnetic freezeout effect.⁽⁴⁸⁾ Note that sample 23 which was more n-type at 300°K than sample 25, as indicated by its higher measured mobility at 300°K (calculated under the assumption of single carrier) shows a magnetic quenching effect at 300°K while sample 25 does not.

For both p-type samples, band c in fig. 5.4 and 5.5, there is an oscillatory behavior for R at 300 and 100°K . This behavior is similar to that calculated theoretically by Beer and Willardson⁽⁴⁹⁾ for Ge and Si with mixed conduction and heavy and light hole valence bands. Their results can be applied to other semiconductors. The magnetic field results therefore confirm that the mobility versus temperature behavior of sputtered films with relatively low mobility is associated with mixed conduction. The holes in the films with p-type behavior are associated with two overlapping valence bands. The results also confirm that the films with sharply rising mobility versus temperature behavior are n-type.

2.5.6 Conclusions on Optimum Annealing and Sputtering Parameters for Nearly-intrinsic Films

The study of the use of annealing to obtain low carrier concentration, high mobility ($\text{Hg}_{0.8}\text{Cd}_{0.2}\text{Te}$) films on Si substrates showed that the optimum annealing temperatures for this purpose depend on the four sputtering parameters given in table 5.2. One of the sputtering parameters, applied rf power and corresponding rate of deposition, was kept at a low value 75 watts; it was assumed that a slow film growth rate would give the best films and that the small loss in arrival energy due to a drop of about 10 percent in the cathode voltage with an applied power decrease from 150 to 75 watts would not be critical. The other three sputter-deposition parameters, pressure of the Hg sputtering gas, P_{Hg} , substrate temperature, T_s , and dc substrate bias were found to strongly influence the film results after annealing. Several combinations of these three parameters were chosen and two annealing parameters, the pressure of Hg (the temperature of the Hg pool) and the substrate temperature, were varied. The total annealing time and the warm-up and quenching processes were not varied. It was assumed that a total annealing time of 48 hours was sufficiently long to allow the film to reach its optimum crystallinity and stoichiometry; however, the results indicated that for low annealing temperature combinations, i.e. 230/225, a longer anneal time should be tried to obtain the best film properties possible after a low temperature anneal.

A most important conclusion of the annealing study was that dc substrate bias can be used to remove sputtered impurities during film growth. Carrier concentrations as low as 10^{15} cm^{-3} at 103°K were obtained (sample No. 18 in Table 5.2). The optimum value of bias is critically dependent on T_s and P_{Hg} . A ten volt bias for T_s of 250°C and P_{Hg} of 1.2 microns appears to be large enough to sufficiently remove impurities to obtain very low carrier concentrations. Higher values of -13 and -20 clearly caused excessive Hg vacancies that could not be filled during the annealing process at 280/275 temperatures. The effect of bias on grain size needs to be studied; it is expected that a small amount of bias promotes some grain growth.

The substrate temperature during sputtering that yielded films with lowest carrier concentration was 250°C. Seven films deposited at 200°C did not yield carrier concentrations below 10^{16} cm^{-3} at 100°K. The experiments indicated that to assure that there are no cadmium vacancies in the sputtered films P_{Hg} should be kept less than 1.2 microns, perhaps as low as 0.9 to 1.0 microns to be on the safe side. The optimum value of T_s for this lower value of P_{Hg} might well be less than 250°C; an educated guess would be about 230°C.

The best results were obtained for a substrate annealing temperature of 280°C with the Hg pressure as high as possible (278°C for the pool of Hg). These temperatures are also accepted to be the best values for bulk crystals. Therefore, in future experiments at NJIT, these temperatures will be kept fixed and the sputtering parameters, particularly P_{Hg} , T_s , and substrate bias more finely tuned. The effect of longer annealing times must also be studied.

Another important parameter that was not changed during these annealing experiments was the substrate and its surface preparation. Because of the high cost of CdTe substrates, high resistivity Si substrates with (111) surface orientation were used. The procedure for introducing the Si wafers into the vacuum with the oxide supposedly completely removed must be examined closely. It is also possible that the use of substrates with surfaces a few degrees off the (111) plane would yield improved crystallinity. The application of Si substrates with micron-sized surface structures might be required to obtain film crystallinity necessary for photoconductors requiring high electron mobility.

Table A Deposition Parameters and Hall-Effect Data for As-Deposited Films

Deposition Parameters						Hall Effect Data Before Annealing			
Film No.	x-value	Deposit. Time [Hrs]	Mercury Pressure [mm]	Cathode Voltage [volts]	Substrate Temp. [°C]	Room Temperature		Low Temperature (-180°C)	
						Mobility [cm ² /volt-sec.]	Carrier Concent. x10 ⁻¹⁶ [cm ⁻³]	Mobility [cm ² /volt-sec.]	Carrier Concent. x10 ⁻¹⁶ [cm ⁻³]
1-CT	.27	8	7	1600	250	1045	61	1727	66
2-CT			↓	↓		1001	67.5	1656	75
3-Si			↓			721	12.6	852	14.1
4-CT			.5	1700		615	8.65	122	4.4
5-Si			↓			678	7.5	241	2.87
6-Si	↓		↓			958	6.6	434	2.5
7-CT	.2		.9			922	26.3	1372	21.2
8-Si			↓			1159	17.1	1527	13.5
9-CT	↓		↓			1051	28.7	1507	29
10-Si			↓	↓		1115	10.9	1781	0.88
11-Si	.18		1.2	2250		689	15	97	58.7
12-Si			↓			1110	7.1	237	15
13-Si			1.4	↓		567	3.3	527	3.3
14-Si			1.8-2.0	2400	300	870	1.2	1100	0.55
15-Si			↓			400	0.83	370	0.44
16-Si		↓	↓	↓	↓	700	3.1	340	2.1
17-Si		5	1.4	↓	250	1300	35	1920	34
18-Si	↓	↓	↓	↓	↓	1000	40	1400	40

Table B Annealing Conditions and Hall-Effect Data for Annealed Films
Data in Parentheses are As-Deposited Values from Table A. Data in Brackets are Values for Bulk Crystals

Annealing Conditions					Hall Effect Data After Annealing			
Film No.	Film Thick [μm]	x-value	Substrate Temp. (°C)	Mercury Pressure (mm)	Room Temperature		Low Temperature (-188°C)	
					Mobility [cm ² /volt-sec.]	Carrier Concent. x10 ⁻¹⁶ [cm ⁻³]	Mobility [cm ² /volt-sec.]	Carrier Concent. x10 ⁻¹⁶ [cm ⁻³]
1-CT	-8	.27			(1045)	(61)	(1727)	(66)
1-CT			280	17.3	514	3.5	33	21
1-CT	↓		280	24	3487	8.3	5473	8.6
					(5200)	(0.4)	(50,000)	(0.2)
2-CT	-8				(1001)	(67)	(1656)	(75)
2-CT			280	74	3799	38	7663	38.5
4-CT					(615)	(8.6)	(122)	(4.4)
4-CT			280	74	3722	28	8277	29
8-CT			280	33	3699	19	6717	19
6-Si					(958)	(6.6)	(434)	(2.5)
6-Si	↓		280	24	3905	11.1	7000	—
9-CT		.18			(1051)	(29)	(1507)	(25)
9-CT	↓		280	.27	1945	185	7132	181
18-Si	5.1				(1000)	(40)	(1400)	(40)
18-Si	↓		350	17.3	8500	3.4	23,800	5.4
					(15,000)	(3)	(150,000)	(0.1)
17-Si	5				(1300)	(35)	(1920)	(34)
17-Si	↓	↓	350	17.3	10,000	22	12900	18

Table 5.1 Annealed Film Data Reported in AFOSR Annual Report, June 1981

Table 5.2 Annealing Parameters and Conduction Properties for Thin Film Samples

No.	Run	Sample	Sputtering Parameter				Annealing			Room Temperature			L.N Temperature			Lowest Temp. (°C)
			Prf (w)	PHg (um)	Ts (°C)	Vb (v)	Temp. (°C)	uH (cm ² /v.sec)	c.c	uH	c.c	uH	c.c	uH	c.c	
1	AA-61	T74-S12	100	0.9	250	0	280/270	5142	n	2176	n	2176	n	2176	n	-170
2	AA-65	T75-S12	100	0.9	200	0	280/275	50	p	226	p	226	p	226	p	-174
3	AA-65	T76-S9	150	0.9	200	0	280/275	3709	n	4224	n	4224	n	4224	n	-174
4	AA-55	T77-S9	100	0.9	200	0	325/200	2736	n	300	n	300	n	300	n	-174
5	AA-55	T77-S11	100	0.9	200	0	325/200	2993	n	306	n	306	n	306	n	-174
6	AA-56	T78-S8	75	0.9	250	0	325/175	2923	n	345	n	345	n	345	n	-170
7	AA-57	T78-S12	75	0.9	250	0	325/175	799	n	981	n	981	n	981	n	-170
8	AA-59	T78-S7	75	0.9	250	0	325/175	751	n	1425	n	1425	n	1425	n	-171
9	AA-62	T78-S5	75	0.9	250	0	280/275	587	n	228	n	228	n	228	n	-174
10	AA-70	T78-S9	75	0.9	250	0	290/285									
11	AA-59	T81-S4	75	1.2	250	0	325/175	1408	n	1669	n	1669	n	1669	n	-170
12	AA-58	T82-S11	75	0.9	150	0	325/175	3062	n	4530	n	4530	n	4530	n	-170
13	AA-58	T82-S12	75	0.9	150	0	325/175	3153	n	4515	n	4515	n	4515	n	-172
14	AA-60	T82-S4	75	0.9	150	0	325/175	2193	n	3503	n	3503	n	3503	n	-170
15	AA-60	T83-S9	75	0.6	250	0	325/175	3453	n	550	p	550	p	550	p	-173
16	AA-57	T84-S3	75	0.9	250	-10	325/175	5131	n	4446	n	4446	n	4446	n	-173
17	AA-64	T85-S8	75	0.9	250	-20	280/275	2650	n	2950	n	2950	n	2950	n	-170
18	AA-67	T87-S4	75	1.2	250	-10	280/278	1345	n	8727	n	8727	n	8727	n	-170
19	AA-68	T87-S2	75	1.2	250	-10	285/283	2201	n	6555	n	6555	n	6555	n	-170
20	AA-69	T87-S3	75	1.2	250	-10	290/288	2697	n	5698	n	5698	n	5698	n	-28
21	AA-66	T88-S5	75	1.2	250	-13	280/275	3020	n	2358	n	2358	n	2358	n	-171
22	AA-77	T88-S6	75	1.2	250	-13	230/225	663	n	194	p	194	p	194	p	-176
23	AA-80	T88-S4	75	1.2	250	-13	310/305	1377	n	36	p	36	p	36	p	-179

Continue on next page.

No.	Annealing Run	Sample	Sputtering Parameter			Annealing Room Temperature		L.N Temperature		Lowest Temp. (°C)
			Pri (w)	PHg (um)	Ts (°C)	Vb (v)	Temp. (°C)	uH (cm ² /v.sec)	c.c (cm ⁻³)	
24	AANI-76	T88-S3	75	1.2	250	-13	230/225	54 p	6.3x10 ¹⁸	238 p 2.0x10 ¹⁸ -170
25	AANI-83	T88-S1	75	1.2	250	-13	280/275	622 n	1.0x10 ¹⁷	77 p 1.1x10 ¹⁸ -151
26	AANI-80	T88-S2	75	1.2	250	-13	310/305	25 p	8.7x10 ¹⁸	146 p 1.8x10 ¹⁸ -176
27	AA-83	T88-S7	75	1.2	250	-13	280/275	2143 n	1.7x10 ¹⁸	1429 n 1.7x10 ¹⁸ -145
28	AANI-75	T90-S2	df00	1.2	250	-10	230/225	406 n	5.8x10 ¹⁷	127 p 8.5x10 ¹⁷ -174
29	AA-79	T91-S2	75	0.9	250	-5	310/305	1682 n	3.8x10 ¹⁷	623 n 1.2x10 ¹⁷ -174
30	AA-82	T91-S5	75	0.9	250	-5	230/225	1073 n	3.0x10 ¹⁹	2501 n 3.0x10 ¹⁹ -168
31	AANI-74	T93-S5	75	1.4	250	-10	270/265	1758 n	2.8x10 ¹⁶	79 n 2.9x10 ¹⁶ -168
32	AA-76	T93-S1	75	1.4	250	-10	270/265	1920 n	3.8x10 ¹⁶	540 n 9.0x10 ¹⁶ -170
33	AA-77	T93-S8	75	1.4	250	-10	230/225	4552 n	1.9x10 ¹⁶	5192 n 4.0x10 ¹⁵ -170
34	AA-79	T93-S6	75	1.4	250	-10	310/305	987 n	6.0x10 ¹⁶	784 n 8.3x10 ¹⁶ -177
35	AANI-81	T94-S4	75	0.9	200	-8	230/225	4730 n	2.5x10 ¹⁶	5805 n 1.2x10 ¹⁶ -179
36	AA-81	T94-S3	75	0.9	200	-8	230/225	808 n	2.6x10 ¹⁸	985 n 2.7x10 ¹⁸ -168
37	AANI-78	T94-S5	75	0.9	200	-8	270/265	4358 n	3.1x10 ¹⁶	2389 n 6.4x10 ¹⁶ -176
38	AA-78	T94-S1	75	0.9	200	-8	270/265	644 n	1.5x10 ¹⁷	5914 n 4.6x10 ¹⁶ -169
39	AA-84	T94-S5	75	0.9	200	-8	280/275	3066 n	9.1x10 ¹⁷	4493 n 9.3x10 ¹⁷ -176
40	AA-84	T94-S1	75	0.9	200	-8	280/275	2169 n	5.5x10 ¹⁷	3961 n 5.5x10 ¹⁷ -177
41	AA-85	T94-S3	75	0.9	200	-8	350/345	507 n	1.5x10 ¹⁸	595 n 1.4x10 ¹⁸ -177

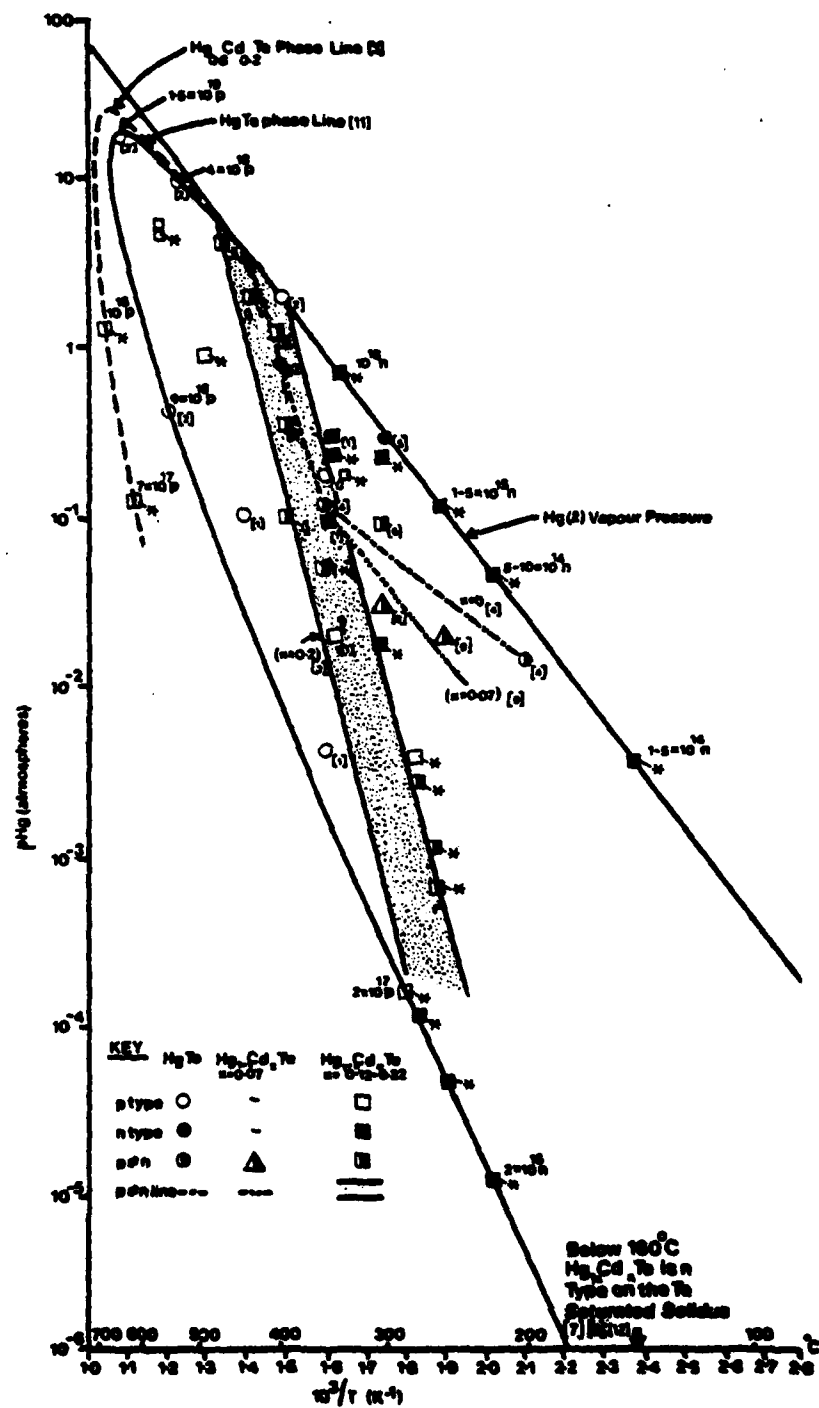


FIGURE 5.1 Pressure-temperature diagram for the $\text{Cd}_x\text{Hg}_{1-x}\text{Te}$ ($0 \leq x \leq 0.3$) system ref. 28

Group	I	II	III	IV	V	VI	VII	VIII
Expected role	Acceptor		Donor		Acceptor		Donor	
Element	Li Na K Cs Ag Au	Cd Hg	B Al Ga In	C Si Sn Ti Pb	N P As Sb Bi	Te	F Cl Br I	Fe Ni

Fig. 5.2 Expected role of impurities

Group	I			II	III			IV			V			VI	VII			VIII		
		M	H			M	H		M	H		M	H			M	H		M	H
Elements	Li	A	A	Cd	B			C			N			Te	F			Fe	I	
	Na			Hg	Al	D	D	Si	D	D	P	A	A		Cl	D	D	Ni		I
	K				Ga		D	Sn		I	As	A	A		Br		D			
	Cs	A	A																	
					In	D	D	Ti			Sb	A	A				D			
	Ag	A	A					Pb		I	Bi									
	Au	I	A																	

M=Majority, H=Minority, A=acceptor, D=donor, I=inactive.

Fig. 5.3 Electrical characters of impurities

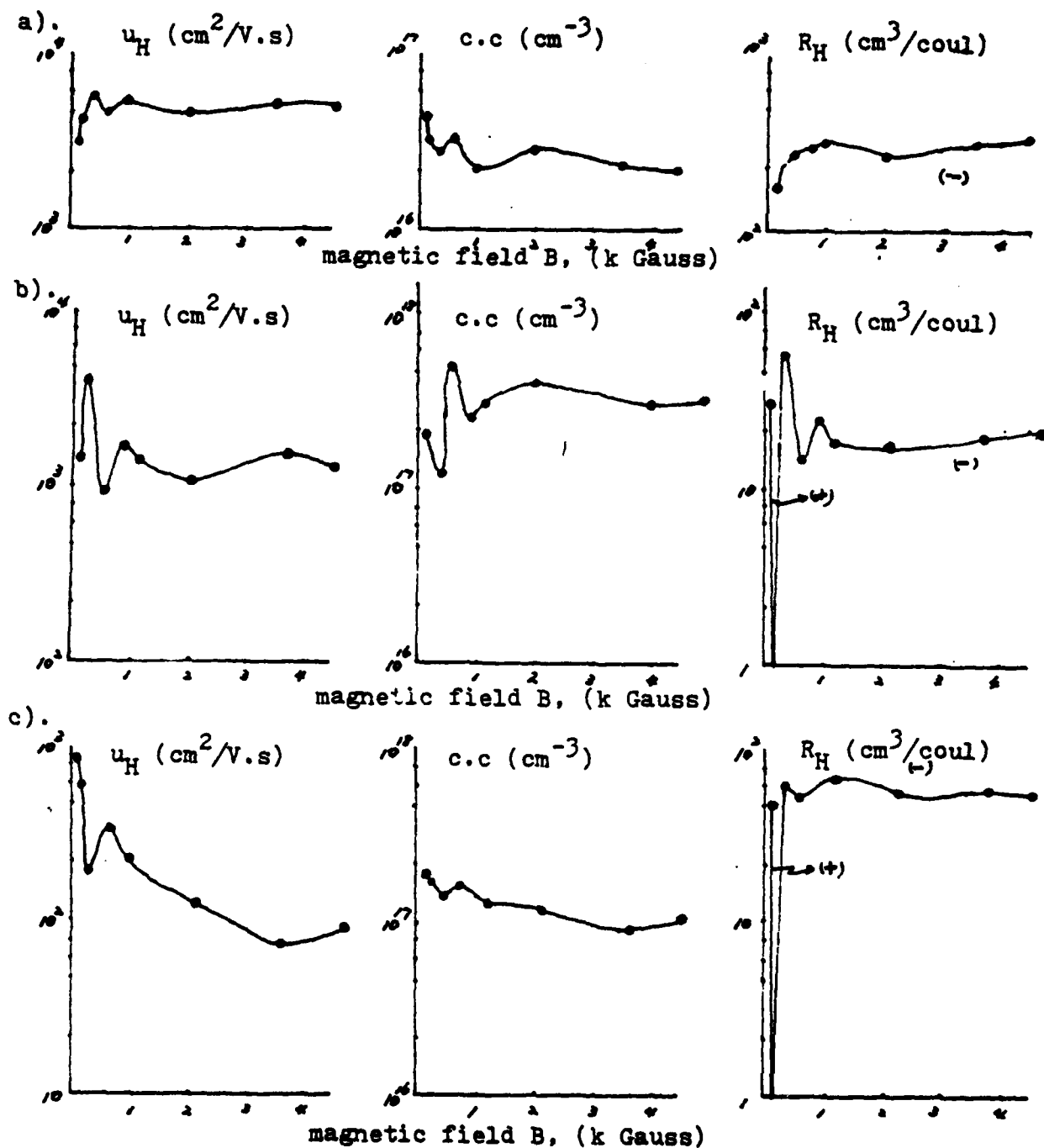


Fig. 5.4 Hall mobility, carrier concentration and Hall coefficient at 300°K vs. magnetic field for a). n-type sample, No. 35 AANI-81 (T94-54), b). p-type sample, No. 23 AA-80 (T88-54), c). p-type sample No. 25 AANI-83 (T88-51).

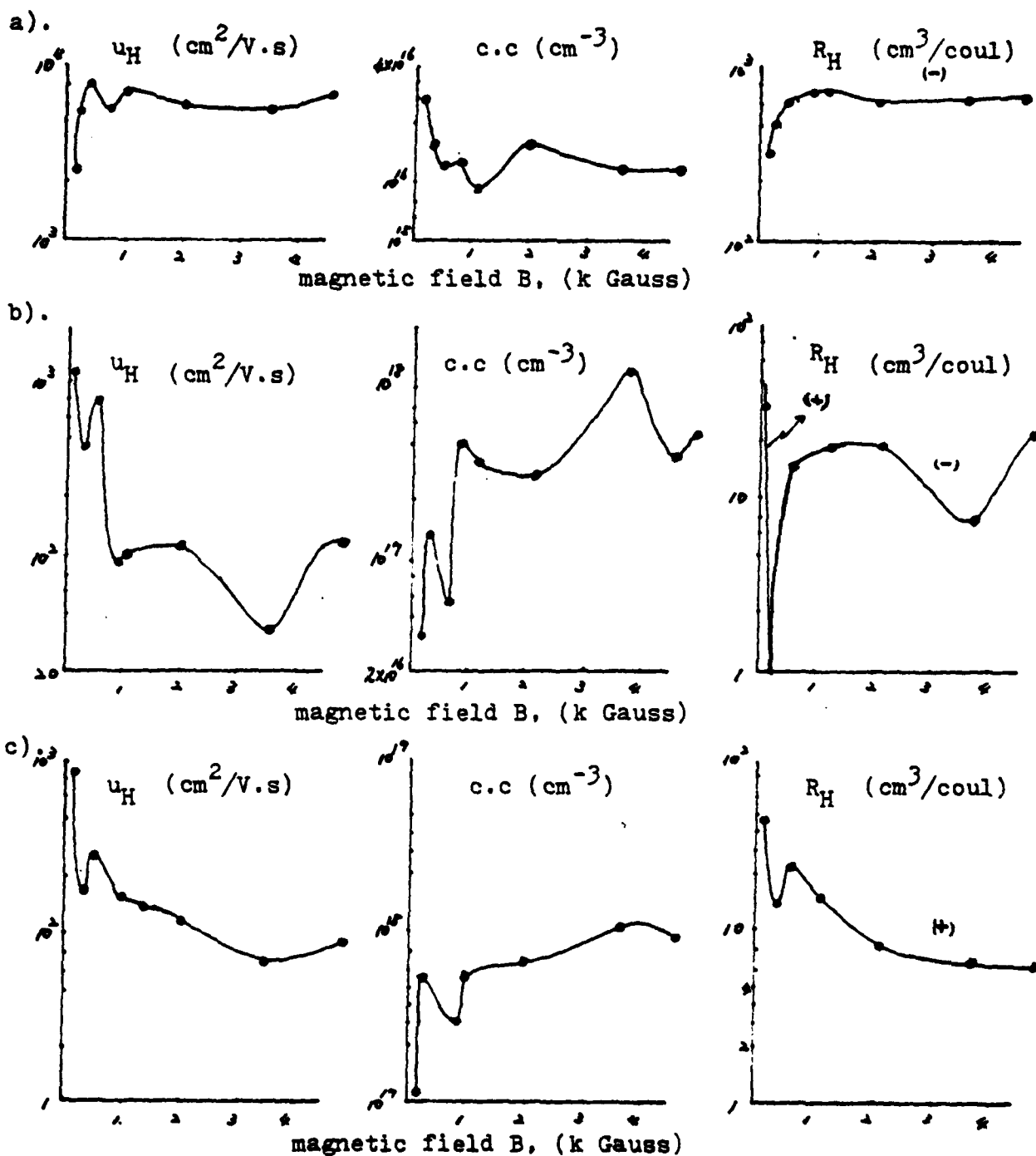


Fig. 5.5. Hall mobility, carrier concentration and Hall coefficient at 100°K vs magnetic for a). n-type sample, No. 35 AANI-81 (T94-54) b). p-type sample, No. 23 AA-80 (T88-54), c). p-type sample No. 25 AANI-83 (T88-51).

APPENDIX A

```

$JOB          MAB          ,P=25
C      THIS PROGRAM CALCULATES ABSORPTION
C      COEFFICIENTS VERSUS INCIDENT ENERGY
C      FOR N TYPE MERCURY CADMIUM TELLURIDE
C      THIN FILMS OF KNOWN BAND GAP ENERGY
C
1      INTEGER T
2      REAL SH,A,P
C
C      READ IN GAP ENERGY, PHOTON ENERGY,
C      TEMPERATURE AND FERMI ENERGY
3      200 READ,COMP,EG,HW,T,CONC,F
C      COMP=COMPOSITION
C      CONC=ELECTRON CONCENTRATION
C      EG=BANDGAP ENERGY
C      HW=PHOTON ENERGY
C      T=TEMPERATURE
C      F=FERMI ENERGY
4      WRITE(6,600) COMP,T
5      600 FORMAT('1','X=',F5.3,2X,'TEMPERATURE=',I3,1X,'W')
6      WRITE(6,700) EG,CONC
7      700 FORMAT('C','BANDGAP ENERGY=',F6.4,2X,
- 'ELECTRON CONCENTRATION=',E8.1)
8      IF(EG.EQ.0.0) GO TO 300
C
9      WRITE(6,400)
10     400 FORMAT('D','INCIDENT ENERGY',4X,'WAVELENGTH',4X,
- 'ABSORPTION COEFFICIENT')
C
C      READ IN CONSTANTS
11     E=12.0
12     P=0.850000E-07
13     SH=0.762001E-15
14     K=0.862860E-04
15     EXP=2.71828
C      E=DIELECTRIC CONSTANT
C      P=BAND MATRIX ELEMENT (EV-CM)
C      SH=BARRED PLANK'S CONSTANT/SQUARE
C      OF ELECTRON REST MASS (EV-CM2)
C      K=BOLTZMAN'S CONSTANT (EV/DEG K)
C      EG=BANDGAP ENERGY
C
C      READ IN NUMBER OF POINTS TO BE PLOTTED
16     N=20
C      CALCULATE SQUARE OF WAVE VECTOR
17     100 QA=(1.5*SH*EG)*(2*HW/EG-1)
18     QB=12.25*SH**2
19     QC=(4*P**2)/3
20     SD=4*QB*HW*(HW-EG)/(QC+QA)**2
21     QD=(1-QD)**0.5
22     SKW=((QC+QA)/CB)*(1-CG)
C      SKW=SQUARE OF WAVE VECTOR

```

APPENDIX A (cont'd)

```

C
C   CALCULATE HEAVY HOLE BURSTEIN-MOSS SHIFT
23  QE=(SKW*SH/D.4)/2
24  JF=-HW/(K*T)
25  JH=-(IF+GE)/(K*T)
26  QI=-(HW-P-GE)/(K*T)
27  BMH=(1-EXP**QF)/((1+EXP**QH)*(1+EXP**QI))
28  CJ=1/(137*(E**D.5))
29  OK=(1+(8*SKW**D**2)/(3*EG**2))**D.5
30  RKW=SKW**D.5
C   RKW=WAVE VECTOR (1/CM)
C
C   CALCULATE ABSORPTION COEFFICIENT
31  QL=(2.625*SH*EG)/(P**2)
32  QH=(RKW*EG)/(2*HW)
33  AHI=(CJ*QH*(QK+1))/(1+(QL*QK))
C
C   CALCULATE HEAVY HOLE ABSORPTION
34  AH=AHI*BMH
C
C   AH=HEAVY HOLE ABSORPTION COEFFICIENT
C
C   CALCULATE LIGHT HOLE ABSORPTION
35  GN=1342.32*P*E**D.5
36  QO=2*(EG/HW)**2
37  CP=(HW**2-EG**2)**D.5
38  ALI=CP*(1+QO)/GN
C
C   CALCULATE LIGHT HOLE BURSTEIN-MOSS SHIFT
39  QR=-(HW+EG-2*F)/(2*K*T)
40  QS=-(HW-EG+2*F)/(2*K*T)
41  BML=(1-EXP**QE)/((1+EXP**QR)*(1+EXP**QS))
42  AL=ALI*BML
C   AL=LIGHT HOLE ABSORPTION COEFFICIENT
C   FIND TOTAL ABSORPTION COEFFICIENT
C   FOR N TYPE FILM
43  AC=AH+AL
C   AC=ABSORPTION COEFFICIENT (1/CM)
C
44  WL=1.24/HW
C   WL=WAVELENGTH (MICRON)
C
45  WRITE(6,500)HW,WL,AC
46  500  FORMAT('D',F8.3,10X,F8.3,10X,E12.3)
C
47  N=N-1
48  IF(N.EQ.0) GO TO 200
49  HW=HW+.01
C
50  GO TO 100
51  300  STOP
52  END

```

SENTRY

25

APPENDIX B - COMPOSITION CALCULATIONS
Sample 1 (T74-S15):

The atomic percentages of the elements as found
by WDX analysis are as follows:

$$\text{Te} = 52.48\%$$

$$\text{Cd} = 8.71\%$$

$$\text{Hg} = 38.81\%$$

Method 1

Using Cd atomic % as determined and assuming Te
atomic % to be 50%,

$$x = \frac{\text{Cd atomic \%}}{50} = \frac{8.71}{50} = 0.1742$$

Method 2

Using the atomic % of both Cd and Hg as found and
assuming Te atomic % to be 50%

$$\text{CdTe mole fraction} = \frac{\text{Cd atomic \%}}{50} = \frac{8.71}{50} = 0.1742$$

$$\text{HgTe mole fraction} = \frac{\text{Hg atomic \%}}{50} = \frac{38.81}{50} = 0.7762$$

$$x = \frac{\text{CdTe mole fraction} + (1 - \text{HgTe mole fraction})}{2}$$
$$= \frac{0.1742 + (1 - 0.7762)}{2} = 0.199$$

Method 3

Using the atomic % of both Cd and Te as found,

$$x = \frac{\text{Cd atomic \%}}{\text{Te atomic \%}} = \frac{8.71}{52.48} = 0.1659$$

Method 4

Using the atomic % of Cd, Hg and Te as found,

$$\text{CdTe mole fraction} = \frac{\text{Cd atomic \%}}{\text{Te atomic \%}} = \frac{8.71}{52.48} = 0.1659$$

$$\text{HgTe mole fraction} = \frac{\text{Hg atomic \%}}{\text{Te atomic \%}} = \frac{38.81}{52.48} = 0.7395$$

APPENDIX B (cont'd)

$$\begin{aligned}
 x &= \frac{\text{CdTe mole fraction} + (1 - \text{HgTe mole fraction})}{2} \\
 &= \frac{0.1659 + (1 - 0.7395)}{2} = \frac{0.1659 + 0.2605}{2} \\
 &= 0.2132
 \end{aligned}$$

Method 5

Based on the assumption of Te atomic percentage being equal to 50% (as in the starting material), the modified atomic percentages of the elements can be calculated as follows:

$$\text{Te} = 50\%$$

$$\begin{aligned}
 \text{Cd} &= \text{Cd At. \%} \left(\frac{50}{\text{Cd At. \%} + \text{Hg At. \%}} \right) \\
 &= 8.71 \left(\frac{50}{8.71 + 38.81} \right) = 9.16\%
 \end{aligned}$$

$$\begin{aligned}
 \text{Hg} &= \text{Hg At. \%} \left(\frac{50}{\text{Cd At. \%} + \text{Hg At. \%}} \right) \\
 &= 38.81 \left(\frac{50}{8.71 + 38.81} \right) = 40.84\%
 \end{aligned}$$

Method 5 (cont'd)

$$\text{Cd mole fraction} = \frac{\text{Cd At. \%}}{\text{Te At. \%}} = \frac{9.16}{50} = 0.1832$$

$$\text{Hg mole fraction} = \frac{\text{Hg At. \%}}{\text{Te At. \%}} = \frac{40.84}{50} = 0.8168$$

$$\begin{aligned}
 X &= \frac{\text{CdTe mole fraction} + (1 - \text{HgTe mole fraction})}{2} \\
 &= \frac{0.1832 + (1 - 0.8168)}{2} = 0.1832
 \end{aligned}$$

The development of an economic sputtering technology for preparation of (Hg,Cd)Te films required attention to many important details associated with the sputtering deposition equipment and the preparation of targets from relatively low-cost HgTe and CdTe powders. These details are discussed in 2.1.1 and 2.1.2. Section 2.1.5 describes the work on control of a critical deposition parameter, the Hg sputtering gas pressure. Another task related to film deposition was preventing the build up and flaking of sputtered layers of (Hg,Cd)Te on various fixtures in the system, such as the substrate platen and the Hall-effect masks. This unexpected problem had to be solved, as discussed in section 2.1.6, to prevent small flakes depositing on the film and shielding it from sputtered material. The flakes caused film pockmarks and the conduction measurements of such films were not reliable. With this problem solved, the films with Hall-effect geometry were smooth, shiny and uniform in every respect, even after annealing.

The behavior of Hg-bombarded sputtering targets is very complex. The study of this behavior was a separate, but closely related, 4 year research project sponsored by the Army Research Office briefly described in section 2.1.3 ⁽⁴⁾. The most important finding of this study of sputtering targets was that Cd tends to be depleted from (Hg_{0.8}Cd_{0.2})Te sputtering targets when the Hg sputtering gas pressure rises above a value in the 1.2-1.4 micron range. It was also found that the time for the elemental concentrations to reach equilibrium on the front surface of the target was of the order of five minutes. The thickness of the altered layer (the region where the concentrations of Hg,Cd and Te are different than the original target material) continues to grow at a decreasing rate with time. The altered layer is typically about 3 microns thick after 6 hours of sputtering. The growth of the altered layer is a function of the sputtering yield of the three elements from the (Hg,Cd)Te matrix and their diffusion coefficients. Mercury diffuses in from the target surface while all three elements diffuse toward the surface from the back of the target. A model was developed and programmed onto the computer to calculate the concentration of Hg,Cd and Te as a function of time and distance from the surface. ⁽³⁾ The constants for the computer model were obtained from experimental XPS data of back-etched targets after they were sputtered. Another result obtained from the target research was that the 25 micron powder particles of CdTe and HgTe making up the low-cost targets tend to fuse together so that effectively the target becomes (Hg,Cd)Te polycrystalline material as it is sputtered with Hg vapor. The target area can be much larger than one can obtain using more-expensive polycrystalline ingots of (Hg,Cd)Te. Targets composed of a combination of pressed-powder and polycrystalline ingots were developed for the target research. Another part of the target research was the study in great detail of the topographical changes that occur in pressed-powder targets bombarded with Hg.

The sputtered film research concentrated on controlling conduction properties of (Hg,Cd)Te films deposited on Si substrates because of the high-cost of single crystal CdTe substrates with (111) surface orientation,

the large number of sputtered film samples required to study the effects of the many sputtering and annealing parameters, and the potential payoff of having (Hg,Cd)Te films on low-cost, electronically active Si substrates. The preparation of the Si substrates is critical and the details of the developed techniques are discussed in section 2.1.4. As pointed out by the author, in the proposal for the 81-82 thin film research, the development of the technology of micron-sized surface features in Si⁽⁷⁾ points to an opportunity for almost ensuring that sputtered (Hg,Cd)Te films on Si substrates can be single crystal. Unfortunately, the contacts developed with Lincoln Labs in 1981 did not result in our being able to obtain a supply of Si substrates with V-slot etched surface features. The study of control of film composition and stoichiometry by sputtering and annealing techniques and other tasks appeared to be of more importance for the development of (Hg,Cd)Te sputtering technology; therefore no significant work on the fabrication of Si substrates with etched surface features was done in 1981-1982. It is of comfort to know that such Si substrates could be used if the crystallinity of sputtered films on Si, even after annealing, limits the desired conduction properties.

Despite the complexity of the elemental concentration changes at the surface of a Hg bombarded target, it was clearly demonstrated that the composition of the film was the same (within the 4 to 5 percent measurement accuracy) as the effective x value of the targets composed of pressed powders of CdTe and HgTe. The results shown in section 2.3 were for the 0.2-0.27 compositional parameter range but most probably can be applied to the wider range of at least 0.18-0.3. This was a most important result that demonstrated a key advantage of the triode-sputtering technology for controlling film composition. The film composition can be shifted by simply changing the percentages of the relatively inexpensive CdTe and HgTe powders composing the pressed-powder target. The x value of the film is determined by the ratio of Cd to Te atoms sputtered at the substrate, since the sticking coefficients of Cd and Te are nearly one for the substrate temperatures used. Therefore, it is only necessary to control the arrival rate of Hg atoms, either sputtered from the target or supplied by the plasma, so that the films are stoichiometric.

The compositions of six sputtered films with x values in the 0.2-0.26 range were measured by Wavelength Dispersive Electronprobe Microanalysis (WDX) analysis at Structure Probe Inc., using as calibration standards a set of (Hg,Cd)Te ingots, borrowed from J. Schmidt of Minn. Honeywell Corp. The x values of the standards were known to be within one mole percent, according to Schmidt. The WDX measurement procedure and the results are discussed in detail in 2.3.4 and 2.3.5. These WDX measurements were supplemented by less expensive optical absorption measurements. A close correspondence between the results from the two measurements were obtained, as shown by the data in table 3.4. The pertinent theory for optical absorption in (Hg,Cd)Te was thoroughly investigated (11) and presented in section 2.3.1. By comparing the optical absorption data of the film samples measured by WDX with theoretical curves calculated for n and p-type films, including the Burstein-Moss shift, it was determined that the as-sputtered

films were p-type. This agreed with the conduction measurement results. It was therefore possible to calculate the x value from the optical absorption data. The problem that remains is to measure the composition of annealed films by optical absorption, rather than the more expensive WDX technique. The optical transmission measurements require larger area samples (about 1 cm in length) than the Hall-effect samples. Samples with 1 cm diameter tended to peel when annealed at temperatures near 280°C. The problem will be solved by further concentration on some of the preparation parameter details.

The structural properties of the sputtered films on Si and CdTe substrates were studied by X-ray diffraction and by SEM of chemically etched samples. As reported in 2.2 and in several publications^(5,6,7), the film samples with highest mobilities and most n-type behavior had nearly 100% (111) orientation for the polycrystallites composing the film. The (444) peak for these films was only 0.8 degrees, the same width as that for LPE films reported to be single crystalline⁽⁸⁾. However, the X-ray diffraction measurements did not reveal as much about the crystallinity of the film as supposed since films composed of differently sized polycrystallites in the plane of the film, but rotated about an axis perpendicular to the film surface, will both have 100% (111) orientation and the same half-width for the diffraction peak, unless the crystallites are less than about 0.1 micron. Rocking curve measurements can reveal the degree of orientation of the (111) crystallites. An NJIT annealed film measured at Marten Marietta⁽⁹⁾ had a rocking curve half-width of 4 degrees. Until films with smaller half-width are prepared or found, it will not be possible to measure the grain size of the crystallites by X-ray topography.

A rocking curve apparatus should be implemented at NJIT to help optimize the crystallite structure of the films. The half-width of the rocking curve peaks should be studied as a function of the sputtering and annealing parameters. It should be possible to exploit the complete (111) orientation of sputtered films on both Si and CdTe substrates to obtain films with a low density of grain boundaries by using a high temperature anneal, if necessary, followed by a low temperature anneal at 280/278°C to minimize native defects. The preparation of the Si substrate surface and the sputtering parameters, particularly the ones used in the initial growth of the film, should be related to rocking curve measurement results.

Although etched vertical lines seen in as-sputtered films were not observed in SEM observations of etched annealed films, direct observation of the grains by some techniques such as X-ray topography is required for a firm conclusion on the effects of annealing on grain size. An important objective, therefore, of future sputtering research is to prepare films with crystallites whose size can be measured and controlled. It will then be possible to compare the decrease in lateral electron mobility due to grain boundary scattering with that due to native defects. Of course for devices that have current flow perpendicular to the surface, such as photovoltaic detectors, the lateral mobility would not be important.

The dependence of the conduction properties on various sputtering parameters, particularly substrate temperature and dc bias, type of substrate and its surface preparation, deposition rate (r.f. power applied to the target), and Hg sputtering gas pressure, was studied and reported in section 2.4. This study, although limited, gave a better understanding of the interdependence of these parameters and pointed to more optimum sputtering conditions for obtaining either as-sputtered films with low carrier concentration and high electron mobility or films with properties such that after being annealed good film properties can be obtained (1).

In the first few years of this sputtering research, films with different x values were studied. However, it became evident that obtaining desired film properties was dependent on optimizing many interdependent sputtering and annealing parameters that were dependent on the x compositional parameter of the film. Therefore in early 1981 it was decided that the research would concentrate on optimizing the properties of films with the composition $x = 0.2$. Table 1.1 and 1.2 summarized the conduction properties of as-deposited $x = 0.2$ films. The highest electron mobility at low temperature, 87°K, was 6080 cm squared per volt second corresponding to a carrier concentration of 4×10^{16} cm⁻³. Samples from run 84 had higher mobilities, 7400, at an intermediate temperature of 175°K but apparently were p-type due to non-perfect stoichiometry. The films with highest mobility at low temperature were prepared with dc bias of 14 volts in the substrate. It is felt that much better results can be obtained for as-deposited bias-sputtered films by further optimizing the sputtering parameters particularly the substrate temperature (trying temperatures between 200 and 250°C), the substrate bias and surface preparation, and the Hg sputtering gas pressure.

The properties that were the main objective of the optimization of the sputtering and annealing parameters were low free carrier concentration and high electron mobility. Since electron mobility is a sensitive function of crystal quality, obtaining high electron mobility would demonstrate that the films were high quality and that the conduction properties could be controlled. The mobilities obtained so far in this research have been less than one tenth of the desired value at temperatures below 100°K. The results from a large number of annealing experiments showed that this is more probably due to the presence of Hg and Cd vacancies and foreign acceptor-like impurities than to a high density of crystal defects. Considerable progress was made in removing the impurities and vacancies by annealing techniques but further work on optimization of annealing parameters remains.

One of the initial annealing results, for an $x = 0.18$ film prepared in a two zone furnace at an annealing temperature of 350°C with 17.3 mm of Hg pressure was very encouraging. The electron mobility at -188°C was 23,800 cm squared per volt sec. or about 16% of the mobility expected for a perfect crystal, even though the film was only five microns thick and the carrier concentration about fifty times that for an intrinsic crystal. However, this film was not quenched after being annealed and it was not possible to reproduce the result, which later results showed was dependent on the improvement in the stoichiometry during the cooling down process and perhaps the introduction of n-type impurities. Later experiments, whose results are reported in table 5.2, were done by quenching the film so that the film properties would depend only on the annealing temperatures and the annealing time.

An important conclusion of the annealing experiments was that negative dc bias applied to the substrate during sputter-deposition effectively removed impurities and that films prepared without dc bias had p-type behavior, even after annealing, due to foreign impurities and not due to stoichiometric defects. An n-type film with a carrier concentration of only 10^{15} cm^{-3} at 103°K was prepared using a negative ten volt dc bias (sample No. 18 in table 5.2). The bias value is not yet optimized. Values in the 8 to 20 volt range were used. The optimum value is dependent on substrate temperature and Hg pressure for minimization of stoichiometric defects, i.e. Hg and Cd vacancies.

Different combinations of temperatures for the pool of Hg and the film-substrate were tried in the range of 230/225 to 310/305. The best results were obtained when the temperature of the Hg pool was as high as possible (slightly less than the substrate temperature) (50,51). The 280/278°C temperature combination will be used in experiments in the near future while fine tuning of key parameters, particularly substrate temperature and bias during the sputtering run, is done. The Hg pressure during the sputtering run should be kept to about 1 micron as higher pressures were shown, from both the annealing experiments and the target research, to result in Cd vacancies in the film that cannot be annealed out. Further details related to the conclusions that were made on optimization of film properties by annealing are given in 2.5.6.

Another important discovery was that films that were tested after sputtering and then annealed were effected by the indium that diffused from under the contact pads across the arms of the Hall effect sample to the tested central region. The indium sometimes improved the result by serving to make the annealed films more n-type. However, to clearly see the effects due to annealing, samples should be annealed without testing after sputtering and their pre-annealing conduction parameters determined by measurement on adjacent samples from the sputtering run. When indium was evaporated over the central region and then thoroughly etched off the surface before annealing, the carrier concentration after annealing was in the 10^{18} cm^{-3} range. Control of film properties with indium should be further investigated; however experiments in the immediate future will continue to concentrate on preparing nearly-intrinsic films.

A further area of research in 1981-82 was the study of the effect of magnetic field changes, in the 0.165-4.65 kilogauss range, on the Hall coefficient, R_H , and the mobility and carrier concentrations (52). These experiments established beyond doubt the conductivity type of the films (52). Films with decreasing mobility with decreasing temperature were p-type; oscillations of R_H with magnetic field were observed as predicted by Beer and Willardson (49) for p-type semiconductor material were overlapping bands with light and heavy holes. The lack of appreciable variation of R_H with magnetic field for the higher mobility films showed that they were n-type; the magnetic quenching effect was seen at low magnetic fields. M. Mulligan (1) also studied whether films were n-type, p-type or compensated based on their mobility versus temperature behavior. His objective was to find the real electron mobility of films from the experimental mobility versus temperature data, calculated from the measured R_H . This calculation assumes single carrier conduction. A computer program was written that calculated R_H and the mobility and carrier concentration that would be calculated, assuming

single carrier conduction, for films composed of different concentrations of acceptors and donors. The hole and electron mobilities were assumed to be that for bulk material. The conclusion drawn was that only if the donor and acceptor concentrations were large but nearly equal, not justifiable at this time, could the relatively low electron mobility versus temperature behavior found from our measurements, assuming single carrier conduction, be attributed to a simple mixed conduction effect. The computer program developed by Mulligan will be useful in analysis of future experimental results.

Another technique for possibly obtaining the real electron mobility of the deposited films and avoiding compensation and possible surface inversion effects is to use an FET structure to obtain material by applying positive gate voltage. Fu-Chung Chang has initiated an MS thesis in this area; a key task is to deposit insulating material on the surface of the film that will not change its material properties significantly. Evaporated ZnS and sputtered SiO₂ and CdTe are being tried with the present emphasis on depositing evaporated high resistivity ZnS that is nearly intrinsic.

Lifetime measurements were done in the 300-100°K range by exciting carriers with a GaAs laser. Lifetimes of about one microsecond were measured that increase only by a factor of three at the lower temperature. It was decided that the research in 81-82 should concentrate on obtaining high mobility films before further lifetime experiments were done since they were time consuming and tied up a vacuum system required for other work. However, lifetime measurements are planned for future research to completely characterize the material. NJIT is also planning to obtain Hall-effect measurements at 4°K to further characterize the material.

The thin film sputtering research has produced many interesting results and shown that high-quality sputtered films can probably be obtained on low-cost silicon substrates with further research. The most promising immediate research paths to achieve this result are further optimization of the sputtering parameters, while keeping the final annealing temperatures constant at 280/278°C. Included in the optimization of sputtering parameters is the use if possible, of starting target materials with higher purity than the 5 nines material which was available and used so far. A second path is to use two-step annealing processes; an initial high temperature anneal at 350°C, to insure sufficient crystallinity, and a second anneal at 280/278°C to insure stoichiometry. It is interesting to observe that MBZ films have been prepared on CdTe substrates with conduction properties similar to the as-sputtered film properties. However, after some experimentation, annealing parameters were found that were able to increase the mobility to much higher values^(53,54).

1. Mulligan, M., "Study of Conduction Properties of Triode-Sputtered ($\text{Hg}_{.8}\text{Cd}_{.2}$)Te Thin Films on Silicon and Cadmium Telluride Substrates, NJIT MSEE Thesis, October, 1982.
2. Gabara, T., "Study of Topographical Changes in Ion-Bombarded Target Surfaces of Mercury Cadmium Telluride", NJIT MSEE Thesis, October, 1980.
3. Bourne, B., "Study of Compositional Changes (Altered Layer) in (Hg,Cd)Te Targets Sputtered with Hg", NJIT MSEE Thesis, June, 1982.
4. Cornely, R. H., Final Technical Report, "Mercury Cadmium Telluride Sputtered Target Research", U.S. Army Research Office - Physics Division, Grant No. DAAG29-78-G-006, June 29, 1982.
5. Cornely, R.H. AFOSR Interim Scientific Report, June 28, 1979.
6. Cornely, R. H., Suchow, L., Gabara, T., Diodato, P., "RF Triode-Sputtered Mercury Cadmium Telluride Thin Films", IEEE Trans. Electron Devices Ed-27, 29 (1980).
7. Cornely, R. H., AFOSR Interim Scientific Report, June 1, 1981.
8. Harman T. C., "Optically Pumped LPE-Grown $\text{Hg}_{1-x}\text{Cd}_x\text{Te}$ Lasers", J. Electron Mat., Vol. 8, No. 2, 191 (1979).
9. Rocking curve X-ray diffraction and Laue measurements were done on a voluntary basis in November 1981 by Dr. William Beck and Dr. Norman Byers in Dr. Byers' research laboratory at Martin Laboratories, 1450 South Rolling Road, Baltimore, Maryland 21227. Dr. Cornely visited the Lab. on Nov. 20, 1981 to discuss the measurements and to give a seminar. A short report on the measurement results was written for Dr. Cornely by Dr. Beck.
10. Kane, E. O., Phys. Chem. Solids, 1, 249 (1957).
11. Haq, R., "The Determination of Composition of RF Sputtered ($\text{Hg}_{1-x}\text{Cd}_x$)Te Thin Films, NJIT MSEE Thesis, October, 1982.
12. Harman, T. C., Strauss, R., J. Appl. Physics, 32 (10), 2265 (1961).
13. Bebb, H. B., Ratliffe, C. R., J. Appl. Phys. 42 (8), 3189 (1971).
14. Andersen, W. W., Infrared Physics, 20, 363 (1980).
15. Andersen, W. W., Personal Communication of Dr. Andersen with Riaz Haq.
16. Bartlett, B. E., J. Material Science 4, 266 (1969).
17. Schmit, J. L., Stelzer, E. L., J. Appl. Physics, 40 (12) 4865 (1969).

- 18) Structure Probe Inc., Report On Microanalysis of the NJIT Samples, July, 1981.
- 19) Duerr, Steve, Personal Communication with Dr. Duerr, Laboratory Director of Structure Probe Inc., Metuchen, N. J.
- 20) Schmit, J.L., Personal Communication of Dr. Schmit with Riaz Haq.
- 21) Woolley, J.C. and Ray, B., J. Phys. Chem. Solids, Vol. 13, 151 (1960).
- 22) Developed by Dr. Lawrence Scuhow of the Dept. of Chem. Engr. and Chemistry and reported in reference 11, page 50.
- 23) Appendices D and E of reference 11.
- 24) Reference 5, page 27.
- 25) Cornely, R.H., Suchow, L., Mulligan, M., Haq, R., SPIE Proceedings, Vol. 285, 107 (1981).
- 26) Diodato, Philip W., "The Structural, Optical and Electrical Properties of RF Sputtered (Hg_{0.75}Cd_{0.25})Te Thin Films", NJIT, MSEE Thesis, Oct. 1980.
- 27) Krikorian, E., Personal Communication by Dr. Cornely with Dr. Esther Krikorian of the Aerospace Corporation, El Segundo, California.
- 28) Ferrar, R.H., Gillham, C.J., Bartlett, B., Ouelch, M., J. Material Science 12, 836 (1977).
- 29) Schmit, J.L. and Stelzer, E.L., J. Electronic Materials 7, 65 (1978).
- 30) Brebick, R.F., Schwartz, T.P., J. Electronic Materials 9, 485 (1980).
- 31) Schmit, J.L. and Bowers, J.E., Appl. Phys. Letters, 35, 457 (1979).
- 32) Reynolds, R.A., Brau, M.J., H. Kraus, Bate, R. T., J. Phys. Chem. Solids 32, suppl. 1, 511, (1971).
- 33) Bartlett, B.E., Capper, P., Harris, J.E., and Oulench M.J., J. Crystal Growth 49, 600 (1980).
- 34) Syllaos, A.J. and Williams, M.J., J. Vac. Sci. Tech. 21 (1), 201 (1982).
- 35) Chu, M., J. Appl. Phys. 51, 5876 (1980).
- 36) Johnson, E.S., and Schmit, J.L., J. Electronic Materials. 6, 25. (1977).
- 37) Capper, P., J. Crystal Growth, 57, 280 (1982).
- 38) Kumar, V. and Kröger, F.A., J. Solid State Chem 3, 389 (1971).

- 39) Hershman, G.H., Zlowanov, V.P., Kröger, F.A., J. Solid State Chem 3, 401 (1971).
- 40) Zanio, K., "Semiconductors and Semimetals" Vol. 13, Academic Press N.Y. (1978).
- 41) Kröger, F. A. "The Chemistry of Imperfect Crystals", North Holland Inc., N.Y. (1973).
- 42) Chern, S.S., Vydyanath, H.R. and Kröger, F.A., J. Solid State Chem. 14, 33 (1975).
- 43) Chern, S.S. and Kröger, F.A., J. Solid State Chem. 14, 44 (1975).
- 44) Belov, V., Personal Communication of Dr. Cornely with Dr. Valery Belov, Vice President of Engineering, Infrared Associates, New Brunswick, N.J.
- 45) Margalit, S. and Nemirovsky, Y., J. Electrochem. Soc. 127, 6, 1406 (1980).
- 46) Vydyanath, H.R., J. Electrochemical Soc. 128, 12, 1981.
- 47) Cornely, R.H., Suchow, L., Mulligan, M. Chan, T.O., Haq, R., J. Vac. Science and Tech., 18 (2), 190 (1981).
- 48) K. Seeger, "Semiconductor Physics", Page 311, Springer-Verlag/Wien, 1973.
- 49) A.C. Beer and R.K. Willardson, Physical Review, 110,6,1286, 1958.
- 50) Professor Robert Brebick suggested to Dr. Cornely at the (Hg,Cd)Te Workshop in Minneapolis in Oct. 1981 that best results would probably be obtained by keeping the temperature of the Hg Pool as close to the annealing temperature as possible.
- 51) Dr. Valery Belov, Vice President of Engineering at Infrared Associates, first suggested to Dr. Cornely that the optimum temperature for annealing would be in the 275-285°C range.
- 52) Wu, Chia-Jen, "Dependence of the Conduction Properties of Annealed Films of (Hg_{0.8}Cd_{0.2})Te on Sputter-Deposition and Annealing Parameters", NJIT MSEE Thesis, Oct. 1982.
- 53) Faurie, J.P., A. Million and G. Jacquier "Thin Solids Films", 90 (1982) 107-12.
- 54) Faurie, J.P., A. Million, Appl. Phys. Lett. Vol. 41, No. 3, Aug. 1, 1982.

5.0 Interactions and Publications

The following important interactions occurred with other scientific researchers during the 1977-82 grant period.

- 1) On July 24, 1978, Dr. Cornely met with Dr. Gerard Cohen-Solal and Dr. P. Bailly at the Central National Scientific Research Laboratory - C.N.R.S. in Bellevue (Paris) France. Dr. Cohen-Solal worked with HgCdTe beginning in the mid-sixties and had been sputtering the material since 1972. He obtained much information about sputtered HgCdTe films, some of which will not be published. Important discussions took place, about our work with Si substrates and pressed-powder targets. The French work resulted in good quality photodiodes being fabricated and these diodes are now manufactured by a French company LETI, according to Dr. Cohen-Solal. Another company was licensed to manufacture a special sputtering system for HgCdTe thin films. The C.N.R.S. research differed from that at NJIT in that their sputtering targets were from single crystal material and smaller (215 mm²) compared to our pressed powder targets of 5.7 cm diameter (2580 mm²) and 2.85 cm diameter (645 mm²). They later reported using larger area pressed-powder target material and Si substrates. Their sputtering system is smaller and their triode plasma is supported by an external magnetic field. They reported problems in making Hall-effect measurements on their polycrystalline films. The films used to make photodiodes with good characteristics were poly-crystalline; however, the grain boundaries, spaced about one micron apart, are perpendicular to the film surface and do not effectively influence photodiode current which flows parallel to these boundaries.
- 2) Dr. M.H. Francombe of Westinghouse Research Laboratories, Pittsburgh, PA 15235 visited the NJIT Laboratory in the summer of 1977. Also, the research progress and problems were discussed with Dr. Francombe several times in telephone conversations during the grant period.
- 3) Dr. Peter Brott, Santa Barbara Research Center, Goleta, Calif. 93017 has continually expressed an interest in the research. Dr. Brott kindly supplied the project with a large number of discarded polycrystalline HgCdTe ingots. These ingot slabs, about 500 grams, were used to make targets for the ARO research.
- 4) Dr. Esther Krikorian, a research scientist at General Dynamics Corp., Pomona, Calif. Division, noted for research on sputtered PbSnTe infrared detector material, visited the NJIT research laboratory with Dr. Lowell Williams of Raytheon Corporation in 1977. Important information was exchanged during her five hour visit. Dr. Krikorian maintained an active interest in the HgCdTe research and was kept aware of the work at NJIT throughout the research period. Dr. Krikorian maintained her interest in the NJIT work after joining the Aerospace Corporation in 1981. At the AVS meeting in Detroit in 1980, she reported on results she obtained at General Dynamics Corp. on Hg triode-sputtering of (Hg,Cd)Te on CdTe substrates.
- 5) Dr. Wolfgang Faist and Mr. Bill Pinkaton of Raytheon Corp., Mass. and Mr. Lowell Williams of Kuras-Alterman Corp. (now a subsidiary of Raytheon Corp.) visited the Laboratory on January 5, 1978. Mr. Williams as a systems engineer at Kuras Alterman Corp., worked with Dr. Cornely as early as 1975

on obtaining government support for Hg,Cd)Te sputtering research at NJIT.

6) Informal discussions concerning the NJIT research were held at the October 1980 A.V.S. meeting with Dr. Esther Krikorian (General Dynamics Corp., Pomona, Calif.), Dr. Joe Greene (Univ. of Illinois), Dr. Richard Gambino (IBM Research Center) and Dr. Francombe (Westinghouse Research Center). Dr. Greene has considerable experience sputtering GaAs and said that although (Hg,Cd)Te is a more difficult material, he believed that good (Hg,Cd)Te thin films could be obtained by optimizing sputtering parameters, even without using annealing techniques. Dr. Krikorian said that she has started a (Hg,Cd)Te sputtering research project and had obtained very high as-deposited mobilities on (111) oriented, single crystal CdTe substrates.

7) At the Electrochemical Society meeting on May 8, 1980 Dr. Cornely met with Dr. Ted Wong and Mr. John Miles of the New England Research Center for several hours. All the experimental results on sputtered (Hg,Cd)Te thin films obtained at NJIT up to that time were presented to them in complete detail. Following the oral presentation at the Electrochemical Society meeting, the results were discussed with various members of the Honeywell Research Center in Boston. The following day Dr. Cornely met for two hours with Dr. Sood (of Honeywell Corp.) and discussed in complete detail the (Hg,Cd)Te research at N.J.I.T.

8) Ted Harmon of Lincoln Labs discussed (Hg,Cd)Te thin films research in several phone conversations and at the SPIE East Symposium in April 20-24, 1981. His experience with LPE grown (Hg,Cd)Te films was very valuable for consultation on the sputtered film research, particularly for verifying the possible annealing temperatures and pressures that can yield good films.

9) Dr. Richard Schooler, the group leader of the Sensor Physics Section at the Aerospace Corporation, visited the NJIT laboratory for several hours. He was interested in learning about the sputtering research program and in meeting potential employees in (Hg,Cd)Te work at Aerospace Corporation. The Air Force sponsored thin films program was discussed in detail along with some mutual problems, particularly the need for basic information on (Hg,Cd)Te (such as absorption versus composition, absorption versus carrier concentration, and mobility versus impurity concentration) that remains unknown or unpublished by (Hg,Cd)Te device manufacturers and scientists. He also was particularly interested in our research of ion-bombardment effects on (Hg,Cd)Te and its meaning with respect to measuring composition.

10) Valuable consultations were held with Dr. Valery Belov, Vice President of Engineering of Infrared Associates, New Brunswick, N.J. Dr. Belov, a recent immigrant from the Soviet Union where he was a Professor of Physics, had considerable experience with diffusion in semiconductors, particularly CdTe and (Hg,Cd)Te.

11) At the October 1980 AVS meeting in Detroit, Dr. Cornely met Michael Geis of Lincoln Labs., who has been actively working for several years on graphoepitaxy. He agreed to send samples of Si with etched surface structure. Films of (Hg,Cd)Te were sputtered on these substrates, which unfortunately were of low resistivity and had a non-optimum saw-tooth structure (were remove overetched and underetched).

- 12) Dr. J. Schmidt of Honeywell Corp., Minneapolis, Minn. kindly lent NJIT a set of about 12 pieces of $(\text{Hg}_{1-x}\text{Cd}_x)\text{Te}$ material with different x values. These standards were used to determine the accuracy of electron microprobe measurements made at Structure, Metuchen, N.J.
- 13) Dr. E. Wiener-Avnear, senior scientist at Hughes Aircraft Co., discussed the NJIT $(\text{Hg},\text{Cd})\text{Te}$ sputtering research for several hours at the AVS 1980 Detroit Symposium. He was sent copies of theses and published papers on NJIT's $(\text{Hg},\text{Cd})\text{Te}$ research.
- 14) U. Solzbach of the Fraunhofer-Inst. Angew. Festkoerperphys., Freiburg, Fed. Rep. of Germany responded to an NJIT inquiry regarding his ESCA research of argon-bombarded $(\text{Hg},\text{Cd})\text{Te}$ material and the growth of oxides on $(\text{Hg},\text{Cd})\text{Te}$.
- 15) A grant received from the Army Research Office Durham, N.C., Physics Division, DAAG29-78-G0066 in March, 1978 supported closely related but distinctly separate HgCdTe target research. This grant was renewed on March 1979 and on March 1980 and continued on a no-cost extension until June 1982. The objective of this grant was to develop an understanding of the complex phenomena involved with sputtering the triconstituent target material HgCdTe and to develop practical methods of making good HgCdTe sputtering targets.
- 16) Mr. Irwin Kudman, President of Infrared Associates, Newark, N.J. served as a valuable consultant to this research since 1977 and also supplied the project with HgCdTe ingots which were used to make targets.
- 17) Dr. Cornely gave a seminar on the $(\text{Hg},\text{Cd})\text{Te}$ research for Dr. Norman Byer's Research Dept. at Martin Marietta's Research Laboratory in Baltimore, Maryland. As reported in reference 9 for the research report, Martin Marietta made x-ray topography measurements on NJIT films.

The following oral technical presentations were made during the grant period:

- 1) "Properties of R.F. Sputtered, Mercury Cadmium Telluride Thin Films" by Dr. R.H. Cornely, L. Suchow, Dennis DeRidder, Thaddeus Gabara, and Phillip Diodato presented at the Electrochemical Society, Inc., Spring meeting in Boston, Mass. May 6-11, 1979 in the Semiconductors and other Electronic Materials Session. Dr. A. Sood of the Honeywell Research Center, Boston was the session chairman.
- 2) "Electrical Properties of R.F. Triode-Sputtered $(\text{Hg},\text{Cd})\text{Te}$ Films" by R.H. Cornely, P. Diodato, T. Gabara, and L. Suchow presented at the National Symposium of the American Vacuum Society on Oct. 4, 1979 in the Thin Films Session. R. Gambino of the IBM Research Center, Yorktown Heights, was the session chairman.

- 3) "The Effects of Annealing in Hg Vapor on the Properties of rf Sputtered Thin Films of $(\text{Hg}_{1-x}\text{Cd}_x)\text{Te}$ by R.H. Cornely, L. Suchow, T. Chan, M. Mulligan, R. Haq and C. Mehta presented at the Thin Films Session on Sputtering and Ion Beam Deposition at the American Vacuum Society's 27th National Symposium in Detroit on October 14, 1980.
- 4) "Properties of rf Triode-sputtered $(\text{Hg}_{1-x}\text{Cd}_x)\text{Te}$ Thin Films" by R. Cornely, L. Suchow, M. Mulligan, and R. Haq was given at the Society of Photo-Optical Instrumentation Engineer's Symposium East (SPIE-East) in Washington, D.C., on April 24, 1981.

The following publications resulted from the research of this grant :

- 1) "Properties of R.F. Sputtered, Mercury Cadmium Telluride Thin Films". by R.H. Cornely, Lawrence Suchow, Dennis DeRidder, Thaddeus Gabara, Philip Diodato, Extended Abstracts volume 79-1, Electrochemical Society Meeting, May 6-11, 1979, Boston, Mass., p. 390.
- 2) "R.F. Triode-Sputtered Mercury Cadmium Telluride Thin Films", by R.H. Cornely, Lawrence Suchow, Thaddeus Gabara, and Philip Diodato, I.E.E.E. Transactions on Electron Devices, Vol. ED27, No. 1, January, 1980.
- 3) R.H. Cornely, L. Suchow, T. Chan, M. Mulligan, R. Haw, C. Mehta, "The Effects of Annealing in Hg Vapor on the Properties of rf Sputtered Thin Films of $(\text{Hg}_{1-x}\text{Cd}_x)\text{Te}$ ", Journal of Vacuum Science and Technology, Vol. 18, No. 2, March 1981, pp. 190-194.
- 4) R.H. Cornely, L. Suchow, M. Mulligan, R.Haq, "Properties of rf Triode-Sputtered $(\text{Hg}_{1-x}\text{Cd}_x)\text{Te}$ Thin Films, Proceedings of the Infrared Materials Session of the Society of Photo-Optical Instrumentation Engineer's Symposium East on April 21-24, 1981 in Washington, D. C.
- 5) Five MSEE theses have been written at NJIT on $(\text{Hg},\text{Cd})\text{Te}$ sputtering research and two theses are close to completion. The abstracts of these theses are given in Section 6.0.
- 6) A patent disclosure written on October 29, 1979 was sent to AFOSR.

6.0 List of Contributing Personnel in the 1977-82 Grants

The Principal Investigator was Dr. Roy H. Cornely, Associate Professor of Electrical Engineering Dr. Lawrence Suchow, Professor of Chemistry in the Department of Chemical Engineering and Chemistry, served as Co-investigator.

The following graduate students were partially supported by the AFOSR grants: Dennis DeRidder, Philip Diodato, Tai-On Chan, Michael Mulligan, and Chia-Jen Wu. Abstracts of Mr. Diodato's and Mr. Mulligan's theses are on the following pages. Mr. Wu's thesis, Dependence of the Conduction Properties of Annealed Films of (Hg_{0.8}, Cd_{0.2})Te on Sputter-Deposition and Annealing Parameters, is scheduled for final typing in October, 1982. Mr. Chan's and Mr. DeRidder's theses work was not completed. Riazul Haq worked on the (Hg,Cd)Te film research while supported by an NJIT graduate research assistantship. The abstract of his completed MSEE thesis is included. The abstracts of the MSEE theses on sputtered target research by Robert Bourne and Thadeus Gabara also follow. Mr. Fu-Chung Chang is presently doing an MSEE thesis on (Hg,Cd)Te FET Structures.

Undergraduate students provided important support for this research. Michael Mulligan, supported by NJIT, worked for several years on the thin film research as an undergraduate student. Chetan Mehta, also supported by NJIT, has been a most valuable contributor to the research effort for more than two years. Other undergraduate students who have been involved with many of the practical tasks associated with the thin film research are: Richard Bystrak, Omar Cassola, Bhavesh Desai, John Hyland, Rolando Ogyueria, and Young-Shin Pyun.

ABSTRACT

Title of Thesis: The Structural, Optical, and Electrical Properties of RF-Sputtered $(\text{Hg}_{0.75}\text{Cd}_{0.25})\text{Te}$ Thin Films

Philip W. Diodato, Master of Science in Electrical Engineering, 1980

Thesis directed by: Roy H. Cornely, Assistant Professor of Electrical Engineering.

The electrical, structural, and optical properties of thin films of $(\text{Hg}_{0.75}\text{Cd}_{0.25})\text{Te}$ from thirty-one RF triode sputtering deposition runs are presented and analyzed. Films 1 - $3\mu\text{m}$ thick were deposited onto Si, CdTe, glass, and mica substrates. Pressed powder targets, 2.1 and 4.6cm diameter, were bombarded with Hg ions with the Hg pressure in the 1 to 2 millitorr range. The targets were made from either a physical mixture of HgTe and CdTe powder or a powder ground from a solid solution ingot of $(\text{Hg}_{0.75}\text{Cd}_{0.25})\text{Te}$. The purpose of the research was to develop large area, high quality thin films for infrared detectors in the 3 to 25 micron wavelength range.

Infrared spectrophotometry revealed that films [on (111) Si and CdTe substrates] which x-ray diffraction showed to have (111) crystal orientation, 100%, had optical absorption comparable with that of single crystals. These films were obtained with an RF power target density of 10 to 20 watts/cm^2 and a substrate temperature of 200 to 260°C . Poorer quality films obtained with other sputtering parameters were found to have a mixture of (311), (111), and other crystal orientations. The highest electron mobility values of $1.8\mu\text{m}$

as-deposited thin films on Si substrates were $550\text{cm}^2/\text{v}.\text{sec}$ at 300°K and $403\text{cm}^2/\text{v}.\text{sec}$ at 85°K . Although annealing parameters were not optimized, a film $3.6\mu\text{m}$ thick annealed at 340°C in a Hg atmosphere of 558mm of Hg had an n-type mobility of $2.2 \times 10^3\text{cm}^2/\text{v}.\text{sec}$ at 300°K .

ABSTRACT

Title of Thesis: Study of Topographical Changes in
Ion-Bombarded Target Surfaces of
Mercury Cadmium Telluride

Thaddeus John Gabara, Master of Science in Electrical
Engineering, 1980

Thesis Directed By: Dr. Roy H. Cornely, Assistant
Professor of Electrical Engineering

Two 2.86cm diameter pressed powdered targets were extensively studied using scanning electron microscopy and energy dispersive x-ray analysis. The targets were rf sputtered for 6 hours in a triode sputtering system, using a plasma confinement box and an rf power density of $28.87\text{W}/\text{cm}^2$. One target was made by grinding a polycrystalline ingot of Mercury Cadmium Telluride, with 25 mole percent of CdTe, so that the powder particles have an average size of about $7\mu\text{m}$. Only particles larger than $3\mu\text{m}$ were measured. The powder for the other target (physical mixture) had the same mole percent of CdTe and about the same particle size; however, it was made by mixing powders ground from HgTe and CdTe ingots.

It was revealed that cones with heights ranging from less than 1 μ m to as much as 150 μ m form as the surface is eroded away. The height depends on the initial particle size, depth of erosion, surface migration and redeposition. The nonuniform ion dosage across the target, due to the target mask, enabled the cone formation and other surface erosion processes to be studied as a function of total ion dosage.

It was found that the largest cones possessed the smallest vertex angles. Unlike the solid solution target, the cones of the physical mixture target had two distinct vertex angle distributions, corresponding to HgTe and CdTe cones.

The smallest vertex angles of HgTe, CdTe and (Hg,Cd)Te were 28°, 17.5° and 23.5°, respectively. These cones all occur in a groove about 0.88cm from the target center, where the erosion rate is a maximum of about 175 Å/sec, due to the higher bombarding ion dosage.

The cones deteriorate after the large particle at the vertex of the cone is eroded away. In the solid solution target this form of deterioration occurs often; for the physical mixture targets most of the cones fracture before the peak deteriorates. The fractures are possibly due to the expansion coefficient differences between HgTe and CdTe. It appears as if the fractured material remains ^{on} the surface of the target.

The compositional studies indicate that the lightly bombarded regions of the solid solution target have an in-

crease in cadmium and a decrease in mercury concentration, while the vertex midpoints of large cones are depleted of Cd. The energy dispersive x-ray mapping of the physical mixture target revealed that in the lightly bombarded regions CdTe is possibly migrating on the surface while a mapping of the larger cones reveals that back-scattering is evident. Despite these compositional changes, optical absorption studies of the deposited films showed that their composition was that of the original unspattered target.

ABSTRACT

Title of Thesis: Study of Conduction Properties of Triode-Sputtered $(\text{Hg}_{0.8}\text{Cd}_{0.2})\text{Te}$ Thin Films on Silicon and Cadmium Telluride Substrates

Michael A. Mulligan. Master of Science, 1982

Thesis directed by:

Dr. Roy H. Cornely
Associate Professor

Department of Electrical Engineering

The dependence of the conduction properties of $(\text{Hg}_{0.8}\text{Cd}_{0.2})\text{Te}$ thin films triode-sputtered onto silicon and cadmium telluride substrates on deposition parameters (particularly substrate bias and temperature, Hg sputtering gas pressure, and deposition-rate) was studied. Five to ten micron thick films were characterized on the basis of free electron mobility measured by the Hall effect at temperatures between 77 and 300 degrees Kelvin. Highest electron mobilities were 4330 cm square per volt

second at 300 degrees Kelvin and 7400 at 175 degrees. with carrier concentrations in low 10 to the sixteenth range. Best film results were obtained with a substrate dc bias of 14 volts. a substrate temperature of 250 degrees centigrade. and an applied rf power density of 1.32 watts per square cm. The mercury pressure for sputtering. in the 0.9-1.4 micron range studied, was found to have a strong effect on films grown with dc bias applied to the substrate. Further fine tuning of these parameters, as well as deposition rate and substrate temperature should yield better results. A computer model was used to investigate the possible effects of mixed conduction on Hall measurement results.

ABSTRACT

Title of Thesis: Study of Compositional Changes (Altered Layer) in (Hg,Cd)Te Targets Sputtered with Hg Vapor.

Robert Granville Bourne: Master of Science in Electrical Engineering, 1982

Thesis directed by: Roy H. Cornely
Associate Professor of Electrical Engineering

Six mercury cadmium telluride targets (5.74 cm diameter) with six polycrystalline ($\text{Hg}_{0.8}\text{Cd}_{0.2}\text{Te}$) ingots (1 x 3 x 0.7 cm \pm 20%) epoxied on them, were r.f. sputtered

in an MRC-8800 triode system for 1, 2, 3, and 5 minutes. The six sputtering runs were made with 3 different Hg pressures of 1.0, 1.25, and 1.6 μm while the uniform target power density was kept constant at 7.7 w/cm^2 . After sputtering a target, $\text{Br}_2 + \text{CH}_3\text{H}$ was used to chemically etch the sputtered ingots to different depths. The surface composition of the etched ingots was measured with x-ray Photo Spectroscopy (XPS). The Hg, Cd and Te concentrations were thus obtained at six different depths into the target. From these data, the formation of the altered layer as a function of Hg pressure and sputtering time was studied.

The compositional studies indicated that the first 4000⁰Å of the sputtered ingots was enriched in Te and depleted of both Hg and Cd. The results also revealed that it takes three minutes for the surface composition to reach equilibrium. As the Hg sputtering gas pressure increased, the Hg surface concentration increased while the Te concentration decreased.

A mathematical model was developed for computing the altered layer composition of (Hg, Cd)Te targets under different sputtering conditions and as a function of time. Some experimental data were used to obtain constants for the mathematical model. Computer results using the mathematical model were in good agreement with experimental results.

Below 1.45 μm Hg gas pressure, the surface concentration ratio was experimentally found to be 12:1:87 (Hg:Cd:Te). As

the Hg gas pressure increased to 1.6um, the Hg concentration increased, and the Te concentration decreased. The computer analysis showed that above 1.6um of Hg pressure the concentration ratio remains constant at 31:1:68 (Hg:Cd:Te).

- ABSTRACT

Title of Thesis: The Determination of Composition and General Characterization of $\text{Hg}_{1-x}\text{Cd}_x\text{Te}$ Thin Films.

Riazul Haq, Master of Science in Electrical Engineering, 1982.

Thesis Directed By: Roy H. Cornely,
Associate Professor of Electrical Engg.

Two methods were used for measuring the control over composition 'x' and compositional uniformity of $\text{Hg}_{1-x}\text{Cd}_x\text{Te}$ triode sputtered thin films. The films were deposited on high resistivity Si substrates in controlled Hg pressure by r.f. sputtering of cold-pressed targets made from a homogenized physical mixture of HgTe and CdTe powders. Three 5.7 cm diameter targets, containing 20, 25 and 27 mole percent of CdTe powder, were used to deposit six samples which were studied in detail.

The two methods for finding the composition of the samples were: (a) infrared spectroscopy, (b) WDX electron microprobe analysis. The estimation of the x-value through optical measure-

ments involved the comparison of the measured infrared absorption with absorption curves calculated from k.p. theory. Before making measurements on the r.f. sputtered thin film samples, the accuracy of the WDX electron microprobe measurements was determined to be within $\pm 5\%$ by using EDX standards obtained from the Honeywell Corporate Research Center, Min. With the exception of one sample with target $x = 0.27$ the 'x' values of the samples determined by the two methods were in agreement within the accuracy ($\pm 5\%$) of the microprobe measurement. It was shown that the x-values of the films could be controlled within $\pm 5\%$ of 0.20, 0.25 and 0.27 CdTe mole fraction in the respective targets. For example, the optically estimated x-value of one sample deposited using a target with $x = 0.200 \pm 0.004$ was 0.204 and the microprobe measured value was 0.20 ± 0.01 . The optical measurements were also correlated with x-ray diffraction and Hall-effect measurement. The absence of the Burstein-Moss shift in all six samples indicated that the samples were not n-type. This was also confirmed by Hall measurements with varying magnetic field. On the basis of the Hall measurements on both as deposited and annealed films, it was also proposed that the electrical properties of the films were determined by the residual and/or unintentionally incorporated impurities.

7.0 Acknowledgement

The author is indebted to the AFOSR monitor Mr. Max Swerdlow for his suggestions, help and encouragement throughout this research and to Dr. Arnold Allentuch and the NJIT Research Foundation for being most supportive of the research of the Microelectronics Laboratory and for helping to provide supplemental funding for graduate students and equipment. The support of the Electrical Engineering Chairperson, Dr. Joseph Strano, and past Chairperson, Prof. Robert Anderson, is gratefully acknowledged.

The author is also most grateful to the following persons:

a) Ms. Brenda Walker, for typing and helping with the organization of many reports, proposals, and theses associated with this work. Timely typing assistance was also received from Ms. Debby Murray and Ms. Virginia Broughton.

b) Dr. Jerome Drexler, an NJIT alumnus, for providing funds and encouragement for the Microelectronics Lab. This was very important for obtaining needed extra student support at critical times of the research.

c) The graduate students, listed in section 6.0 and many other hard-working NJIT students, particularly Mr. Chetan Mehta, who enthusiastically pitched in to help with the numerous small but critical tasks associated with this thin film research.

d) Numerous colleagues in industry, particularly Mr. Irwin Kudman and Dr. Valery Belov of Infrared Associates Inc., for consultations concerning this research.

e) The NJIT Machine Shop personnel, particularly Mr. Anthony J. Emanuele for making many mechanical fixtures.

f) Dr. Leon Buteau and Dr. Eliot Farber of the NJIT Physics Dept. for letting us use their x-ray diffraction and S.E.M. equipment.

g) The Dept. of Chemical Engineering and Chemistry for the use of their spectrophotometers, other equipment, and space.

h) Dr. Stephen Duerr of Structure Probe Inc., for providing skillful guidance on surface analysis measurements at Structure Probe.